INAUGURAL - DISSERTATION

zur

Erlangung der Doktorwürde

der

Naturwissenschaftlich-Mathematischen Gesamtfakultät

der

Ruprecht-Karls-Universität

Heidelberg

2009

vorgelegt von

Diplom-Biologe

Thorsten Bus

aus Münster / Westfalen

Tag der mündlichen Prüfung:

Genetic investigations into the role of ionotropic glutamate receptors in hippocampal learning

Hiermit erkläre ich, daß ich die vorliegende Dissertation selbst verfaßt und mich dabei keiner anderen Mittel als der von mir ausdrücklich bezeichneten Quellen und Hilfsmitteln bedient habe. Des weiteren erkläre ich, daß ich an keiner Stelle ein Prüfungsverfahren beantragt oder die Dissertation in dieser oder einer anderen Form bereits anderweitig als Prüfungsarbeit verwendet oder einer anderen Fakultät als Dissertation vorgelegt habe.

Heidelberg, 29.03.2009

Thorsten Bus

Zusammenfassung

L-α-Amino-3-Hydroxy-5-Methylisoxazol-4-Propionsäure (AMPA) und N-Methyl-D-Aspartat (NMDA) Rezeptoren gehören zu der Familie der ionotropen Glutamat-rezeptoren, die erregende Signalweiterleitung im Zentralen Nervensystem vermitteln und an vielen Mechanismen beteiligt sind, die dem kognitiven Lernen und Gedächtnis unterliegen. Mit Hilfe genetischer Manipulationen dieser Rezeptoren, sowohl global in allen Zellen der Maus, als auch spezifisch in Prinzipalneuronen des Vorderhirns, wurden molekulare Mechanismen im dorsalen Hippokampus unterschieden, die dem Referenz- und dem Arbeitsgedächtnis im räumlichen Verhalten zugrunde liegen. In dieser Doktorarbeit wird die Beteiligung der hauptsächlichen ionotropen Glutamat-Rezeptoren (AMPA Rezeptoren, die GluR-A oder GluR-B enthalten und NMDA Rezeptoren) in Prinzipalneuronen spezifischer Hippokampusregionen (DG, CA1 und CA2) in diesen prominenten Gedächtnisformen in erwachsenen Mäusen untersucht.

Gezielte genetische Manipulation mittels Cre Rekombinase in spezifischen Regionen der Hippokampalen Formation und des Olfaktorischen Systems wurde durch die Kombination von transgenen Mäusen der Linien $Tg^{CN12\text{-}itTA}$ und Tg^{LC1} erreicht, die basierend auf dem zeitlich regulierbaren tet-Sytem eine Rekombination im gesamten Vorderhirn in embryonalen Stadien verhindern. Die sukzessive zeitliche Anhäufung von Rekombinationsereignissen wurde mit Hilfe der genetisch veränderten *Rosa26R* Maus (Soriano et al., 1999) sichtbar gemacht. Rekombination wurde zwar auch in weiteren Teilen des Vorderhirns beobachtet, jedoch waren nur sehr wenige Nervenzellen betroffen. Diese Spezifität blieb auch noch in einjährigen Mäusen erhalten.

Die Herstellung von Mausmodellen für die drei prominenten Glutamatrezeptor-Untereinheiten im Hippokampus (GluR-A in $Gria1^{\Delta HipOlf}$; GluR-B in $Gria2^{\Delta HipOlf}$; NR1 in $Grin1^{\Delta HipOlf}$ Mäusen) ermöglichte es, die erregende Signalweiterleitung in drei entscheidenden Eigenschaften mit relativ gleicher räumlicher und zeitlicher Spezifität im erwachsenen Mausgehirn genetisch zu verändern.

Die Mausmodelle $Gria1^{\Delta HipOlf}$, $Gria2^{\Delta HipOlf}$ und $Grin1^{\Delta HipOlf}$ wurden in verschiedenen Tests auf räumliches Arbeits- und Referenzgedächtnis untersucht. Unerwartet von früheren Beobachtungen (Reisel et al, 2002) zeigten $Gria1^{\Delta HipOlf}$ Mäuse keinerlei Beeinträchtigung im räumlichen Arbeitsgedächtnis. Jedoch werden

sie, wie globale GluR-A KO Mäuse, hyperaktiv in neuen Umgebungen, und alternierten wenig im spontanen T-Maze Test. Im Gegensatz dazu zeigten *Gria2$^{\Delta HipOlf}$* Mäuse ein vermindertes Arbeitsgedächtnis unter Standardbedingungen. Das Entfernen der NMDA Rezeptoren in hippokampalen Regionen der *Grin1$^{\Delta HipOlf}$* Mäusen führte zu einem differenzierteren Phänotyp. *Grin1$^{\Delta HipOlf}$* Mäuse konnten sich an räumliche Informationen im T-Maze für etwa drei Sekunden erinnern und entsprechend handeln, aber nicht mehr nach einer Minute. Entgegen einer populären Hypothese, lernten *Grin1$^{\Delta HipOlf}$* Mäuse die Position einer verdeckten Plattform im Morris Wasserlabyrinth im mehrtägigen Versuchsprotokoll. Allerdings hatten sie anschließend mehr Schwierigkeiten als ihre Kontrollmäuse, eine neue Position für die Fluchtmöglichkeit aus dem Wasser zu erlernen.

Mit Hilfe genetischer Manipulation der hauptsächlichen Glutamatrezeptoren in den drei Mausmutanten *Gria1$^{\Delta HipOlf}$*, *Gria2$^{\Delta HipOlf}$* and *Grin1$^{\Delta HipOlf}$* wurde aufgezeigt, daß AMPA Rezeptoren, die GluR-B enthalten und NMDA Rezeptoren in DG, CA1 und CA2 Prinzipalneuronen der hippokampalen Formation essentiell am räumlichen Arbeitsgedächtnis beteiligt sind. AMPA Rezeptoren, die GluR-A enthalten und NMDA Rezeptoren in diesen Nervenzellen scheinen jedoch nicht am räumlichen Referenzgedächtnis beteiligt zu sein.

Summary

AMPA and NMDA receptors are ionotropic glutamate receptors, respectively sensitive to the glutamate analogue α-amino-3-hydroxy-5-methyl-4-isoxazole-propionic acid (AMPA) or N-methyl-D-aspartate (NMDA), and are essential for hippocampus-dependent learning and memory. As indicated by global and forebrain-specific mutant mouse models of AMPA and NMDA receptors, distinct molecular mechanisms coexist in the dorsal hippocampus, underlying spatial behavior in working and reference memory tasks. The present study is focused on the main ionotropic glutamate receptors (AMPA receptors with GluR-A or GluR-B subunit or NMDA receptors) in principal neurons (DG, CA1, CA2) of the hippocampus in adult mice and the role of these receptors in spatial working and reference memory.

Cre recombinase expression in restricted sublayers of the hippocampal formation and the olfactory system was achieved by the use of transgenes of mouse lines $Tg^{CN12\text{-}itTA}$ and Tg^{LC1} employing the *tet*-system to prevent widespread recombination in the mouse embryo. Minor recombination, monitored by the use of gene-targeted *Rosa26R* mice, accumulated in additional forebrain structures but remained sparsely located in one-year-old mice.

By employing the $Tg^{CN12\text{-}itTA}$ / Tg^{LC1} mouse model to deplete GluR-A in $Gria1^{\Delta HipOlf}$ mice, GluR-B in $Gria2^{\Delta HipOlf}$ mice or all NMDA receptors by NR1 ablation in $Grin1^{\Delta HipOlf}$ mice, excitatory neurotransmission was modified in three major ways. Depletion of these receptor subunits was observed with similar spatial and temporal specificity in hippocampal sublayers of adult mice.

With these three $iGluR^{\Delta HipOlf}$ mouse models in hands, behavioral consequences were investigated in spatial working and reference memory tasks in two independent laboratories (Heidelberg, Germany; Oxford, England). Unexpected from our previous observations (Reisel *et al.* 2002), GluR-A depleted $Gria1^{\Delta HipOlf}$ mice performed well in all cognitive tasks of spatial working behavior independent of delay and task composition. However, $Gria1^{\Delta HipOlf}$ mice still expressed hyperactivity in a novel environment and little spontaneous alternation. In contrast, GluR-B depletion in $Gria2^{\Delta HipOlf}$ mice became manifest in impairment in spatial working memory. Unfortunately, testing of spatial reference memory in $Gria2^{\Delta HipOlf}$ mice is still missing. $Grin1^{\Delta HipOlf}$ mice exhibited delay- and task-dependent impairment of the

spatial working memory and in reversal reference learning. Nevertheless, the acquisition of spatial reference memory in Morris watermaze and Y-maze was not affected upon NR1 depletion in dorsal CA1, CA2 and the entire DG subfield of the hippocampal formation.

In summary, genetic manipulation of the main ionotropic glutamate receptors in the three mutant mouse models $Gria1^{\Delta HipOlf}$, $Gria2^{\Delta HipOlf}$ and $Grin1^{\Delta HipOlf}$ demonstrated the essential role of AMPA receptors containing the GluR-B subunit and NMDA receptors in principal DG, CA1 and CA2 neurons of the hippocampal formation in spatial working memory. Spatial reference memory, however, was still intact upon depletion of AMPA receptors containing the GluR-A subunit in $Gria1^{\Delta HipOlf}$ mice and NMDA receptors in $Grin1^{\Delta HipOlf}$ mice.

Table of Content

1. Introduction

The brain is the central and most complex organ in the mammalian body that regulates most physiological processes (e.g. movement, digestion, breathing, heart rate, blood pressure, the endocrine system) and promotes learning and memory-based cognitive functions including consciousness and mind. Underlying mechanisms on the network of over 100 billion interconnected nerve cells in the human brain have been investigated on multiple levels of complexity. Our knowledge of brain systems, local neuronal networks, and cellular and molecular properties in the brain increased extensively over the last two centuries. Excitatory neurotransmission mediated by ionotropic glutamate receptors plays an essential role in hippocampus-dependent spatial forms of cognitive behavior. The main focus of this Ph.D. thesis is the role of ionotropic glutamate receptors in principal DG, CA1 and CA2 neurons of the hippocampal formation in adult mice and its role in spatial working and reference memory. Three mutant mouse models of the main ionotropic glutamate receptors (AMPA receptors that contain the GluR-A or GluR-B subunit and all NMDA receptors) were generated with similar spatial and temporal specificity.

1.1. Signal transmission in the nervous system

The nervous system is composed of individual nerve cells called neurons and neuro glia. Whereas neurons (*Greek* for „*nerve*") are the main structural and functional units of the nervous system that acquire, store and pass on information (*neuron doctrine*, Cajal 1911), the roughly ten times more abundant glia (*Greek* for „*glue*") were long considered as „brain glue" providing exclusively structural, metabolic and neuro-protective support. However, recent reports highlighted a more direct role of glia cells in the interplay with neuronal networks. Glia cells secrete trophic factors, promote axonal outgrowth (development of the nervous system), form axonal myelination to enable long-range signaling and were even shown to secrete neurotransmitter and coordinate neuronal activity (reviewed in Fields and Stevens-Graham, 2002; Haydon and Carmignoto 2006).

Nevertheless, the network of interconnected neurons fulfills the main properties of the nervous system. Neurons convert stimuli of various sensory modalities (e.g. visual, auditory, olfactory, endocrine), integrate multiple inputs of neurons or other

cells and generate directed output signals. These 'integrated information-processing units' are organized in discrete cellular layers forming local networks and discrete brain systems to separate brain functions with highly balanced hierarchy.

1.1.1. Neurons

Neurons developed into a broad class of electrochemically responsive cells with different shapes, sizes, morphologies and functions to process stimuli of different qualities, control the homeostasis and refine the action of the animal's body. Based on their function in the signal transmission in a neuronal network, neurons can be divided into two main classes: *principal* (or *projection*) *neurons* and *interneurons*. Principal neurons convey information to the next processing stage in neuronal networks and usually, activate other neurons by excitatory neurotransmission. In contrast, interneurons connect mainly local neurons in a discrete neuronal cell layer and inhibit their target neurons.

Although neurons differ from one another, depending on location and discrete function, they share some morphological features. In addition to the cell body (termed *soma*) that contains the nucleus and most of the protein synthesis machinery, neurons extend differentiated structures for receiving input (*dendrites*) and transmitting output (*axons*). Signals are received in the highly branched, tree-like *dendrites* (also called *dendritic tree*) and the *soma*. Thereby, little membranous protrusions, so-called *spines*, on the dendritic tree are the main input structures and get innervated typically by single axon terminals (*boutons*) of other cells. Up to 10.000 of these *synapses* receive signals in a single neuron (Stevens 1979) that are transmitted via electrical discharges across the plasma membrane to the neuron's soma. Combined with received signals on dendritic shafts and somatic contacts, electrical signals are processed at the *axon hillock* where the axon emerges from the soma. This zone is the most electrically sensitive part of the neuron and initiates the regenerative, all-or-none output signal, the so-called *action potential* or *electrical spike*. Usually a single axon transmits the action potential in one direction, away from the soma (*law of dynamic polarization*, Cajal 1911). To enable the communication with many target neurons, the axon usually branches in multiple axon terminals. Axons of many projection neurons, involved in fast, long-range signaling, are insulated by a myelin sheet (80% lipids and 20% proteins), which is regularly interleaved by the so-called *nodes of*

Ranvier. Here, electrical signals are transmitted via saltatory conduction from node to node in direction to axonal terminals. Myelinated axons form the white matter in the brain.
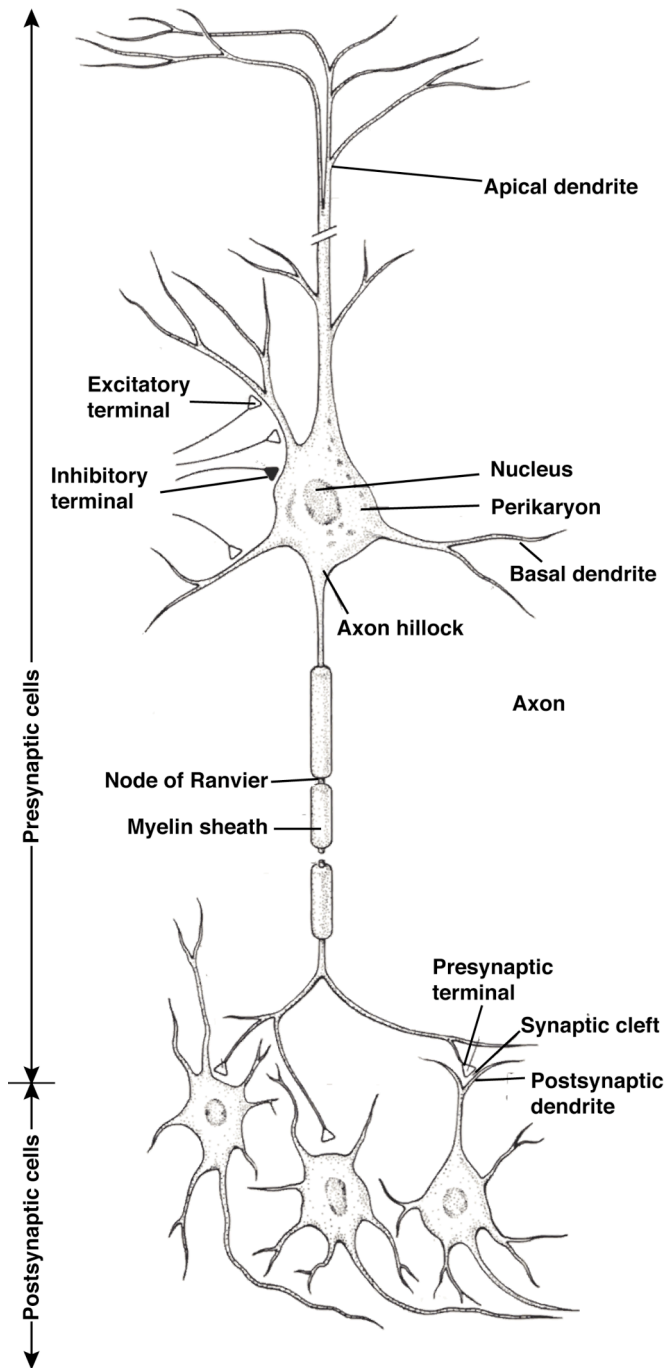
Fig. 1.1. Morphological features of neurons

The cell body (soma) contains the nucleus and perikaryon, and gives rise to two types of processes: dendrites (apical and basal) and axons. The axon is the transmitting element of the neuron. Axons vary greatly in length, with some extending > 1 meter. The axon hillock, the region of the soma where the axon emerges, is the initiation site for action potentials, based on the high density of voltage-gated Na+ and K+ channels. Many axons are insulated by a fatty myelin sheath, which is interrupted at regular regions known as nodes of Ranvier. Branches of the axon form synaptic connections with dendrites of postsynaptic neurons. The branches of the axon may form synapses with as many as 1000 other neurons (adapted from "Principles of Neural Science", E.R. Kandel, J.H. Schwartz, T.M. Jessel).

1.1.2. Transient changes in the membrane potential

Double-layered lipid membranes (6-8 nm thin), permeable *per se* only for small gases and dipolar substances (e.g. chloroform, ethanol), separate the interior from the exterior of all living cells and serve as a physical barrier for the highly conductive fluids on both sides. By consuming energy (mainly ATP), selective ion pumps and transporters (e.g. *sodium potassium pump*) embedded in the double-layered lipid membrane accumulate ion gradients of mono- and divalent ions (mainly K^+, Na^+, H^+, Ca^{2+}, Cl^-) in both directions across the membranes. In turn, additional membrane-spanning protein complexes, forming ion channels and transporters with regulated and selective permeability, allow for the facilitated diffusion along the *electrochemical gradient* across the membrane. While an ion crosses the membrane through a protein pore (ion pump, transporter or channel) and separates the charge of the interior and the exterior of a cell, the lipid double layer works like a dielectric phase in a plate capacitor. The electrical field across the membrane aligns electrons differently in both layers, whereas the strong hydrophobic characteristic of the lipid layer prevents the electron transition into the hydrophilic space. The *electrical force* (charge difference) effective in the plasma membrane i.e. the *membrane potential*, stores potential energy that counterbalances the *molecular force* (concentration difference) of the electrochemical ion gradient. The potential energy is coupled to thermodynamically unfavorable processes like passive transport (e.g. other ions or metabolites) and even ATP synthesis (proton-motive force in F1F0-ATP synthase; reviewed in Devenish et al., 2008).

While most living cells depend on a cell type-specific *resting potential* (between -50 and -100 mV) to ensure the continuous exchange with the environment, electrically-excitable cells like neurons, muscle or certain gland cells in addition, are capable to communicate via transient changes in the *membrane potential*. In particular, neurons differentiated to highly specialized 'microprocessors' that form highly compartmentalized and selective membrane permeabilities for Na^+, K^+, Ca^{2+} and Cl^- (*ligand- and voltage-gated ion channels*) and membrane conductance (density of ion channels and pumps, lipid composition, myelination) to receive, process and transmit transient changes in the membrane potential.

First, neurons are capable to receive electrical signals and to convert chemical signals of connected cells in local transient deviations from the resting potential, so-called *graded potential*. So, if opening of ion channels results in a net gain of positive charge (mainly influx of Na^+), the membrane becomes *depolarized*. Depolarization changes the resting potential in direction to the *firing threshold* (typically -50mV) and is therefore referred to as *excitatory postsynaptic potential* (EPSP). In turn, if selective ion channels mediate a net loss of positive charge (e.g. efflux of K^+) or a net gain of negative charge (influx of Cl^-), the membrane is *hyperpolarized*; the evoked potential is called *inhibitory postsynaptic potential* (IPSP). Neurons experience several hundreds or thousands of EPSPs and IPSPs at the same time that are spatially and temporally summated.

The axon initial segment close to the soma, the axon hillock, receives the incoming EPSPs and IPSPs and „compares" them to the firing threshold of the neuronal output signal across the membrane, the *action potential* or *firing spike*. The action potential is an all-or-none, stereotyped, transient depolarizing electrical signal, which spreads along the axon without attenuation. The underlying generation and propagation of action potentials reflect the interplay of voltage-gated Na^+ and K^+ channels. Above a certain membrane potential threshold (typically -50 mV), which is reached upon depolarizing postsynaptic signals terminating on the neuron, voltage-gated Na^+ channels have a higher probability to be in the open conformation (i.e. the channels open). This results in further depolarization, since the membrane potential is driven towards the reversal potential of Na^+ (around +60 mV). Neighboring stretches of the membrane, which also contain voltage-gated Na^+ channels, are subsequently equally depolarized resulting in a spread of the excitation along the membrane. By way of this regenerative self-amplifying process, most of the Na^+ channels can switch to their open state in less than 1 ms. Then the voltage-gated Na^+ channels rapidly inactivate, thereby reducing the Na^+ permeability of the membrane. Voltage-gated K^+ channels, which have opened during the depolarization, lead to a K^+ efflux into the cell and cause a rapid hyperpolarization of the membrane back to the resting potential.

Action potentials do not just travel down the axon to cause transmitter release at the presynaptic boutons and terminals; they also invade the dendritic tree, which is mainly the input region of a neuron. Dendrites of most neurons also contain voltage-gated Na^+ channels, which allow the back-propagation of action potentials initiated at

the soma (Stuart, Sakmann, 1994). The back-propagating action potential signals the state of activity (i.e. firing of an action potential) of a neuron back to its input region.
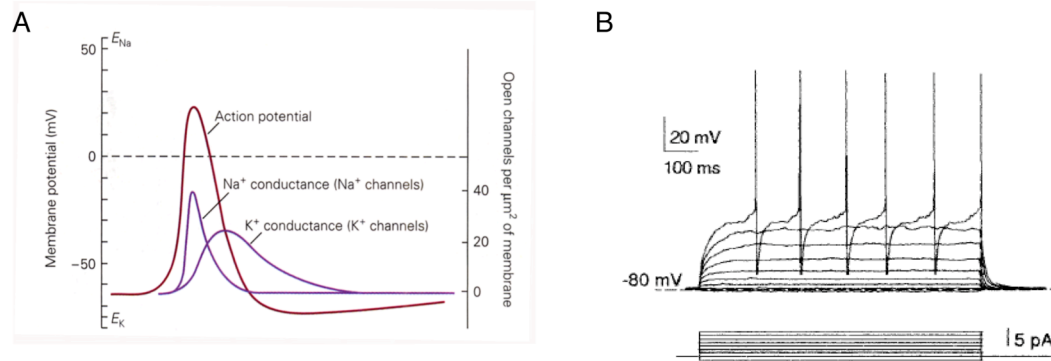
Fig. 1.2. Action potentials

(A) The shape of an action potential can be calculated from the changes in g_{Na} and g_K that result from the opening and closing of voltage-gated Na^+ and K^+ ion channels. The Na^+ current is responsible for the depolarizing and the K^+ current for the hyperpolarizing phase of the action potential, respectively. (B) When a nerve is depolarized above a certain threshold (typically -50 mV) action potentials are generated. In this case, the depolarization was provided by current injections into the soma in a current-clamp experiment. Action potentials are all-or-none events having the same shape and amplitude, which are characteristic for each cell type, as is the firing frequency (adapted from "Principles of Neural Science", E.R. Kandel, J.H. Schwartz, T.M. Jessel).

1.2. Synaptic neurotransmission

Synapses (synapsis, *Greek* for *conjunction*) form the main point of contact between neurons. Transmission via synaptic connections can be mediated either *electrically* or *chemically*. While the direct electrical coupling of connected neurons via *electrical synapses* allows for fast, bi-directional transmission of neuronal activity (action potentials and graded, sub-threshold deviations from the resting potential) without latency, signal transmission via *chemical synapses* is delayed and unidirectional because the presynaptically released neurotransmitter diffuses across the synaptic cleft (10 nm gap) to activate specific neurotransmitter receptors embedded in the postsynaptic membrane. Since the two main classes of neurotransmitter receptors acts either fast as selective ion channels (*ionotropic receptors*) or slower as G protein-coupled *metabotropic receptor*, released neurotransmitters can induce postsynaptic changes with various latencies and decays dependent on the activated postsynaptic receptors. Chemical synapses are more abundant in the central nervous system and

implement numerous features for a major role in activity-dependent prolonged changes in the synaptic transmission between neurons (*synaptic plasticity*).

1.2.1. Chemical synapses

Chemical synapses are specialized structures, where the membrane of the presynaptic neuron is in close apposition to the postsynaptic membrane of the connected neuron, being just separated, and thus electrically isolated, by the 10 nm synaptic cleft. At the point of contact, both membranes contain a high density of proteins for signal transduction linked to synaptic transmission (reviewed in Specht and Triller, 2008). The presynaptic active zone is characterized by a cluster of vesicles containing neurotransmitter close to the membrane and a high density of voltage-gated Ca^{2+} channels. The postsynaptic density is composed of neurotransmitter receptors, their scaffolding molecules, various down-stream signaling complexes and cell adhesion molecules.

When an action potential reaches a bouton or axonal terminal, the voltage-gated Ca^{2+} channels open. This results in Ca^{2+} influx into the presynaptic active zone. Ca^{2+} binds to proteins (e.g. *synaptobrevin, -tagmin*) that trigger the fusion of the transmitter vesicle with the plasma membrane. Subsequently, a fusion pore opens, expands and releases neurotransmitter into the synaptic cleft. This mechanism of neurotransmitter release is called exocytosis, a highly regulated process of multiple protein-protein interactions for which influx and binding of Ca^{2+} is prerequisite. The vesicle membrane is usually recovered from the plasma membrane by endocytosis and reloaded with neurotransmitter. The neurotransmitter diffuses across the synaptic cleft and binds to specific receptors on the postsynaptic membrane, mainly located on a spine head or a dendritic shaft of the connected neuron.

In the CNS, synaptic transmission can either be excitatory or inhibitory. The main excitatory transmitter in the brain is glutamate, which acts on three different types of ionotropic receptors termed α-amino-3-hydroxy-5-methyl-4-isoxazole-propionic acid (AMPA), kainate and N-methyl-D-aspartate (NMDA) receptors and on metabotropic (G-protein coupled) glutamate receptors (mGluRs). The main inhibitory transmitters in the CNS are γ-amino butyric acid (GABA) and glycine. GABA receptors are divided into ionotropic $GABA_A$ receptors and metabotropic $GABA_B$ receptors.

1.2.2 Ionotropic glutamate receptors

Ionotropic glutamate receptors (iGluR) are ligand-gated channels that are selectively permeable for cations, principally Na^+, K^+ and sometimes Ca^{2+}. On the basis of their responsiveness to certain glutamate derivatives, iGluRs are classified into AMPA, NMDA and kainate receptors. The ionotropic glutamate receptors are encoded by six gene families of which a single one encodes all AMPA receptors, three for NMDA receptors and two for kainate receptors (reviewed in Dingledine et al., 1999). All ionotropic glutamate receptors share certain structural features. AMPA, NMDA and kainate receptors form functional, tetrameric receptor complexes. Each subunit of ionotropic glutamate receptors consists of three transmembrane segments (M1, M3 and M4) and one intra-membranous loop (M2). In addition, each subunit contains a bipartite ligand-binding site formed by two domains (S1 and S2, reviewed in Mayer, 2005).

AMPA and kainate receptors have fast activation and deactivation kinetics (Trussel and Fischbach, 1989) as well as usually low Ca^{2+} permeability (Jonas and Burnashev, 1995). In contrast, NMDA receptors exhibit voltage-dependent, slow gating kinetics with prolonged channel opening after binding of agonists (Jonas and Burnashev, 1995), high Ca^{2+} permeability (MacDermott et al., 1986) and a need for glycine as a co-activator (Benveniste and Mayer, 1991).
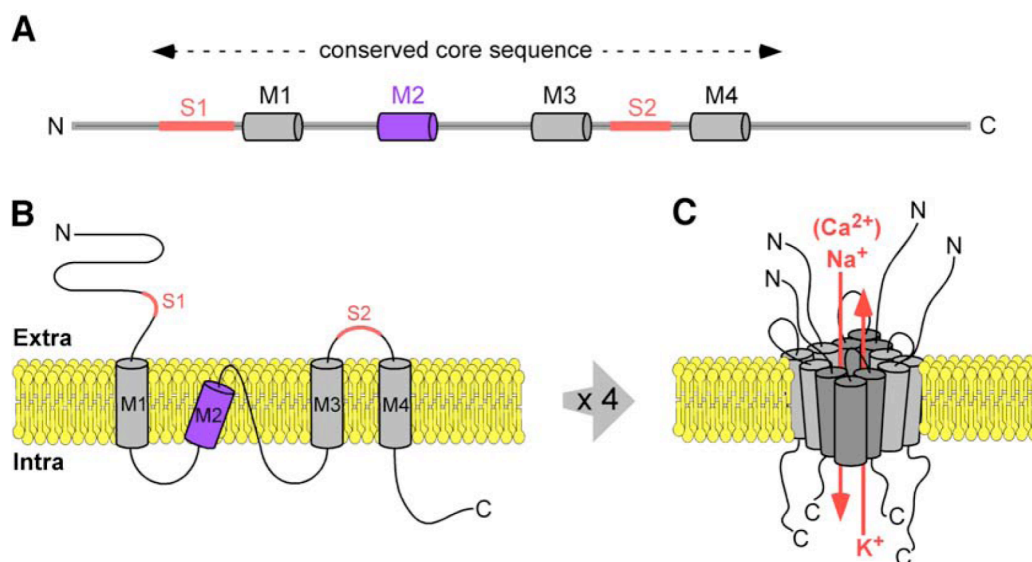
Fig. 1.3. Schematic representation of the common structure of ionotropic glutamate receptors
(A) Linear arrangement of a single subunit from the amino- (N) to the carboxyl-terminus (C). Gray barrels indicate the transmembrane segment (M1, M3, M4), the purple barrel the membrane loop (M2)

forming the channel pore in functional, tetrameric receptors. The segments S1 and S2 form the glutamate-binding site. **(B)** Schematic arrangement of a single subunit in the plasma membrane. The amino-terminus (N) is located on the extracellular side, the carboxyl-terminus (C) on the cytoplasmatic side of the membrane. **(C)** Schematic arrangement of functional ionotropic glutamate receptors. AMPA, NMDA and kainate receptors form tetrameric receptor complexes permeable for Na^+, K^+ and sometimes for Ca^{2+} by non-edited GluR-B containing or GluR-B lacking AMPA and NMDA receptors (adapted from Mihaljevic, MD thesis, Uni Heidelberg, 2005).

1.2.2.1. AMPA receptors

AMPA receptors are glutamate-gated cation channels that are sensitive to the glutamate analogue α-amino-3-hydroxy-5-methyl-4-isoxazolepropionic acid (AMPA). Four different AMPA receptor subunits, termed GluR-A to GluR-D or GluR-1 to GluR-4 (novel nomenclature GluA1 to GluA4), are encoded in the mammalian genome (Keinanen et al., 1990) and assemble the functional tetrameric AMPA receptors. GluR-A and GluR-B subunits are ubiquitously expressed in the mammalian CNS, GluR-C mRNA is found in hippocampal and cortical cell layers as well as in the Purkinje cell layer of the cerebellum and GluR-D mRNA mainly in GABAergic interneurons. While most principal neurons in the hippocampus express mainly GluR-A/-B heteromers, some GluR-B/-C heteromers, and a few GluR-A homomeric channels (Derkach et al., 2007; Petralia and Wenthold, 1992; Wenthold et al., 1996), GluR-D-containing AMPA receptors are found in hippocampal interneurons (Jensen et al., 2003).

Upon binding of glutamate, AMPA receptors are permeable for Na^+ and K^+, typically with rapid onset, offset, and desensitization kinetics (Dingledine et al., 1999; Gouaux, 2004; Sprengel, 2006). Opening of these channels at resting potential leads to a rapid depolarization of the postsynaptic membrane. The cationic depolarization current flowing through AMPA receptors can be measured in voltage-clamped condition as EPSC (excitatory postsynaptic current).

Ca^{2+} entry through AMPA receptors is restricted by the GluR-B subunit. While GluR-B-lacking AMPA receptors are permeable for Ca^{2+}, incorporation of RNA-edited GluR-B(R) into functional AMPA receptors decreases single channel conductance (Swanson et al., 1997) and renders the channel impermeable to Ca^{2+} (Burnashev et al., 1992b). Hydrolytic deamination of adenosine to inosine by enzymes termed adenosine deaminases acting on RNA (ADARs) changes the coding information on the GluR-B transcript from a glutamate (Q) residue at position 607

(C$\underline{A}$G) to arginine (R; C$\underline{I}$G). The Q/R editing site is located in the pore forming segment M2 and RNA editing of GluR-B transcripts converts the Ca^{2+} permeable GluR-B(Q) to the impermeable GluR-B(R). Q/R editing is developmentally, cell- and region-specifically regulated (Lerma et al., 1994; Nutt and Kamboj, 1994), in the adult hippocampus however ~ 99 % of the GluR-B mRNA is edited (Sommer et al., 1991; Higuchi et al., 1993).

Additional editing (reviewed in Seeburg et al., 1998) and alternative splicing of pre-mRNA (Sommer et al., 1990; Mosbacher et al., 1994; Kohler et al., 1994) as well as cell- and region-specific and developmentally regulated expression of all receptor subunit isoforms generates a remarkable variability of functional AMPA receptors that differ in many properties, including single channel conductance and desensitization properties (Lomeli et al., 1994; Mosbacher et al., 1994). In addition, AMPA receptors embedded in the postsynaptic membrane undergo various posttranslational modifications (reviewed in Palmer et al., 2005). Most prominent in hippocampal processing, GluR-A and GluR-B contain two phosphorylation sites within the C-terminal domain. Protein Kinase C (PKC) and Calcium/Calmodulin-dependent Protein Kinase II (CaMKII) mediate phosphorylation of the GluR-A protein at Ser 831 and Protein Kinase A (PKA) at Ser 845. Modification of GluR-A-containing AMPA receptors at these phosphorylation sites increases channel open probability and single channel conductance (Mammen et al., 1997; Roche et al., 1996). The GluR-B subunit is phosphorylated at Ser 880 and Tyr 876. Phosphorylation regulates the interaction of GluR-B with the binding proteins ABP/GRIP1 and PICK1, causing internalization of GluR-B-containing AMPA receptors from synaptic sites (Chung et al., 2000; Matsuda et al., 1999; Seidenman et al., 2003).

Global inactivation of the GluR-A gene mostly affected AMPA receptors in the hippocampus and amygdala, where GluR-A expression is high (Molnár et al., 1993). In the absence of GluR-A, in global GluR-A-deficient mice (GluR-A$^{-/-}$, Zamanillo et al., 1999), the expression of the other AMPAR subunits is not only delayed, but also the final expression level of GluR-A partners, GluR-B and GluR-D, is reduced compared to wild-type mice (Jensen et al., 2003). Because GluR-B and GluR-D are the principal GluR-A partners in hippocampal AMPA receptors, absence of GluR-A leaves much of the GluR-B and GluR-D unassembled, resulting in a shorter half-life of these subunits. Depletion of GluR-A also impairs the cellular localization of the

other AMPAR subunits, as immunolabelling studies showed that GluR-B subunits are largely restricted to soma in the absence of GluR-A (Zamanillo et al., 1999, Jensen et al., 2003).

1.2.2.2. NMDA receptors

NMDA receptors, sensitive to the glutamate analogue N-methyl-D-aspartate, form heteromeric channel complexes combined of the principal subunit NR1 and NR2 (A to D) or NR3 (A, B) subunits (Seeburg et al., 1995). In principal neurons of the forebrain, functional NMDA receptors are mainly formed by two NR1 and two NR2A or NR2B subunits. Interestingly, NR2B containing receptors are expressed predominately in the mouse brain until the end of the second postnatal week (Monyer et al., 1982). As for AMPA receptors, heterogeneity of NMDA receptors is based on combination of different subunit isoforms (alternative splicing variants) and various post-translational modifications. However, RNA editing of NMDA receptor transcripts does not occur.

AMPA and NMDA receptors exhibit a number of unique electrophysiological features that make them key players in activity-dependent prolonged changes in synaptic neurotransmission (*synaptic plasticity*). Both receptor types colocalize at most synapses of the CNS (Chen et al., 2000; Liao et al., 1999; Petralia et al., 1999). Both are activated by the neurotransmitter glutamate but differ in their affinity for that ligand, their channel kinetics and ion permeability. Furthermore, NMDA receptors require glycine as a co-activator.

Upon binding of glutamate, AMPA receptors open and close rapidly (Mayer and Westbrook, 1987), thereby leading to a depolarization of the postsynaptic membrane creating an excitatory postsynaptic potential (EPSP). Activated NMDA receptors on the other hand open at resting potential but Na^+, K^+ or Ca^{2+} cannot pass the cannel pore since Mg^{2+} blocks it. A simultaneous depolarization of the membrane, however, removes the Mg^{2+} block and leads to high permeability to Na^+, K^+ and also to Ca^{2+}. Thus, NMDA receptors act as *coincidence detectors*: presynaptic release of glutamate must coincide with postsynaptic depolarization in order to unblock NMDA receptors and to increase postsynaptic depolarization (Koester *et al.* 1998). While most AMPA receptors are Ca^{2+} impermeable due to the incorporation of edited GluR-B subunits, NMDA receptors are permeable to Ca^{2+}. The Ca^{2+} influx through NMDA

receptors activates second messenger cascades such as the Calcium/Calmodulin-dependent protein kinase II (CaMKII, Lisman et al., 2002; Malenka and Nicoll, 1999) and is an essential step in some forms of activity-dependent changes in synaptic strength at the single synaptic contact level.
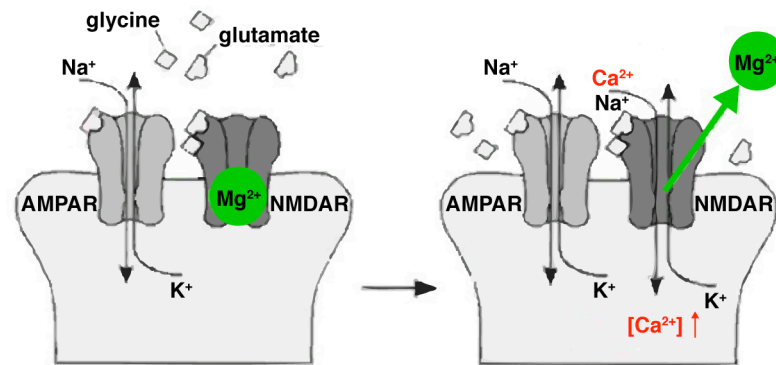
Fig. 1.4. Coincidence detection of the NMDA receptor

Model of the activity-dependent increase in transmission at a AMPA and NMDA receptor co-localized, glutamatergic synapse. L-glutamate release from the presynaptic membrane opens AMPA receptors but not NMDA receptors that are blocked by Mg^{2+} in the channel pore at resting membrane potential (left diagram). Sufficient depolarization of the postsynaptic membrane by AMPA receptor activation releases the Mg^{2+} block at the NMDA receptor channel pore and permits high membrane permeabilities for Na^+, K^+ and in particular, for Ca^{2+} that are essential for the activation of intracellular signaling processes (*second messenger* function) (adapted from Shimshek, PhD thesis, Uni Heidelberg, 2003).

1.2.3. Synaptic plasticity: Activity-dependent modulations of synaptic transmission evoke prolonged changes in the efficacy of synaptic contacts

Synaptic plasticity, i.e. activity-dependent changes in synaptic efficacy, is an intriguing feature of neuronal networks and is believed to be the neurophysiologic correlate underlying memory and behavior. Originally hypothesized by Cajal (*neuron doctrine*, 1913), information storage between two active neurons is based on changes of their synaptic connections. Hebb (1949) supported this hypothesis and proposed that time-dependent, local and highly interactive mechanisms as a function of repeated pre- and post-synaptic activity lead slowly to the formation of ``cell-assemblies''. In his book, *The Organization of Behaviour*, Hebb postulated how learning could occur. Specifically;

"When an axon of cell A is near enough to excite a cell B and repeatedly or persistently takes part in firing it, some growth process or metabolic change takes

place in one or both cells such that A's efficiency, as one of the cells firing B, is increased."

One usually refers to changes in synaptic efficacy that last for a short time window (milliseconds or several seconds) as short-term plasticity, whereas changes lasting for hours or even days are considered as long-term plasticity.

Activity-dependent short-term plasticity was demonstrated by an increase (facilitation) or a decrease (depression) of synaptic transmission between two subsequently administered action potentials in field or cellular recordings (Thomson et al., 2003; Stevens and Wang, 1995; Markram and Tsodyks, 1996). Short-term effects are mainly accounted by the release probability of transmitter vesicle as a function of presynaptic mechanisms (Katz and Miledi, 1968; Betz, 1970; Zucker, 1989). However, the exact determinants of facilitation and depression at a synapse are more complex. Observations in cortical layers II and III between principal and inhibitory neurons indicated that the action potential frequency of postsynaptic cells determines the direction of the short-term plasticity (Reyes et al., 1998).

Several distinct types of activity-dependent long-term plasticity have been described (reviewed in Malenka, 2004) of which long-term potentiation (LTP) (Bliss and Lomo, 1970, 1973) is the most prominent. LTP describes the observation that a brief high-frequency train of stimuli increases the amplitude of the excitatory postsynaptic potential (EPSP) in an input-specific manner. It has become clear that various forms of LTP exist dependent on synaptic connectivity, developmental stage and induction protocol (Esteban et al., 2003; Jensen et al., 2003; Yasuda et al., 2003). Bliss and Lomo first reported LTP experimentally in the hippocampus (Bliss and Lomo, 1970). Since then LTP and the contrary long-term depression (LTD) have been observed at many synapses in different brain regions. It is widely believed that these phenomena provide an important key to our understanding of the cellular and molecular mechanisms by which memories are formed and stored (Bliss and Collingridge, 1993). Furthermore, LTP and LTD might underlie the development and refinement of neuronal networks (Crair and Malenka, 1995).

1.2.5. The role of AMPA and NMDA receptors in hippocampal long-term potentiation (LTP)

The LTP model comprises an early phase (E-LTP) and a late phase (L-LTP) that are further divided in 3 distinct parts: induction, expression and maintenance. While E-LTP (first 30 to 60 minutes) is thought to rely mainly on direct changes in the membrane permeability for Na^+, K^+ and Ca^{2+} via ionotropic glutamate receptors in the hippocampus, the prolonged increase in synaptic strength lasting over hours, days or weeks (late phase, L-LTP) is a much more complex structural process including gene transcription and protein synthesis (Deadwyler et al., 1987; Frey et al., 1988; Stanton and Sarvey, 1984; reviewed in Lynch 2004).

LTP in the hippocampus was induced by different patterns of stimulation in field or cellular (*patch clamp*) recordings. Widely used induction protocols are presynaptic tetanization[1] or pre- and postsynaptic pairing such as low frequency stimulation[2] and theta burst pairing[3] (TBP). Although each of the protocols induces long lasting synaptic changes, the time course of expression of the early phase (0-5 min) LTP differs. After tetanic stimulation the peak increase in synaptic efficacy is expressed rapidly (1-3 min) after the stimulation and then drops gradually over time (Malenka and Nicoll, 1999). The pairing protocol results in a gradual, saturating increase in synaptic efficacy without a large initial peak (Chen et al., 1999; Hoffman et al., 2002). Finally, theta-burst pairing generates a rapid potentiation of synaptic strength, which then increases with time (Magee and Johnston, 1997; Pike et al., 1999). The difference in the time course of LTP expression induced by different protocols suggests different molecular pathways involved in the expression of these different forms of LTP.

With the exception of cAMP-dependent LTP at mossy fiber-CA3 synapses, all described forms of LTP in the hippocampus of wild-type mice are NMDA receptor-dependent (for review Malenka and Bear, 2004; Sprengel 2006). Application of the

---

[1] Tetanization consists of a 1 s long high frequency (100 Hz) stimulation of presynaptic neurons.

[2] Pairing protocol is a low frequency (0.7-1.5 Hz) presynaptic stimulation paired with prolonged (~ 3 min) postsynaptic depolarization at 0 mV, which aims to mimic postsynaptic action potential initiation upon presynaptic neural input to the postsynaptic neuron.

[3] Theta-burst pairing is a theta rhythm-mimicking train of 5 action potential bursts delivered at 5 Hz, with each burst consisting of 5 presynaptic EPSPs and postsynaptic action potentials paired at 100 Hz.

competitive NMDA receptor antagonist AP5 or the non-competitive NMDA channel blocker MK801 blocks LTP substantially in cellular or field recordings (Coan and Collingridge, 1987; Collingridge et al., 1983; Errington et al., 1987). The synaptic connections of principal neurons between the CA3 region and the CA1 region of the hippocampus (Schaffer collateral/commissural - CA1 synapses) are the most studied synapses to elucidate mechanisms of field and cellular LTP (Bliss and Collingridge, 1993). The CA1 principal neurons gain further impact for neurobiological research since transgenic mice with restricted ablation of NMDA receptors failed to induce Schaffer collateral - CA1 LTP and exhibited severe impairment in spatial behavior (Tsien et al., 1996). This was the first finding of a molecular and neurophysiologic correlate in a single cell layer that underlies memory-based behavior (for more details, please refer to 1.3.4.).

Successful LTP induction has been shown to require a rapid rise in the concentration of Ca^{2+} in the postsynaptic cell. Here, the capability of NMDA receptors to act as molecular coincidence detector is essential. Repeated stimulation at Schaffer collateral - CA1 synapses depolarizes the postsynaptic membrane by activation of AMPA receptors. This then causes the release of the Mg^{2+} blocking NMDA receptors in the postsynaptic membrane and allows the influx of Ca^{2+} via NMDA receptor channels (Collingridge et al., 1983; Ascher and Nowak, 1986). Hence, LTP is only induced if two time-dependent events occur, AMPA and subsequently additional NMDA receptor activation.

In principle, a rapid rise in the concentration of Ca^{2+} in the postsynaptic cell can also be mediated by AMPA receptors lacking GluR-B. In GluR-B KO mice, the AMPA receptor-mediated Ca^{2+} influx leads to an enhanced NMDA receptor-independent CA3-to-CA1 LTP (Jia et al., 1996). This form of NMDA receptor-independent LTP was also observed in the wild-type situation outside the hippocampus. In cerebellar interneurons, high frequency, presynaptic stimulation induces a rapid rise in local postsynaptic Ca^{2+} via GluR-B lacking AMPA receptors that triggers the insertion of GluR-B containing AMPA receptors at the synapse (Liu and Cull-Candy, 2002).

In the hippocampus however, enhanced and NMDA receptor-independent LTP was not reproduced in forebrain-specific GluR-B mutant mice (Shimshek et al., 2006). Here, GluR-B depletion was restricted to principal forebrain neurons by the use of transgenic Tg^{Cre4} mice (Mantamadiotis et al., 2002) directing Cre recombinase

under the αCaMKII promoter to excitatory neurons. Even though we do not have any evidence for the neurophysiologic differences in global (Jia et al., 1996) and forebrain-specific GluR-B mutants (Shimshek et al., 2006), one might speculate that the interplay between excitatory and inhibitory circuits or developmental, long-term changes induced by AMPA receptor-mediated Ca^{2+} influx (e.g. observed in kainate acid-mediated status epilepticus, Friedman et al., 1994; Friedman and Koudinov, 1999) are responsible for this kind of 'enhanced' LTP that was observed in global GluR-B mutant mice.

Following a rapid and strong Ca^{2+} influx[4], intracellular, Ca^{2+}-dependent signaling complexes convey the increase of Ca^{2+} into prolonged changes in synaptic efficacy. The most prominent candidate among protein kinases is the calcium/calmodulin-dependent protein kinase II (CaMKII), since pharmacological and genetic experiments indicated that its activation is essential for LTP induction (Fukunaga et al., 1993; Lledo et al., 1995; Otmakhov et al., 1997). CaMKII phosphorylates AMPA receptors and thereby, increases their single-channel conductance (Barcia et al., 1997; Benke et al., 1998). In addition, activation of CaMKII leads to insertion of GluR-A containing AMPA receptors at extrasynaptic sites, followed by lateral diffusion into synaptic sites (Chen et al., 2000; Passafaro et al., 2001). However, many other Ca^{2+}-dependent kinases are implemented in the LTP expression and maintenance. These include tyrosine kinases of the Src family (Salter and Kalia, 2004), protein kinase C (PKC, Bliss and Collingridge, 1993; Malenka and Nicoll, 1999), the protein kinase M zeta (PKMζ, Hrabetova and Sacktor, 1996; Ling et al., 2002), mitogen-activated protein kinase (MAPK, Sweat 2004) and cAMP-dependent protein kinase A (PKA, Roberson et al., 1999).

Nevertheless, like LTP induction, LTP expression at the Schaffer collateral - CA1 synapses relies heavily on ionotropic glutamate receptors. The discovery of silent synapses lacking AMPA receptors, and the evidence that LTP un-silences these synapses (Isaac et al., 1995; Liao et al., 1995), convinced most researchers that LTP involves the activity-dependent rapid recruitment of synaptic GluR-A containing AMPA receptors. Direct support comes from physiologically tagged AMPA receptor subunits (Liu and Cull-Candy, 2000) and experimentally un-caging glutamate onto

---

[4] It was hypothesized that a fast and strong influx of Ca^{2+} leads to LTP, whereas a smaller and more prolonged increase in intracellular Ca^{2+} ions induces LTD (Ismailov et al., 2004).

single spines (Bagal et al., 2005; Matsuzaki et al., 2004). It appears that there is a fairly constant turnover of GluR-B/C AMPA receptors at the synapse, whereas the trafficking of GluR-A/B AMPA receptors requires neural activity (Shi et al., 2001). Interestingly, while LTP expression has been associated with an increased number of GluR-A-containing AMPA receptors in synapses, there is also evidence that NMDA receptor-dependent LTD is associated with a decrease in AMPA receptors (Carroll et al., 1999).

Complete inactivation of the GluR-A gene in global GluR-A$^{-/-}$ mice impaired the NMDA receptor-dependent LTP in the tetanus as well as in the low frequency pairing protocol (Zamanillo et al., 1999; Mack et al., 2001). However, significant CA3-CA1 LTP could be induced in young (P14-P28) *GluR-A$^{-/-}$* mice in both LTP protocols (Jensen et al., 2003). This 'juvenile' GluR-A-independent form of LTP was shown to be NMDA receptor-dependent, postsynaptically expressed and, likely to rely on different molecular mechanisms than GluR-A-dependent LTP in adult wild-type mice. In addition, theta burst pairing of hippocampal CA3-CA1 synapses elicited robust LTP in adult *GluR-A$^{-/-}$* mice (P41-56). The initial component was substantially reduced and hence, GluR-A dependent. However, the slow developing LTP component in adult *GluR-A$^{-/-}$* mice was indistinguishable from control mice (Hoffman et al., 2002). It was hypothesized that GluR-A dependent and GluR-A independent LTP might be relevant for different forms of information storage and that a specific LTP deficit might result in the impairment of only a certain memory type, while preserving others (Hoffman et al., 2002).

1.3. The hippocampal formation in mice and rats: model system for anterograde amnesia

The hippocampal formation is located in the medial temporal lobe of the cerebellar cortex, part of the forebrain (telencephalon) and contains the *entorhinal cortex*, the *hippocampus*, the *dentate gyrus* (DG) and the *subicular complex*. Together with the adjacent amygdala, it forms the central axis of the limbic system (Squire et al., 2004). In contrast to the six-layered neocortical brain areas and the entorhinal cortex, the central parts of the hippocampal formation belongs to the allocortical brain areas of the cerebellar cortex and exhibits a characteristic three-layered structure (principal cell layer II and inhibitory cell layers I and III that include the principal fibers). The

entorhinal cortex connected to the perirhinal and parahippocampal cortex within the temporal lobe, receives neocortical information via monosynaptic inputs from higher-order sensory areas of each modality and pre-processed multimodal information from cortical association areas (e.g. *frontal association cortex*). Subcortical information, mainly from the septum, is transmitted via the *fimbria-fornix* bundle into the hippocampus. A rudimentary component of the hippocampus, the so-called '*hippocampal attenuation*' (*indusium griseum* or *supracallosal gyrus*) located above the corpus callosum, connects the olfactory system with hippocampal processing (reviewed in Cenquizca and Swanson, 2007). Most hippocampal research in the last fifty years was directed to the hippocampus and the DG, the central structures of the hippocampal formation. Both structures form the most prominent internal circuit of the hippocampal formation, the excitatory trisynaptic loop that is believed to be the relay station of polymodal stimuli in cognitive brain functions.

The hippocampal formation, in particular the hippocampus, has long been recognized as a key structure in the human brain for its capacity of conscious recollection of facts and autobiographical events (declarative memory). The observations of patients HM (Scoville and Milner, 1957) and RB (Zola-Morgan et al., 1986), which suffered from anterograde amnesic syndromes related to damage to their temporal lobes, explicitly identified the important role of the hippocampus and medial temporal lobe structures in memory. In HM, a large portion of the hippocampus was lesioned whereas damage in RB was just restricted to the CA1 subfield. Studies of HM and RB demonstrated that the hippocampus was important for the formation and retrieval of memories. HM was unable to retain and recall new information over a delayed period of time and RB could not acquire new long-term memories. Aside from memory formation and recall however, both patients had normal levels of perceptual and cognitive ability, and some remote memory sparing (Scoville and Milner, 1957; Zola-Morgan et al., 1986).

In rodents, the hippocampal formation is involved specifically in spatial forms of episodic memory (Morris et al., 1982; O'Keefe and Nadel, 1978). With improvement of lesion and transgenic techniques and development of various cognitive tasks of spatial behavior, the rodent's hippocampal formation became an attractive model to investigate acquisition, consolidation and recall of spatial short- and long-term memory.
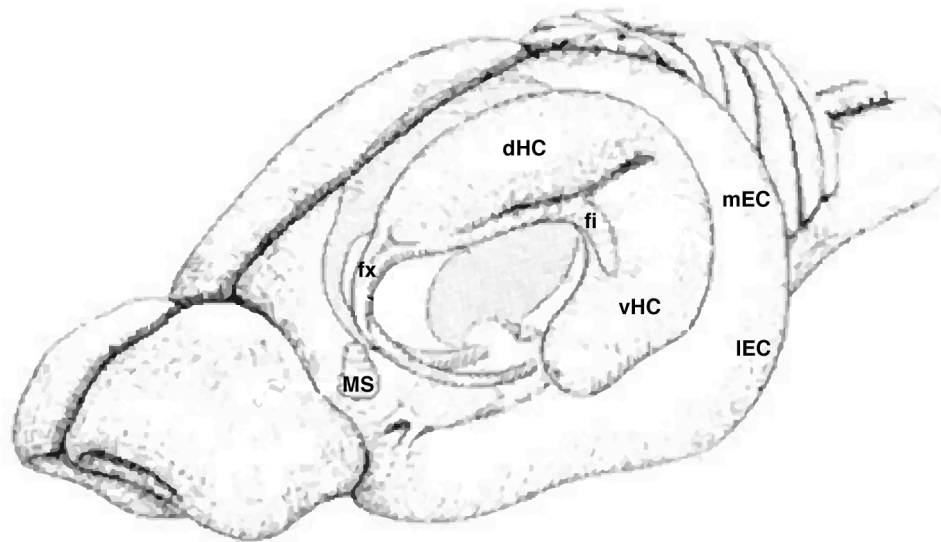
Fig 1.6. Three-dimensional location of the hippocampus (including the Dentate Gyrus) in the mouse brain

dHC/vHC, dorsal/ventral hippocampus; fi, fimbria; fx, fornix; mEC/lEC, medial/ventral entorhinal cortex; MS, medial septum (adapted from Amaral and Witter, 1989).

1.3.1. Hippocampus - the central processing unit of the hippocampal formation

The hippocampus (seahorse, *Greek*: *hippos* for horse, *kampos* for sea monster) including DG is a curved, tube-like structure deeply buried in the temporal lobe. Located along the rostro-caudal plane of the rodent's brain in a way that, roughly, one end is near the top of the brain (the dorsal hippocampus or septal pole) and another end near the bottom of the brain (the ventral hippocampus or the temporal pole). This structure consists of two C-shaped interlocking regions, the Ammon's horn (cornu ammonis, CA) of the hippocampus and the fascia dentata of dentate gyrus (DG). Both composed of one principal cell layer; the pyramidal cell layer in CA (*stratum pyramidale*) and the granular cell layer in DG (*stratum granulosum*) (Ramón y Cajal, 1893). CA is further subdivided in the subfields CA1-CA3 (Amaral and Wittner, 1989), based on the classification of the arrangement of different cells in each area (Lorente de Nó, 1934). Pyramidal cells extend their main apical dendritic shafts in *stratum radiatum*, terminating in *stratum lacunosum-moleculare*, and basal dendrites in *stratum oriens*. Axons of pyramidal cells run in *stratum alveus* where they form numerous collaterals before leaving the hippocampus. Granule cell dendrites stretch

out to *stratum moleculare* and axons (mossy fibers) runs through the polymorphic cell layer in the DG hilus that is often considered a separated subfield (CA4).

The most prominent pathway of informational processing through the hippocampus forms an excitatory feed-forward circuit, which has been termed the 'trisynaptic loop or circuit' (Andersen, Holmqvist and Verhoeve, 1966; Andersen, 1975; Swanson et al., 1978). First, granule cells in DG receive synaptic input from layer II of the entorhinal cortex via the perforant path (Stewart and Scoville, 1976). DG granule cells send axonal mossy fibers terminating in str. radiatum on the proximal apical dendrites of the large CA3 pyramidal cells. Finally, CA3 pyramidal cells project to the pyramidal CA1 neurons via the Schaffer collateral system (Lorente de Nó, 1934; Blackstad, 1956; Amaral, 1978) terminating in the distal two-third of str. radiatum. CA1 pyramidal neurons send their axons to the subiculum and deep layers of the entorhinal cortex. This unidirectional loop is thought to process most of the hippocampal information (Amaral and Wittner, 1989). Within all fields of the hippocampus a large number of interneurons are present. These interneurons often have extensive axon arborization, usually staying within the boundary of a given region. They can interact with many hippocampal principal neurons modulating hippocampal activity both by feed-forward and feedback inhibition (Lopes da Silva et al., 1990).
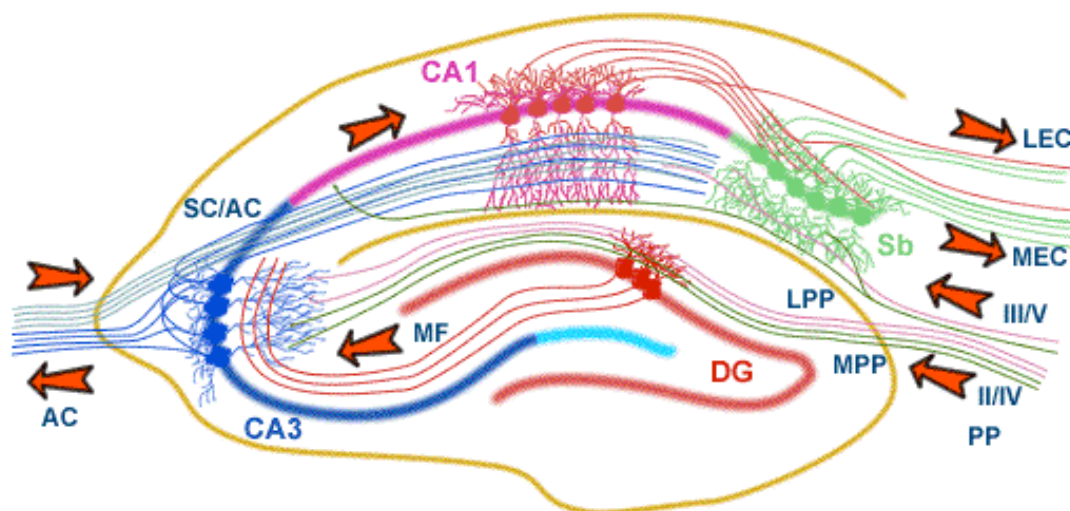
Fig 1.6. The most prominent, unidirectional pathway in the hippocampus, originally based on the 'trisynaptic loop' (Andersen et al., 1966)
The main cortical information, converged in the entorhinal cortex, is received via the Perforant Path (PP, splits into lateral and medial) that innervate mainly the granule cells of the Dentate Gyrus (DG) as well pyramidal CA3 neurons. Axons of DG neurons (mossy fibers, MF) innervates CA3 pyramidal

neurons that send Schaffer Collateral (SC) axons to the CA1 pyramidal neurons in the same transversal plane and axons via the Associational Commissural pathway (AC) to CA1 neurons of the contra lateral hippocampus. CA1 neurons send hippocampal information via principal neurons in the subicular complex (subiculum, pre- and parasubiculum) and directly back to the entorhinal cortex, forming the mainly unidirectional loop. CA1 pyramidal neurons receive pre-processed information via DG and CA3 neurons from layer II and also V of the entorhinal cortex but also directly from layer III and V of similar regions in the entorhinal cortex and are hypothesized as the central relay station of hippocampal processing (adapted from Collingridge G, MRC laboratory, Bristol).

The observation of preserved connections in thin, electrophysiological slices was the basis of the *lamellar hypothesis* for the anatomical organization of the hippocampus (Andersen et al., 1971). It proposes a functionally independent operation of a series of parallel stripes and hence, hippocampal processing predominately via the 'trisynaptic loop' in the transversal plane.

However, in the last decade, more insight was gained on additional intrinsic connection in the longitudinal axis of the hippocampus connecting the transverse planes of the trisynaptic loops. For example, DG granule and CA3 pyramidal cells have extensive associational fibers projecting widely in the longitudinal direction (Swanson et al., 1978). These recurrent and distributed sites along the dorso-ventral axis of the hippocampal formation could become associated during spatial learning (McNaughton and Morris, 1987; Hasselmo et al., 1995). In addition, neurons in the hippocampus receive input from commissural afferents from the contra lateral hippocampus. Therefore, it is most reasonable to consider the hippocampus as a three-dimensional subcortical structure with important informational processing taking place in both the transverse and longitudinal axis (Amaral and Witter, 1989).

Originally indicated by Tolman (1948) and hypothesized by O´Keefe and Dostrovsky (1971) with the discovery of hippocampal place cells, the whole hippocampus is thought to generate a cognitive map of the environment that aids the animal to navigate flexibly. Place cells fire whenever the animal is in a particular location of the environment. Interestingly, spatially-related firing cells (place, grid and head-direction cells) were discovered throughout the hippocampal formation, including the entorhinal cortex (Quirk et al., 1992; Fyhn et al., 2004; Hafting et al., 2005; Sargolini et al., 2006), the presubiculum (Cacucci et al., 2004), the postsubiculum (Sharp, 1996), the parasubiculum (Taube et al., 1995; Cacucci et al., 2004) and the subiculum (Sharp and Green, 1994). These findings supported the view

of the hippocampal formation as 'whole structure' with the hippocampus in its central position.

1.3.3. Behavioral studies of hippocampal lesion and drug infusion in rodents

Hippocampal lesion and drug infusion studies in rodents are studied as models for human amnesic syndromes. Behavioral analysis in rodents included various spontaneous (e.g. spatial open-field, Save and Poucet, 1992), associative (e.g. Pavlovian fear conditioning, plus maze, reviewed in Bannerman et al., 2004) and cognitive forms of spatial and non-spatial behavior (t-maze, Morris watermaze, differential reinforcement of low rates of responding (DRL) task; reviewed in Bannerman et al., 1999; 2004). Most prominent in comparison to memory deficits in human patients suffering from anterograde amnesia, rodents are studied mainly in two spatial types of cognitive learning and memory: *spatial reference memory* - where the relationship between a goal and the environment is consistent throughout the trials (*matching-to-place paradigm*, MTP; Morris et al., 1982); and the *spatial working memory* - where the relationship between the goal and the environment in a first, sample run has to be stored flexibility and remembered for successful performance in the subsequent choice run after a certain delay. Thereby, the relationship between spatial cues and goal changes on a trail-to-trail basis (*delayed non-matching-to-place paradigm,* DNMTP, Rawlins and Olton, 1982)[5]. Spatial working and reference memory were tested in various behavioral tasks with different complexity like the elevated T-maze, Y-maze, radial maze, watermaze (reviewed in Bannerman et al., 2004; Reisel et al., 2002; Deacon et al., 2002) that use sweet milk as reward (*appetitive*) or water as motivation to escape onto a hidden platform (*aversive*).

With improvement of lesion techniques by e.g. fiber-sparing *ibotenic acid* (IBO, a kainate acid derivate extracted from mushroom *Amanita muscaria*), discrete lesions of certain parts of the hippocampus were performed to elucidate function of those areas (Jarrad et al., 1989). Behavioral experiments have shown that both aspiration and IBO lesions of dorsal and ventral parts of the hippocampus have different effects

---

[5] Notably, many researchers, in particular working with primates, often use the term *working memory* for a short-term, on-line memory supported by frontal lobe structures (Goldman-Rakic, 1987) in contrast to the flexible memory system dependent on the hippocampal formation.

(Moser et al., 1993, 1995). Dorsal hippocampal lesions in rats disrupted the learning of appetitive and aversive spatial memory tasks (elevated T-maze, six-arm radial maze and watermaze; Bannerman et al., 1999, 2002; Pothuizen et al., 2004). These animals performed at a level resembling complete hippocampal lesions (Olton and Papas, 1979; Rawlins and Olton, 1982; Morris et al., 1982; reviewed in Bannerman et al., 2004). Yet, ventral lesions showed no effect on performance in these tasks (Bannerman et al., 2004). These findings suggested that the dorsal hippocampus has a greater role in spatial learning and memory than the ventral portion.

The ventral hippocampus however has been implicated in some spatial learning tasks (Frebinteanu and McDonald, 2001; de Hoz et al., 2003), indicating that the ventral hippocampus contributes at least under certain conditions to the learning of spatial reference memory tasks. Moser and Moser (1998) found that small hippocampal lesions disrupted retrieval of a previously learned spatial reference memory task in a retention test. But these lesions did not affect the learning or retrieval of a new task post-operatively. These data suggested that spatial memory was encoded, stored and retrieved in the hippocampus-wide network and that disruption of this network by a lesion affects retrieval of previously learned tasks. However, new tasks were encoded and stored in the available network, they were retrieved effectively as without disruption (Moser and Moser 1998).

The ventral hippocampus might be involved in the processing of information during fear conditioning. Reduced levels of freezing were observed in the contextual conditioning task (Richmond et al. 1999). Discrete lesions to the ventral portion of the hippocampus resulted in attenuated responses in the conditioned freezing task but normal levels of learning in the watermaze task (Richmond et al., 1999). It was concluded that the connection between the ventral portion of the hippocampus and the amygdala is involved in anxiety-related behaviors (Bannerman et al., 2003, 2004). Discrete lesion studies suggested that the ventral and dorsal hippocampus support separate learning and memory systems of spatial behaviors, but are not mutually exclusive in function.

Techniques that prevent LTP by NMDA receptor blockage showed similar, although not identical, results as hippocampal lesion studies. Using the NMDA receptor antagonist 2-Amino-5-phosphonopentanoic acid (AP5), Morris et al. (1986) found spatial reference learning in the watermaze was disrupted by blockage of LTP. The rats failed to learn to locate the submerged platform, in a similar manner as rats

with hippocampal lesions, indicating that LTP may be a crucial factor in spatial learning. Bannerman et al. (1995) found that blocking NMDA receptors did not completely disrupt spatial reference learning in the watermaze, however. Saucier and Cain (1995) also found that pharmacological blockage of NMDA receptor activity blocked dentate gyrus LTP but had no effect in spatial learning. These results were both attributed to the pre-training, the animals had received prior to treatment and testing. It was hypothesized that hippocampal NMDA receptor-dependent synaptic plasticity is not necessary for spatial reference memory (reviewed in Bannerman et al., 2006). There is also the implication that AP5 affects sensorimotor skills, and that pre-treatment allows the animals to develop the procedural skills effectively prior to drug treatment (Bannerman et al. 2006).

However, Hippocampal-dependent spatial working memory requires NMDA receptors. Steele and Morris (1999) found impairment in watermaze performance using a delayed matching-to-place paradigm with AP5-treated rats. Their results showed that the impairment was delay-dependent and that animals, which had received pre-training on the task prior AP5 infusion, were still impaired in spatial working memory. Tonkiss and Rawlins (1991) also used AP5 and found impairment in choice accuracy and a delay-dependent impairment: a small retention interval impaired the AP5-treated animals initially but they recovered over days. However a second 20 s retention interval did impair the choice accuracy of the AP-treated animals significantly.

1.3.4. Spatial working and reference memory in *iGluR* mutant mice

Genetic engineering of the mouse genome allowed the generation of mice with selective deletion of distinct AMPA and NMDA receptor subtypes. Initially, global gene knock-out (KO) mice of distinct AMPA and NMDA receptor subtypes were generated to investigate the overall role of certain glutamate receptors in the mouse brain.

Behavioral testing of *GluR-A$^{-/-}$* mice was performed in a variety of hippocampus-dependent tasks. First of all, adult *GluR-A$^{-/-}$* mice were found to be normal with respect to most behavioral patterns (Bannerman et al., 2004). Despite the lack of CA3-CA1 LTP, the *GluR-A$^{-/-}$* mice exhibited normal spatial reference memory performance in the Morris water maze and Y-maze tasks (Schmitt et al., 2004;

Schmitt et al., 2003; Zamanillo et al., 1999). Nevertheless, *GluR-A$^{-/-}$* mice showed specific and profound spatial working memory impairment, as tested on the T-maze alternation task and six-arm radial maze (Reisel et al., 2002; Schmitt et al., 2003). Importantly, both LTP and spatial working memory was partially restored by transgenic expression of GluR-A in the forebrain, providing direct evidence that GluR-A-containing AMPA receptors are critical for spatial working memory (Mack et al., 2001; Schmitt et al., 2005).
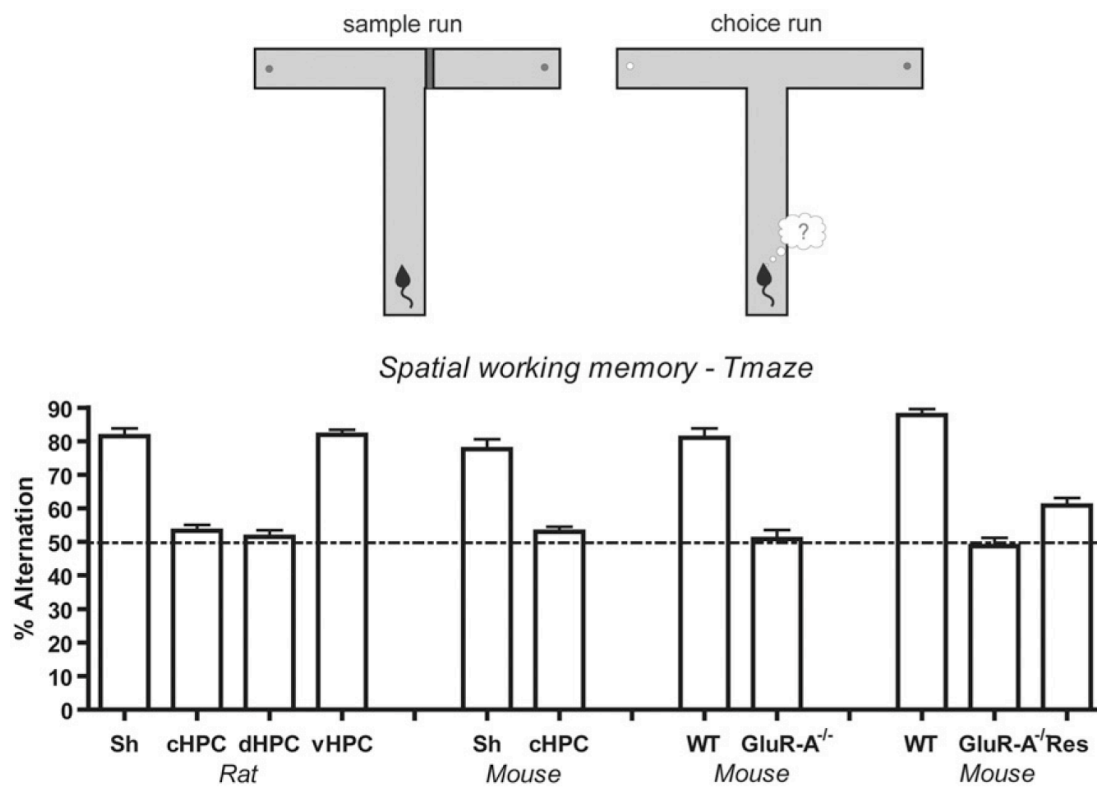
Fig 1.7. Hippocampal lesions and GluR-A deletion both impair spatial working memory performance during the DNMTP task on the elevated T-maze (*rewarded alternation*).
Top: The mouse is forced into either the left or right goal arm, according to a pseudorandom sequence, and receives a milk reward. During the choice run (right) the mouse has to go directly to the opposite (previously unvisited) goal arm to find a second milk reward. Both runs are delayed by the standard inter run interval (IRI) of 15 seconds. 40 trials in total on 5 successive days were performed. **Bottom:** Mean percentage of trials on which the mouse alternated successfully (± SEM). *Left:* Performance of sham, complete (cHPC), dorsal (dHPC) and ventral (vHPC) lesioned rats (data taken from Bannerman et al., 2002). *Center left:* performance of sham and complete (cHPC) hippocampal-lesioned mice. *Center right*: performance of wild-type and GluR-A$^{-/-}$ mice (data taken from Reisel et al., 2002). *Right:* Performance of wild-type (WT), *GluR-A$^{-/-}$* mice and GFP-labeled GluR-A rescued GluR-A$^{-/-}$ mice (data taken from Schmitt et al. 2005). Broken line equates to chance performance of 50% (adapted from Sanderson et al., 2008).

However, global KO mice had certain drawbacks. For example, global $NR1^{-/-}$ mice displayed a lethal phenotype. These mice died around birth from respiratory failure (Forrest et al., 1994). Global $GluR\text{-}B^{-/-}$ mice had poor motor coordination, exhibited low explorative activity, and did not breed (Jia et al., 1996; Shimshek et al., 2005). However, $GluR\text{-}A^{-/-}$ mice displayed only a slight hyperactivity but otherwise appeared normal (Bannerman et al., 2004). With improvement of transgenic techniques (*pronucleus injection*, use of spatially- and temporally-restricted promoters and induction systems), more selective mouse models with gene inactivation of distinct receptor subtypes were generated to test animals in adulthood and to avoid compensatory and developmental effects.

Forebrain principal neuron-specific inactivation of the GluR-B gene in $Gria2^{\Delta Fb}$ (Shimshek et al., 2006) was generated by transgenic expression of the Cre recombinase driven by a 3.5kb αCaMKII promoter fragment in the homozygous background of floxed $Gria2^{loxP/loxP}$ mice. The GluR-B mutant mice displayed both, impairment in spatial working memory on the elevated T-maze and in spatial reference memory tested on the elevated Y-maze. However, the strong GluR-B lacking AMPA receptor-mediated Ca^{2+} influx evoked long-lasting changes in the hippocampal circuitry, either direct (moderate mossy fiber sprouting in DG; loss of CA3 neurons) or indirect (loss of parvalbumin-positive interneurons in DG; reduced neurogenesis). Therefore, behavioral deficits in spatial memory might be due to developmental, second-order failures rather than changes in synaptic neurotransmission (Sprengel et al., 2006).

Arguably the most discussed mutant mouse model of hippocampal processing features the CA1-restricted deletion of the NR1 gene (Tsien et al., 1996). These CA1-KO mice were severely impaired in the acquisition of spatial reference memory in the Morris watermaze. By contrast, AP5 infusion in the dorsal hippocampus did not produce this impairment (Bannerman et al., 1995), and even the effect in dorsally lesioned rats was weaker than in CA1-KO mice (Bannerman et al., 1999). Notably, AP5-infused mice received pre-training prior to treatment and testing, that CA1-KO mice did not receive. Furthermore, CA1-KO mice also showed evidence of a mild and transient deficit in a visible platform version of the watermaze task. A later study (Fukaya et al., 2003) investigated the age-dependent gene manipulation in these mutants. In the brains of one-month-old mutants, the levels of NR1 mRNA were

significantly reduced in CA1 and subiculum. At two months of age, however, the reduction of NR1 mRNA was further decreased in these areas but reduction was also observed in other brain areas, most conspicuously in the deep layers of the neocortex. At later age (2-4 months), the NR1 knock-out extended to other telencephalic structures (e.g. CA3, DG). Therefore, it was speculated that the strong effect in acquisition to find the hidden platform and the mild and transient deficit in the visible platform version may be due, at least partially, to the nature of the mutation, which spread to the cortex with age. Hence, the contribution of a cortical NR1 deletion cannot be excluded.
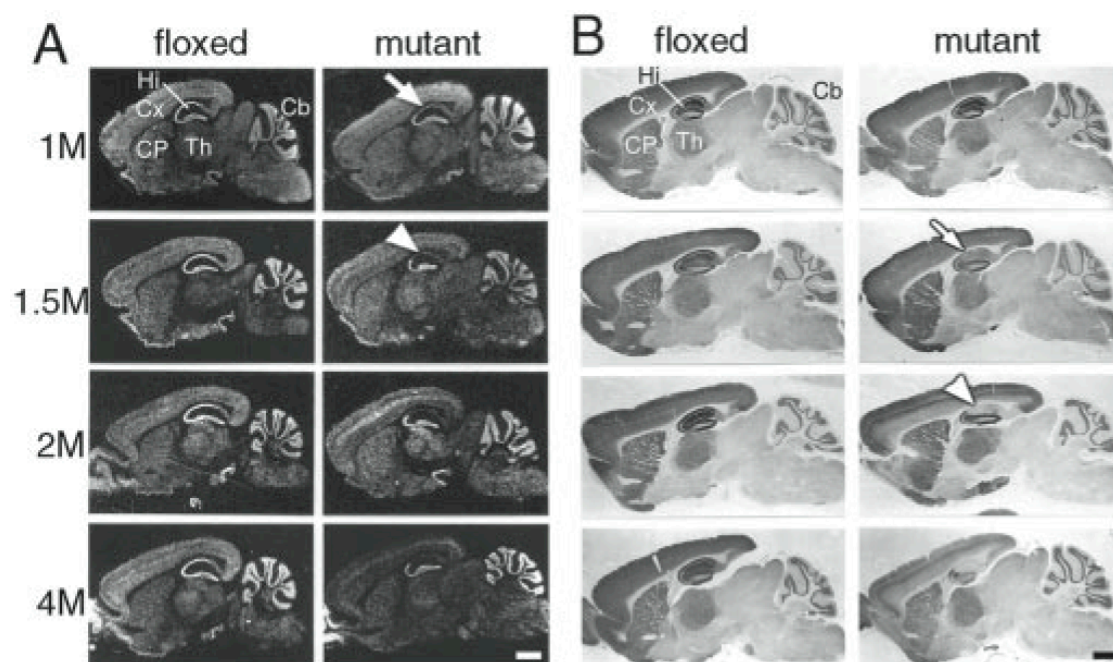
Fig 1.8. Age-dependent depletion of the NR1 subunit in the CA1-NR1 KO mice (Tsien et al., 1996)

(A) *In situ*-hybridization with antisense NR1 probe. **(B)** Immunoperoxidase stainings against the principal NMDA receptor subunit NR1. Pairs of control (floxed) and mutant mouse brains at different ages (1, 1.5, 2 and 4 months) are depicted. Arrows and arrowheads indicate the hippocampal CA1 region at stages when NR1 reduction is first observed or reaches the lowest level, respectively. Cb, cerebellum; CP, caudate putamen; Cx, cortex; Hi, hippocampus; Th, thalamus. Scale bars, 1 mm (adapted from Fukaya et al., 2003).

Deletion of the NR1 subunit in CA3 (Nakazawa et al., 2002) allowed normal Morris watermaze performance under training conditions. Yet, with the removal of the spatial guiding cues, the animals revealed a clear deficit in the same task. It was hypothesized that NMDA receptors in CA3 are important for pattern completion. The

mutant mice were unable to form a representation of the environment to solve the maze when some of the cues were absent. In a later study, these CA3-NR1 mutant mice exhibited impaired spatial working memory in a delayed matching-to-place watermaze task (Nakazawa et al., 2003).

NMDA receptor mutant mice with NR1 deletion in the DG showed a spatial working memory deficit on a radial maze task, but intact spatial reference memory on the same maze (Niewoehner et al., 2007). McHugh et al. (2007) found that mice having NR1 deleted in the DG showed normal spatial reference memory performance in the watermaze and acquired and retained a contextual fear-conditioning task. These animals did, however, show a transient, significant deficit when required to distinguish between two slightly different contexts in the fear-conditioning task. It has been proposed that this deficit reflects the role of NMDA receptors of the DG in pattern separation. However, one should note, that 'classical' pattern separation in spatial behavior was not observed by Niewoehner et al. (2007) or McHugh et al. (2007) and that the applied electric foot shock in the contextual fear conditioning paradigm was relatively high and the training relatively long (0.75 mA on day 1; 0.65 mA on days 2-17).

Taken together, gene activation of prominent AMPA and NMDA receptors in the hippocampus of transgenic mice demonstrated the important role of excitatory glutamatergic neurotransmission in different spatial forms of cognitive memory. It has been hypothesized that spatial working memory is dependent on GluR-A containing AMPA and NMDA receptors (delay- and task-dependent), whereas spatial reference memory is only dependent on NMDA receptors (at least to some extent). The exact role of GluR-B containing AMPA receptors in spatial behavior could not be addressed properly since GluR-B depletion evoked an altered hippocampal circuitry.

1.4. Aim of thesis

The primary objective of this work is to contribute to the understanding how the main excitatory glutamate receptors (AMPA that contain the GluR-A or GluR-B subunit and NMDA receptors) in restricted sublayers of the hippocampal formation of adult mice are involved in distinct spatial forms of cognitive memory. The Ph.D. thesis is composed of three parts:

1. Generation and evaluation of a selective model system that allows for restricted recombination of floxed target genes in prominent sublayers of the hippocampus. Transgenic targeting should include at least the CA1 pyramidal cells of the hippocampal formation and has to be as little invasive as possible (no surgery). In addition, gene manipulation should not be effective in early postnatal or pubertal ages but has to remain stable until at least 10-12 months to assess extensive behavioral analysis in adult mice.

2. Use of the established, selective genetic model system to generate three conditional mutant mouse models in parallel, each deficient in one of the three main iGluR subunits GluR-A, GluR-B and NR1 in the hippocampal formation.

3. Analysis of these three adult *iGluR* mutant mouse models in various spatial forms of cognitive behavior.

1.4.1 Induction of transgenic gene expression in restricted sublayers of the hippocampal formation and the olfactory cortex in $Tg^{CN12-itTA}$ mice

The most important step in the Ph.D. thesis is the genetic approach to manipulate the endogenous genes for GluR-A (*Gria1*), GluR-B (*Gria2*) or the principal NR1 subunit (*Grin1*). In order to investigate the role of functionally dissected glutamatergic neurotransmission in cognitive memory in the adult mouse, specific and stable transgenic targeting of principal cell layers in the hippocampal formation is required. In addition, the genetic system should be temporally controlled but any traumatic event (e.g. surgery) should be avoided.

Jinhyun Kim, a previous member of our lab, generated two transgenic founder mouse lines, $Tg^{CN10-itTA}$ and $Tg^{CN12-itTA}$, in her Ph.D. thesis (Ruprecht-Karls-Universität, Heidelberg, 2001) that might fulfill these requirements. The *pronucleus-injected* CN construct contains an improved version of the tetracycline-dependent transactivator (itTA; Shimshek et al., 2002) under the control of a chimeric, so called αCaMKII-NRSE promoter to allow for the temporal control of gene manipulation, specifically in forebrain principal neurons.

Temporal control of transgenic gene expression can be achieved by use of the tTA system in mammalian cells (Gossen and Bujard, 1992). This binary system is based on the prokaryotic Tn10 tetracycline resistance operon of *Escherichia (E.) coli*

and makes use of its *repressor* protein (tetR) and the tetR-binding *operator* sequence (tetO). Usually, tetR binds to the tetO sequence and blocks downstream transcription. However, tetR is released and transcription is unblocked by presence of tetracycline that binds to tetR with high affinity, changes its conformation and thereby induces transcription of proteins for its own export (*tetracycline resistance*).

In the tTA system (Gossen and Bujard, 1992), the tetR protein is combined with an activation domain of the virion protein (VP) 16 of the *herpes simplex virus* in the tTA fusion protein to induce transgenic transcription from a minimal promoter composed of adjacent tetO (usually five or seven; $TetO_5$, $TetO_7$) and promoter sequences of the *human cytomegalovirus* (hCMV). Furthermore, flanking the seven-tetO target sequences with two minimal promoters (bi-directional P_{tetBi}) allows the co-regulation of two transgenes at the same time (Baron et al., 1995; Krestel et al., 2001). Transactivation of P_{tetBi}-controlled genes can be blocked with tetracycline derivates like doxycycline that can be administered via the drinking water (usually 50mg/l dox). By modification of the prokaryotic tTA sequence according the mammalian codon usage and replacement of the VP16 domain (high *quenching* of cellular transcription factors) by three minimal F domains (Baron, Gossen and Bujard, 1997) the improved version of tTA, termed itTA, was developed (J. Kim, Ph.D. thesis, Ruprecht-Karls-Universität, Heidelberg, 2001).
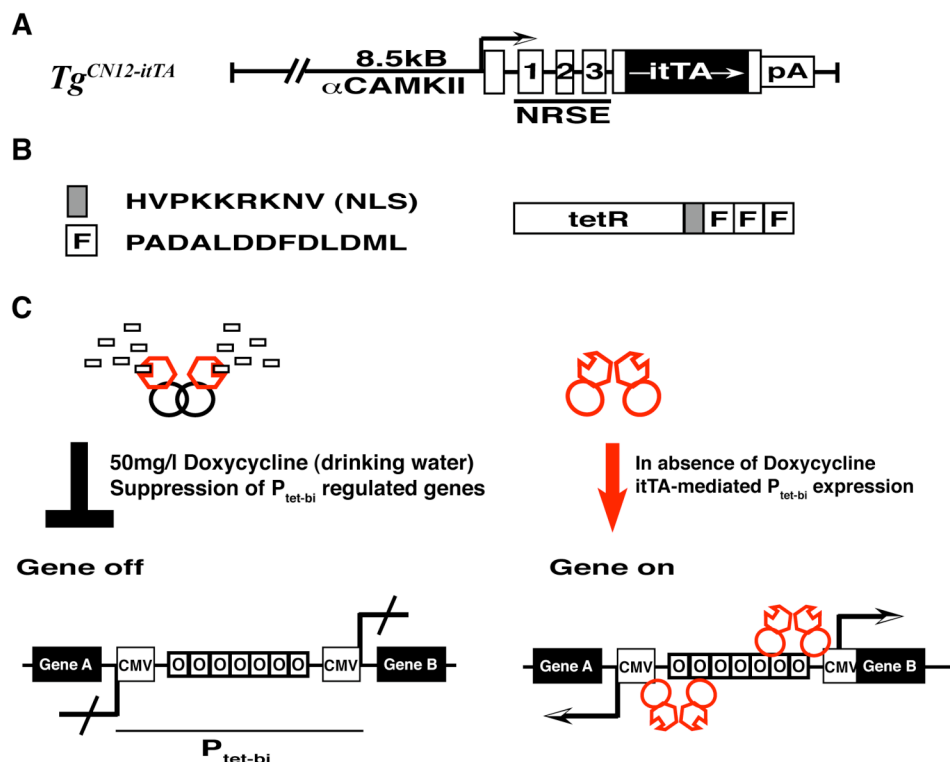
Fig. 1.9. Temporal control of transgenic activity using the tet-system

(A) Schematic construct of the 8.5kb αCaMKII promoter, neuron-restrictive silencing element (NRSE) of the NR2C gene, itTA minigene used for pronucleus injection to generate $Tg^{CN12\text{-}itTA}$ mice. **(B)** Representation of domains in the transgenic itTA fusion protein. The 207 amino acid (aa) repressor of the Tn10 tetracycline (tet) operon of *E. coli* (tetR) is fused C-terminally to the 9 aa nuclear location sequence (NLS, gray box) and three minimal activation domains of VP16 (F domains, 13 aa each). Numbers indicate position of amino acids (aa) and capital letters are single letter aa. **(C)** Schematic outline of the itTA regulatory activity (tTA system). ItTA fusion protein (red circle and open hexagon) forms dimers, which elicit transactivation activity in absence of tetracycline or its derivates. ItTA binds to an array of seven tet operator sequences (TetO7, O in open box) flanked by minimal CMV promoter (bidirectional P_{tetO7}; $P_{tet\text{-}Bi}$), recruit other endogenous transcription factors and enable $P_{tet\text{-}Bi}$ promoter activity (right panel). In presence of 50 mg/l Doxycycline (Dox, black, open box) in the drinking water of transgenic mice itTA undergoes conformational change whereby losing its DNA-binding ability (black circle). Hence, transgenic expression of $P_{tet\text{-}Bi}$ regulated genes can be suppressed efficiently (left panel).

The forebrain-specific αCaMKII promoter has been widely used to direct forebrain-specific expression of the tTA (Mayford et al., 1996); rtTA (Malleret et al., 2001; Mansuy et al., 1998), Cre recombinase (Minichiello et al., 1999; Mantamadiotis et al., 2002) and many other transgenic proteins. To further restrict transgenic itTA expression in $Tg^{CN12\text{-}itTA}$ mice, the chimeric promoter in the CN minigene was composed of the 8.5 kb αCaMKII promoter fragment, followed by the tripartite leader sequence of the *adenovirus* known to enhance mRNA stability and translation efficiency (Choi et al., 1991; Sheay et al., 1993), and the 1.0 kb untranslated fragment (exons 1-3) of mouse NMDA receptor subunit NR2C which contains a neuron-restrictive silencer element (NRSE)-like sequence. The chimeric αCaMKII-NRSE promoter was thought to suppress transcription selectively in low αCaMKII-expressing principal neurons in the forebrain and to permit a more restricted transgenic expression as observed in previous αCaMKII-driven transgenes.

Indeed, transgenic itTA expression under this αCaMKII-NRSE promoter in both founder lines, $Tg^{CN10\text{-}itTA}$ and $Tg^{CN12\text{-}itTA}$, induces tissue-restricted expression of transgenic responder elements. $Tg^{CN10\text{-}itTA}$ was used to drive Cre recombinase from Tg^{LC1} (Schoenig et al., 2002) and delete the NR1 subunit selectively in the DG (Niewoehner et al., 2007). But even more suitable for this Ph.D. thesis, $Tg^{CN12\text{-}itTA}$-induced expression from the bidirectional responder element in Tg^{OCN1}, encoding β-galactosidase and GFP-tagged GluR-B protein, was restricted to DG and CA1 of the

hippocampus and piriform cortex (PC) of the olfactory system. Expressed in genetic background of forebrain-specific GluR-B deletion in *Gria2^AFb* mice, the combination of *Tg^CN12-itTA* / *Tg^OCN1* mice was able to rescue partially the previously observed GluR-B dependent olfactory memory deficit of simple odor discrimination, presumably by transgenic GluR-B restoration in the central part of the primary olfactory cortex (PC). Unfortunately, spatial behavior was not analyzed in these *GluR-B^Rescue* mice (Shimshek et al., 2005).
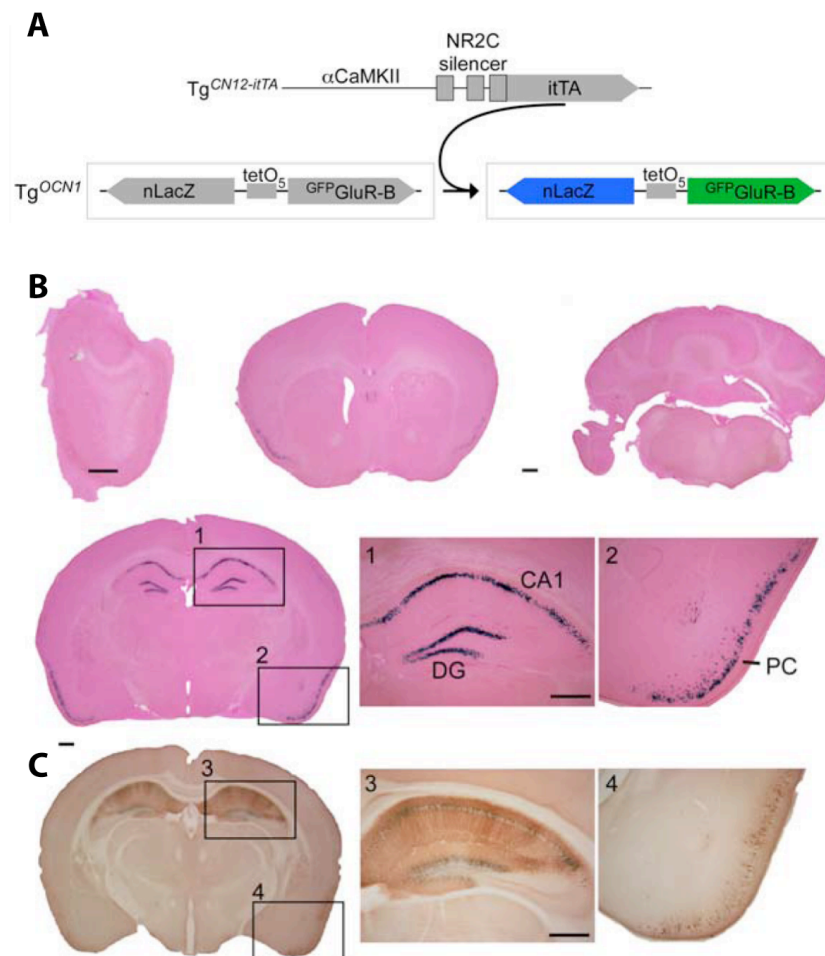
Fig. 1.10. Specific expression of transgenic ^GFP GluR-B in hippocampus and piriform cortex
(A) Diagram depicting itTA-dependent expression of nucleus-localized β-Galactosidase (nLacZ) and GFP-tagged GluR-B in *Tg^CN12-itTA* / *Tg^OCN* mice. **(B)** In coronal sections of *Tg^CN12-itTA* / *Tg^OCN* mice, β-galactosidase activity (blue, X-gal, counterstained with eosin) is restricted to hippocampal neurons in CA1, DG and neurons in the piriform cortex. The same brain regions show GFP-GluR-B expression when adjacent sections were stained with an antibody against GFP. Scale bars 500 μm (adapted from Shimshek et al., 2005).

2. Results

2.1. Generation and evaluation of the $Tg^{CN12\text{-}itTA}$ / Tg^{LC1}-driven, conditional KO mouse model

In a previous study, we used transgenic itTA expressed by a chimeric αCaMKII-NRSE promoter in the $Tg^{CN12\text{-}itTA}$ mouse model to induce transgenic GFP-tagged GluR-B and β-gal expression from the bidirectional tet-responder element (P_{tetBi}) in Tg^{OCN} mice specifically in sublayers of the hippocampal formation (DG, CA1, CA2) and the olfactory cortex (PC) (Shimshek *et al.* 2005). To engage the restricted itTA-dependent transactivation for generation of conditional gene knock out (cKO) via the Cre/loxP system, $Tg^{CN12\text{-}itTA}$ mice were bred with transgenic Tg^{LC1} mice (Schoenig *et al.* 2002) that expressed Cre recombinase and luciferase (luci) from the transgenic P_{tetBi} minimal promoter upon induction by itTA. The combination of itTA-system and Cre/loxP recombination allowed the temporal control of irreversible gene manipulations in cKOs by application of dox via the drinking water. Binding of dox changed the itTA conformation along with its DNA-binding ability to tet-responder elements (as P_{tetBi}) and thus, prevented the itTA-dependent irreversible recombination of loxP-flanked target genes.

Sensitive monitoring of accumulated Cre/loxP recombination events during the animal's life was achieved by the use of gene-targeted *Rosa26R* mice (Soriano *et al.* 1999). The ubiquitously expressed *Rosa26* locus was modified by insertion of a gene construct that contains a loxP-flanked transcriptional stop cassette upstream of the β-gal coding sequence. Thereby, even transient Cre expression that mediated recombination was detected. The irreversible recombination of the modified *Rosa26R* locus induced constitutive β-gal expression until the animal is death.

2.1.1. Adult, sublayer-specific recombination by embryonic Cre suppression

To assess the accumulated maximal recombination potential[6] of $Tg^{CN12-itTA}$ / Tg^{LC1}-mediated recombination, coronal sections of dox-naive $Tg^{CN12-itTA}$ / Tg^{LC1} / $Rosa26R$ mice were analyzed by X-gal staining at postnatal day 45 (P45). The sensitive approach utilizes the β-gal enzymatic activity to convert colorless X-gal to a blue precipitate. Surprisingly, positive X-gal signals accumulated in a much more widespread manner in the forebrain of $Tg^{CN12-itTA}$ / Tg^{LC1} / $Rosa26R$ mice than expected from the X-gal pattern of $GluR-B^{Rescue}$ mice that used $Tg^{CN12-itTA}$ to induce β-Galactosidase from the Tg^{OCN1} responder element (Shimshek et al., 2005; please refer to 1.4.1.). Next to X-gal signals in the piriform cortex (PC) as well as CA1/2 and dentate gyrus (DG) of the hippocampal formation, the olfactory bulb (OB, data not shown), caudate putamen (CPu), amygdala (Amy), hypothalamus and septum appeared intensively blue, and even cortical areas showed elaborate X-gal staining. Unexpected recombination was presumably induced from transient itTA expression in late embryonic or early postnatal days. The nuclear Cre protein (temporal recombination potential) was not detected in adjacent slices. In fact, positive Cre signals (visualized as brown dots with diameters of 2-6 µm) at P45 were observed only in PC, OB, CA1/2, DG, CPu, around lateral ventricles and very sparsely in cortical areas.

These results indicated that the exclusion of transgenic activity at early ages might reveal the sublayer-restricted recombination, as expected from previous work using $Tg^{CN12-itTA}$-driven transgenes (Krestel *et al.* 2004, Shimshek *et al.* 2005). Therefore, we applied 50 mg/l dox in the drinking water during breeding of $Tg^{CN12-itTA}$ / Tg^{LC1} / $Rosa26R$ mice and removed dox from the drinking water of the mothers when offspring was born. Triple positive animals (termed $Rosa26R^{ΔHipOlf}$ mice) were analyzed for X-gal activity and Cre immunostaining at P45. And indeed, we observed the expected recombination potential in restricted sublayers of the hippocampal formation (CA1/2, DG) and the olfactory cortex (PC) in both stainings of

---

[6]Maximal recombination potential represents the accumulated efficiency of itTA-induced Cre activity to recombine the single allele in heterozygous *Rosa26R* mice. In functional cKO mouse models, one needs to consider that two alleles have to be recombined and that the endogenous loci might show different accessibility in certain brain areas.

Rosa26R$^{\Delta HipOlf}$ mice. Very sparse labeling was observed in posterior CPu, Amy and cortical areas.

Slow induction of P$_{\text{tet-bi}}$-regulated gene expression in the brain after suppression in the mouse embryo has been described previously (Krestel *et al.* 2004). To evaluate the first time point of P$_{\text{tet-bi}}$-induction in *Rosa26R*$^{\Delta HipOlf}$ mice, we analyzed animals by enhanced Cre immunostaining at two (P14), three (P21) and four (P28) weeks of age. We isolated the offspring from their mothers at birth and nursed them by dox-naive NMRI foster mothers to exclude further dox exposure. Cre recombinase protein is first detected in four-week-old *Rosa26R*$^{\Delta HipOlf}$ mice. Dense brown signals in the dentate gyrus (DG) and looser pattern in CA1/2 of the hippocampal formation were observed as well as single positive signals in PC and CPu. Cre suppression in the mouse embryo together with the slow P$_{\text{tet-Bi}}$ initiation in the *Tg*$^{CN12\text{-}itTA}$ / *Tg*^{LC1} model allowed the generation of conditional gene knock-outs (cKOs) in well-established neuronal networks of adult mouse brains.
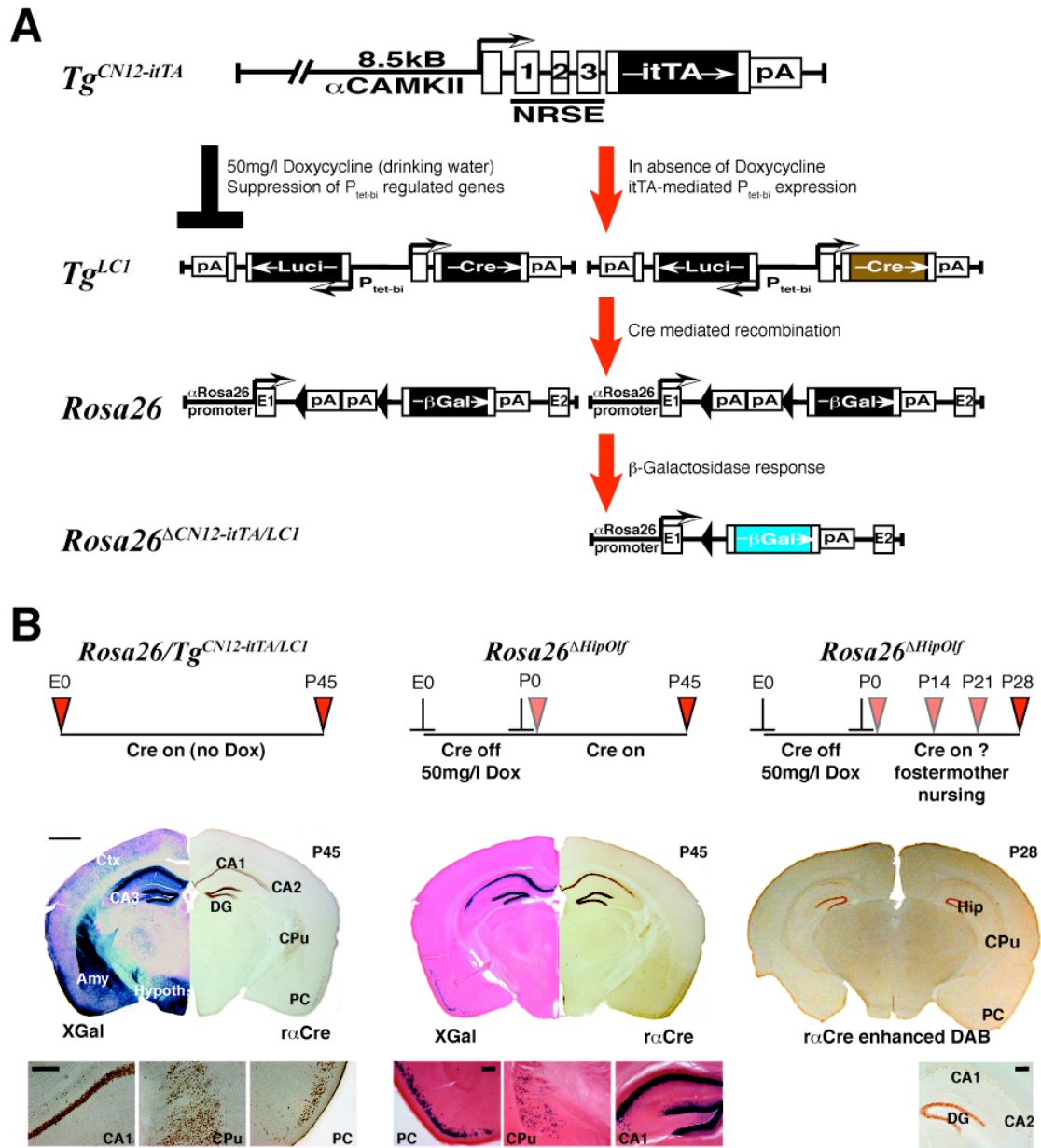
Fig. 2.1.1 Sublayer-restricted recombination in $Tg^{CN12-itTA}$ / Tg^{LC1} / $Rosa26R$ mice (P45) by Cre suppression in the mouse embryo (now called $Rosa26^{\Delta HipOlf}$ mice)

(A) Genetic elements and temporal regulation of mouse models used to establish sublayer-restricted recombination by $Tg^{CN12-itTA}$-induced Cre expression. Luci, luciferase; pA, polyadenylation signal; pApA, floxed transcriptional stop cassette **(B)** Evaluation of maximal (X-gal, left hemisphere) and temporal (rαCre, right hemisphere) $Tg^{CN12-itTA}$ / Tg^{LC1}-mediated recombination potential in absence of dox (left panel) and by Cre suppression in the mouse embryo (middle panel, 50mg/l dox until birth). Postulated initiation time point of $Tg^{CN12-itTA}$-induced transactivation was investigated by nursing $Rosa26^{\Delta HipOlf}$ offspring from dox-naive foster mothers and detection using enhanced Cre immunostaining. Ctx, cortex; Amy, amygdala, Hypo, hypothalamus Scale bar, overviews, 1 mm; higher magnifications, 100 µm.

2.1.2. Stability of sublayer-restricted recombination in *Rosa26R$^{\Delta HipOlf}$* mice during behavioral testing

Using conditional recombination systems to generate cKOs requires transgenic specificity at early time points as well as stability of the system during the time of analysis. In particular, temporally controlled gene manipulation at an age when the functional gene product already exists, requires a critical time period before the manifestation of functional consequences. The duration of protein depletion depends on expression levels and specific turnover rate of the protein of interest. In addition, analysis of behavioral consequences usually involves handling time and long lasting test protocols. Hence, gene manipulation of excitatory glutamate receptors in restricted hippocampal sublayers of adult mice and analysis of the behavioral impact requires a recombination system with extraordinary stability of transgenic activity for at least several months.

To evaluate the stability of sublayer-restricted recombination in *Rosa26R$^{\Delta HipOlf}$* mice, we analyzed the accumulated maximal recombination efficiency in animals at several ages (P150, P180, P240, data not shown) until the very end of behavioral analysis (P365, fig. 2.1.3). β-gal expression upon recombination was not confined to the nucleus in *Rosa26R* mice (Soriano *et al.* 1999) but precipitated within the entire cell shape of recombined neurons in *Rosa26R$^{\Delta HipOlf}$* mice at older age. X-gal signals increased with age in the recombined sublayers (CA1, CA2, DG, PC) and accumulated in basal and apical fibers. Light blue labeling was visible in dendritic and axonal processes of excitatory CA1, CA2 and DG neurons in the corresponding layers (so, stratum oriens; sr, stratum radiatum; ml, molecular layer; ff, fimbria-fornix; mf, DG mossy fibers). At P365, even hippocampal connections into the lateral part of the substantia nigra (SNL) were labeled. Compared to the highly restricted X-gal pattern at P45, *Tg$^{CN12-itTA}$* / *Tg^{LC1}*-mediated recombination in *Rosa26R$^{\Delta HipOlf}$* mice targeted additional sublayers of the hippocampal formation (IG, S) and in particular, of the olfactory system (e.g. OB, DTT, VTT, Tu) until the beginning of behavioral analysis (P150). Sparse cellular X-gal signals were also detected in the CA3 subfield and in defined layers (II and V/VI) of cortical (e.g. FrA, M1, M2, AuD) and subcortical (e.g. BLA) structures. Nevertheless, recombination was highly concentrated in restricted sublayers of the hippocampal formation and the olfactory system, and this pattern remained stable until the very end of behavioral testing at P365. To evaluate the

contribution of $Tg^{CN12\text{-}itTA}$ / Tg^{LC1}-targeted cells in their neuronal networks, we had a closer look into the accumulated X-gal pattern of $Rosa26R^{\Delta HipOlf}$ mice at P365 and performed various co-localization studies to quantify and verify the nature of recombined cells at ages of stable transgenic activity (P150-P365).

2.1.3. $Tg^{CN12\text{-}itTA}$ / Tg^{LC1}-driven recombination in the hippocampal formation

Strong recombination in the hippocampal formation of $Rosa26R^{\Delta HipOlf}$ mice at P365 was restricted to DG, CA1 and, to a lesser extent, also to CA2. As observed with other transgenes that employed the αCaMKII promoter (Krestel *et al.* 2004, Shimshek *et al.* 2005), the X-gal profile in CA1 proceeded gradually along the dorso-ventral axis, whereas it remained relative stable in DG (fig.2.5). In CA3 and CA4 hardly any recombination was observed indicating that the functional networks were not essentially affected. Recombination in the subiculum was restricted to a small region adjacent to dorsal CA1. Other regions of the subicular complex (inclusive of presubiculum, PrS and parasubiculum, PaS) remained free from transgenic activity. The main relay station of cortical information, the entorhinal cortex (Ent), exhibited sparse recombination events in specific layers of its lateral part (lEnt). Superficial pyramidal cell layer II and deeper layers V and VI showed only isolated X-gal signals. The medial area (mEnt) that is potentially more important for spatial behavior was not targeted by $Tg^{CN12\text{-}itTA}$ / Tg^{LC1}-driven recombination in $Rosa26R^{\Delta HipOlf}$ mice. Additionally to the main components of the hippocampal formation, the X-gal pattern of $Rosa26R^{\Delta HipOlf}$ mice revealed also the remnant structure of the indusium griseum (IG) that extends centered on top of the corpus callosum (cc) to the dorsal tenia tecta (DTT, fig. 2.1.5). Usually, hippocampal investigations did not refer to this structure, even though it forms a direct link to olfactory cortices.
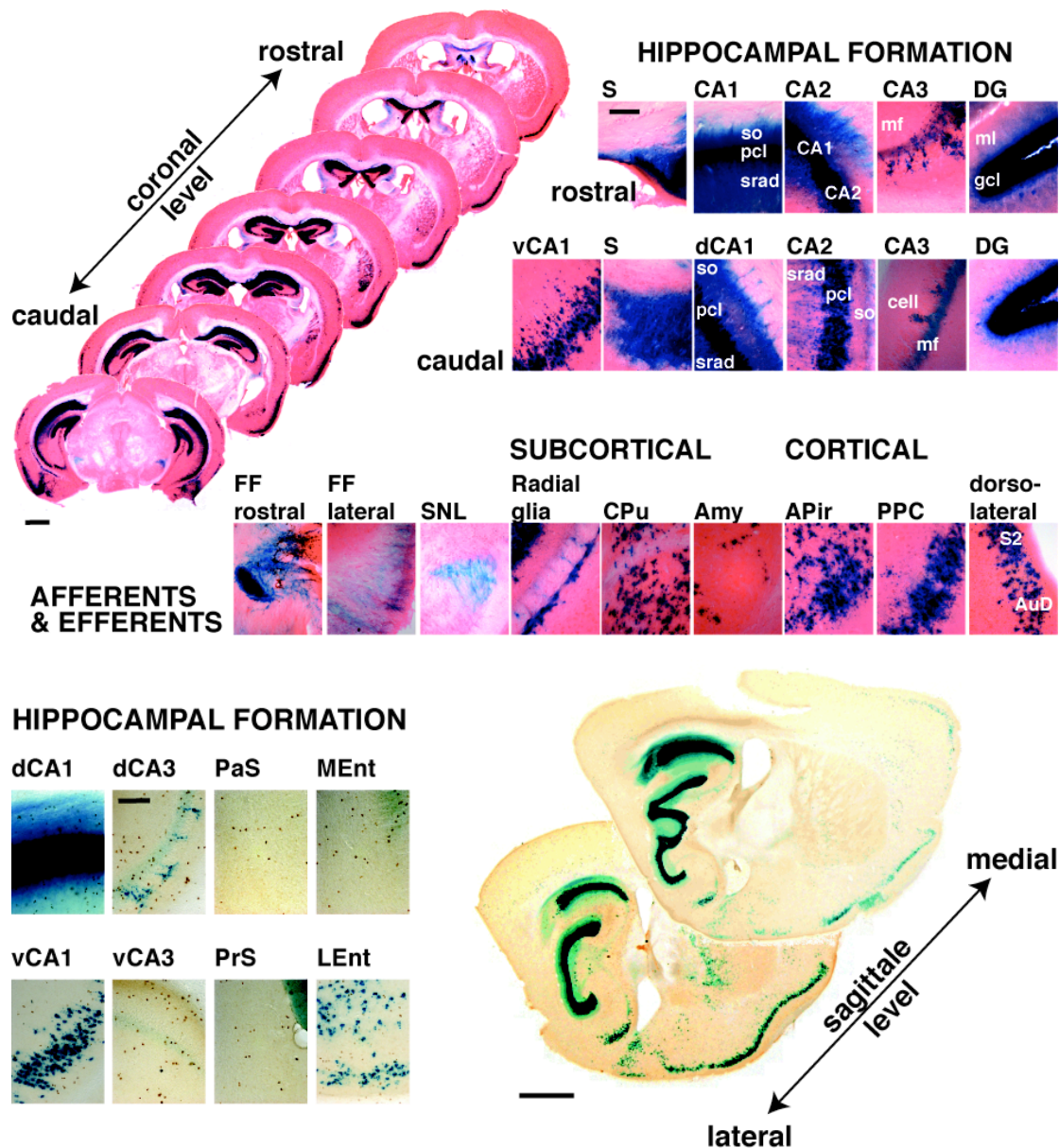
Fig. 2.1.2. Recombination in the posterior forebrain of *Rosa26R^ΔHipOlf* mice at the very end of behavioral analysis (P365)

Amy, amygdala; APir, amygdalopiriform transition area; AuD, secondary auditory cortex, dorsal area; CPu, caudate putamen; FF, fimbria-fornix; LEnt, lateral entorhinal cortex; MEnt, medial entorhinal cortex; PaS, parasubiculum; PPC, posterior piriform cortex; PrS, presubiculum; S, subiculum; S2, secondary somatosensory cortex; SNL, substantia nigra, lateral part; so, stratum oriens; pcl, pyramidal cell layer; srad, stratum radiatum; mf, DG mossy fibers. Scale bar, overviews, 1 mm; higher magnifications, 100 µm.

The accumulation of β-gal along the entire cell and the high sensitivity of X-gal staining hindered cellular resolution of recombined neurons in hippocampal sublayers. To estimate the ratio of affected neurons, double immunostainings against the

transgenic Cre protein and the neuronal nuclear marker protein (NeuN) were performed in $Rosa26R^{\Delta HipOlf}$ mice (n = 6, P 180 - P 240). By use of horizontal slices, transgenic expression ratios of dorsal and ventral regions were separated. $Tg^{CN12\text{-}itTA}$ / Tg^{LC1}-driven Cre expression was observed exclusively in NeuN-stained neurons in the hippocampal formation. As expected from the X-gal pattern in $Rosa26^{\Delta HipOlf}$ mice, high co-localization was found in the granule cell layer (gcl) of DG (97.8 ± 2.9%; mean ± SD) and in the pyramidal cell layer (pcl) of dorsal CA1 (dCA1, 85.1 ± 12.1%). However, transgenically affected neurons in the CA1 subfield did not show homogeneous co-localization throughout the three-dimensional structure. Within dCA1, Cre expression exhibited a slight anterior-posterior gradient (97.2 ± 2.5% vs. 77 ± 8.6%), but along the dorso-ventral axis it decreased substantially (medial, 53.4 ± 19.1%; ventral, 19.2 ± 9.8%). In CA2, co-labeling also decreased from its dorsal (41 ± 21%) to ventral part (19.5 ± 14.1%). All other parts of the hippocampal formation (CA3, lEnt, mEnt, Sub) feature negligible recombination (<1% co-labeling).
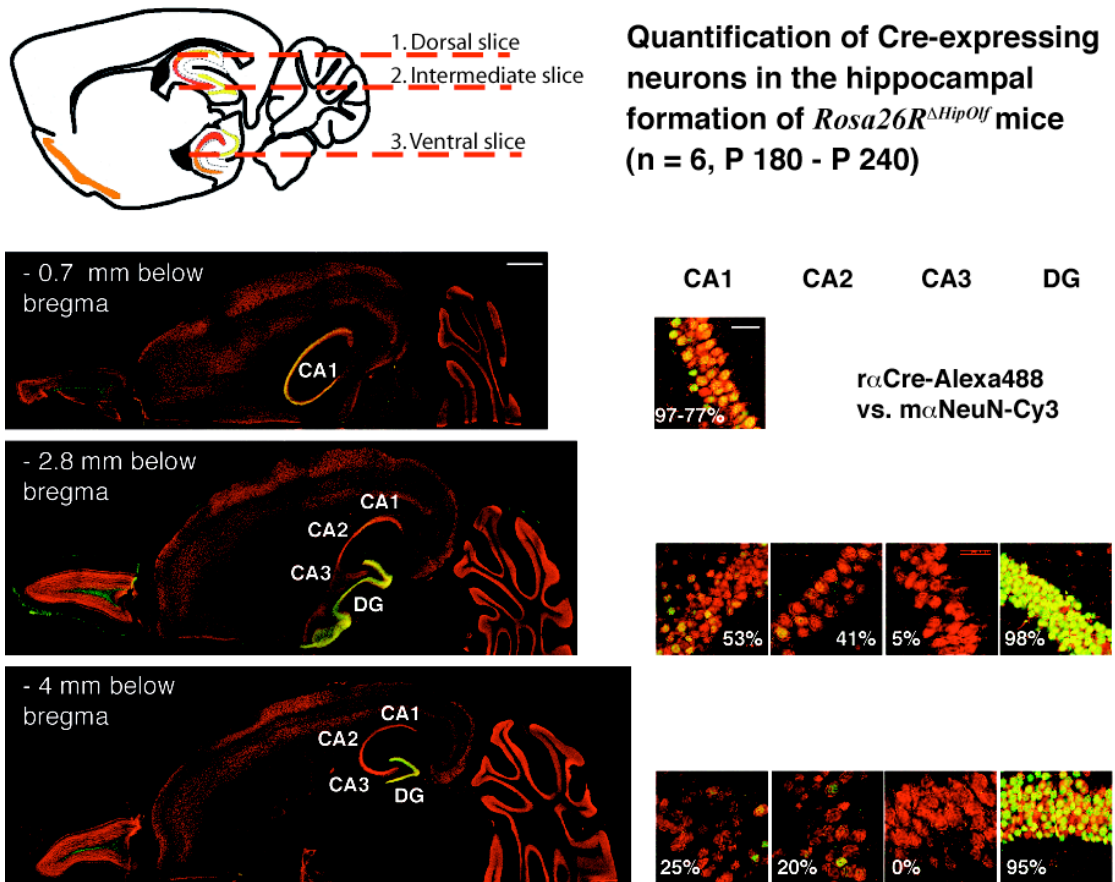
Fig. 2.1.3 Quantification of $Tg^{CN12\text{-}itTA}$-driven Cre expression in the dorsal and ventral hippocampal formation

Horizontal vibratome sections of six *Rosa26R*^{AHipOlf} mice were immunostained against NeuN (Cy3, red) and Cre (Alexa488 or FITC, green). Images were recorded within a single optical plane using confocal microscopy for four to six slices per animals at various depth. Cre-expressing neurons in individual sublayers were counted manually. Data reflect mean values. Scale bar, overviews, 1 mm; higher magnifications, 50 µm.

As expected from various transgenic models employing the αCaMKII promoter (Krestel *et al.* 2004, Shimshek *et al.* 2005, Mayford *et al.* 1996), *Tg*$^{CN12-itTA}$-driven Cre expression in the hippocampal formation was detected exclusively in excitatory neurons[3]. In co-localization studies against the glial cell-specific fibrillary acidic protein (GFAP) and interneuronal markers (GAD67, Parvalbumin, Calretinin), no overlapping signals with transgenic Cre protein were observed.
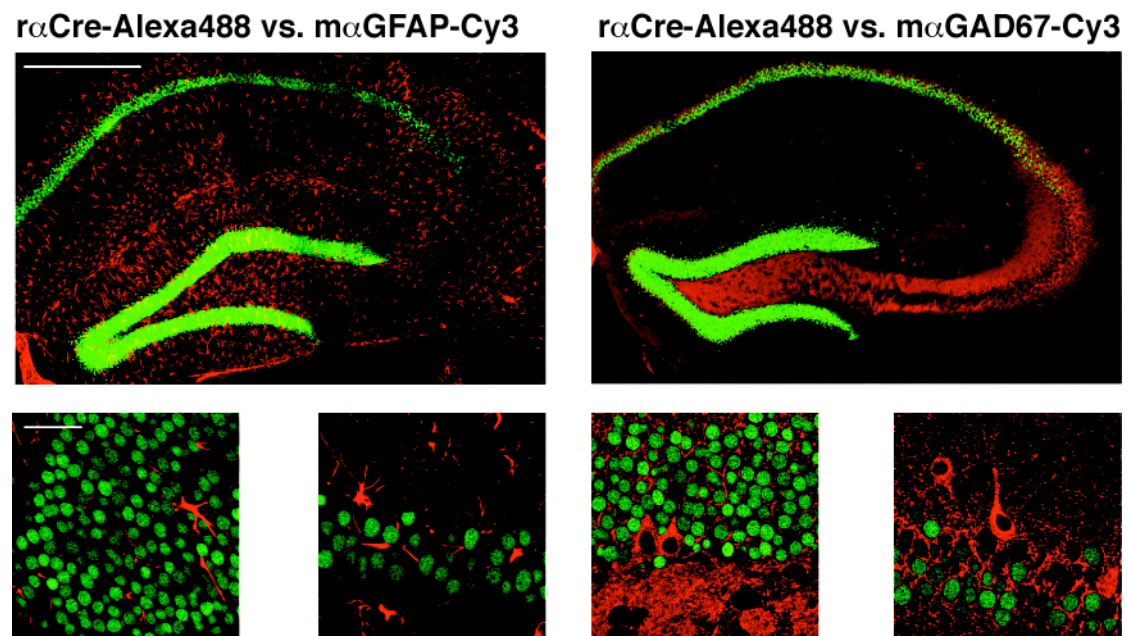
Fig. 2.1.4 Co-labeling of transgenic Cre recombinase and GFAP- or GAD67-positive cells
Tg$^{CN12-itTA}$-driven Cre expression (Alexa488, green) in the hippocampal formation did not colocalize with marker proteins of glial cells (GFAP, Cy3, red, left panel) or inhibitory neurons (GAD67, Cy3, red, right panel). Scale bar, overviews, 500 µm; higher magnifications, 50 µm.

2.1.4. $Tg^{CN12-itTA}$ / Tg^{LC1}-driven recombination in the olfactory system

Strong recombination in P365 $Rosa26R^{\Delta HipOlf}$ mice was observed in various brain structures responsible for discrimination, learning and memory of olfactory information. Unexpected from the highly restricted X-gal pattern at P45, various structures of the olfactory cortex showed strong accumulation of recombination events[7]. Interestingly, the anterior olfactory cortex (AOC, dorsal, external and lateral parts of the anterior olfactory nucleus (AON), AOD, AOE, AOL) remained mainly unstained, but the medial (MOC) and the primary olfactory cortex (POC) showed strong X-gal staining. Positive signals in MOC were detected in neurons of the dorsal and ventral tenia tecta (DTT, VTT), whereas the medial part of AON (AOM) and the dorsal peduncular cortex (DP) exhibited only sparse labeling. POC, comprised of the olfactory tubercle (Tu), anterior and posterior PC (APC, PPC), showed recombination events along its longitudinal brain axis. Location and shape of X-gal signals as well as positive co-localization of $Tg^{CN12-itTA}$ / Tg^{LC1}-driven Cre expression with the neuronal marker protein NeuN (data not shown) indicated transgenic activity in excitatory layer II neurons of the medial and primary olfactory cortices (OC).

Furthermore, also projection neurons in several transition zones of the olfactory cortex exhibited strong accumulation of X-gal signals. Direct connection from the dorsal tenia tecta (DTT) of the medial olfactory cortex to the indusium griseum (IG) of the hippocampal formation, as well as the islands of Calleja (ICj) and ventral pallidum (VP) that link the olfactory tubercle (Tu) and anterior piriform cortex (APC) to limbic and basal forebrain structures, were stained intensively blue. Multiple connections from the primary olfactory cortex to the amygdala were also affected in $Rosa26R^{\Delta HipOlf}$ mice. Cortex-amygdala transition zone (CxA) and anterior cortical amygdaloid nucleus (ACo) are connected to the olfactory tubercle (Tu) and anterior piriform cortex (APC) as well as amygdalopiriform transition area (APir) that is linked to the posterior piriform cortex (PPC).

---

[7] Classification of subregions of the olfactory cortex was reviewed by Brunjes *et al.* 2005 and was based on the wiring model proposed by Haberly 2001 (Please refer to the discussion).
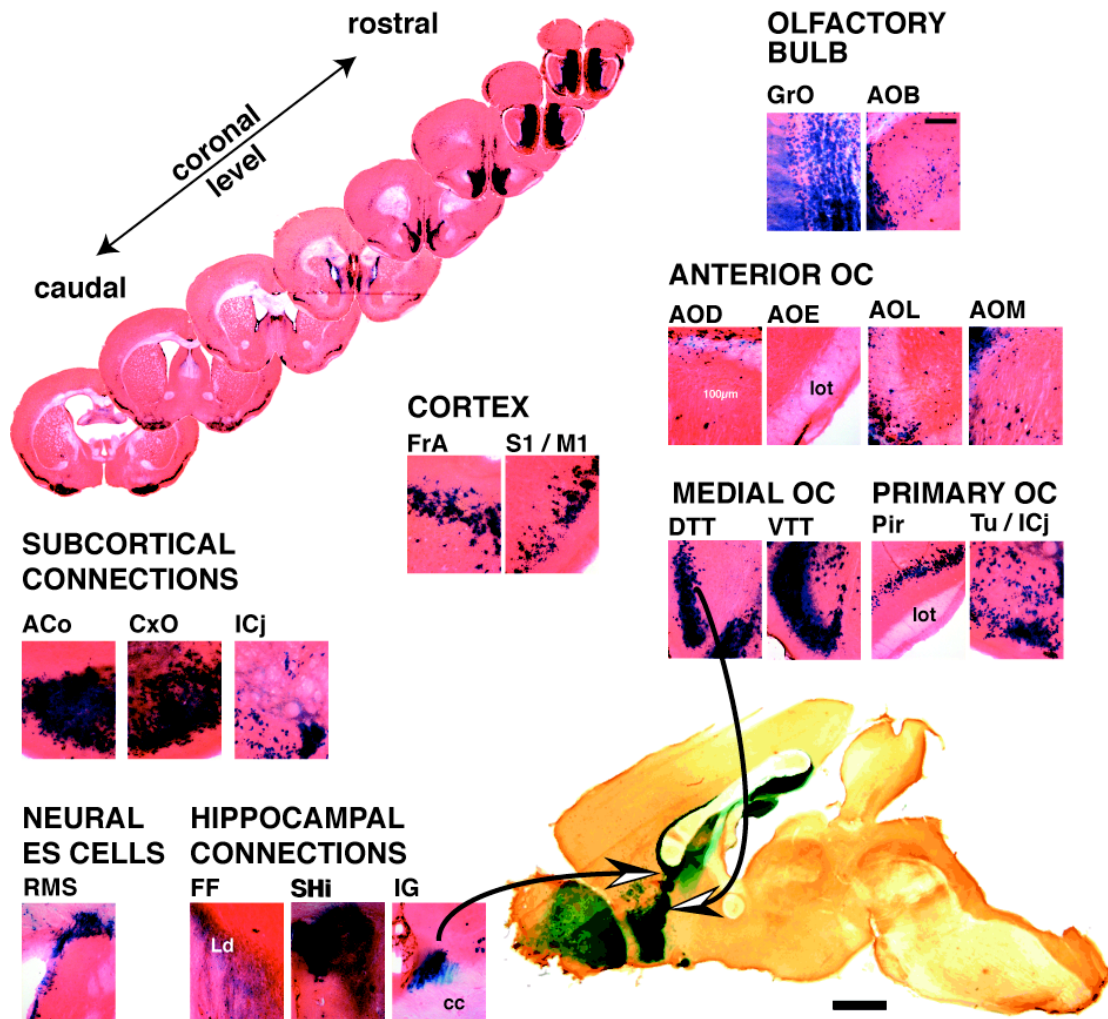
Fig. 2.1.5 Recombination in the anterior forebrain of *Rosa26R^{ΔHipOlf}* mice at the very end of behavioral analysis (P365)

ACo, anterior cortical amygdaloid nucleus; AOB, accessory olfactory bulb; AOD, anterior olfactory nucleus, dorsal part; AOE, external part; AOL, lateral part; AOM, medial part; CxA, cortex-amygdala transition zone, DTT, dorsal tenia tecta; FF, fimbria-fornix; FrA, frontal association area; GrO, granular OB cell layer; ICj, islands of Calleja; IG, indusium griseum; Ld, lambdoid septal zone; lot, lateral olfactory tract; M1, primary motor cortex; RMS, rostral migratory stream; S1, primary somatosensory cortex; Tu, olfactory tubercle; VTT, ventral tenia tecta. Scale bar, overviews, 1 mm; higher magnifications, 100 μm.

But even more striking, positive X-gal signals appeared in the posterior caudate putamen (pCPu), around lateral ventricles and in the main olfactory bulb (MOB), and increased with age. The temporal increase of recombination events along these structures of the rostral migratory stream (RMS) and subsequently, in all cellular layers of the MOB, indicated transgenic activity in migratory, neural stem cells (nES)

and not in the established networks of the MOB *per se*. Further co-localization studies underlined this hypothesis.

Non-neuronal $Tg^{CN12\text{-}itTA}$-driven Cre expression was detected in structures of adult neurogenesis in the olfactory system (pCPu, along lateral ventricles and MOB). In the MOB, it was concentrated in the deepest area, the subependymal layer (SEL) that includes the intrabulbar portion of the RMS. In contrast, Cre expression in all processing MOB layers was decreased drastically and only a few Cre-positive cells co-localized with NeuN. Similar pattern of Cre immunostaining was observed during all tested ages (P100-P365).

Further confirmation of $Tg^{CN12\text{-}itTA}$-driven Cre expression in olfactory neuroblasts was obtained by co-localization studies against the marker protein doublecortin (DCX) and against the SVZ astrocyte marker protein GFAP. Transgenic activity is observed in all DCX-positive neuroblasts and even a subset of GFAP-positive cells in SEL of the main olfactory bulb showed overlapping Cre expression (fig. 2.1.6).
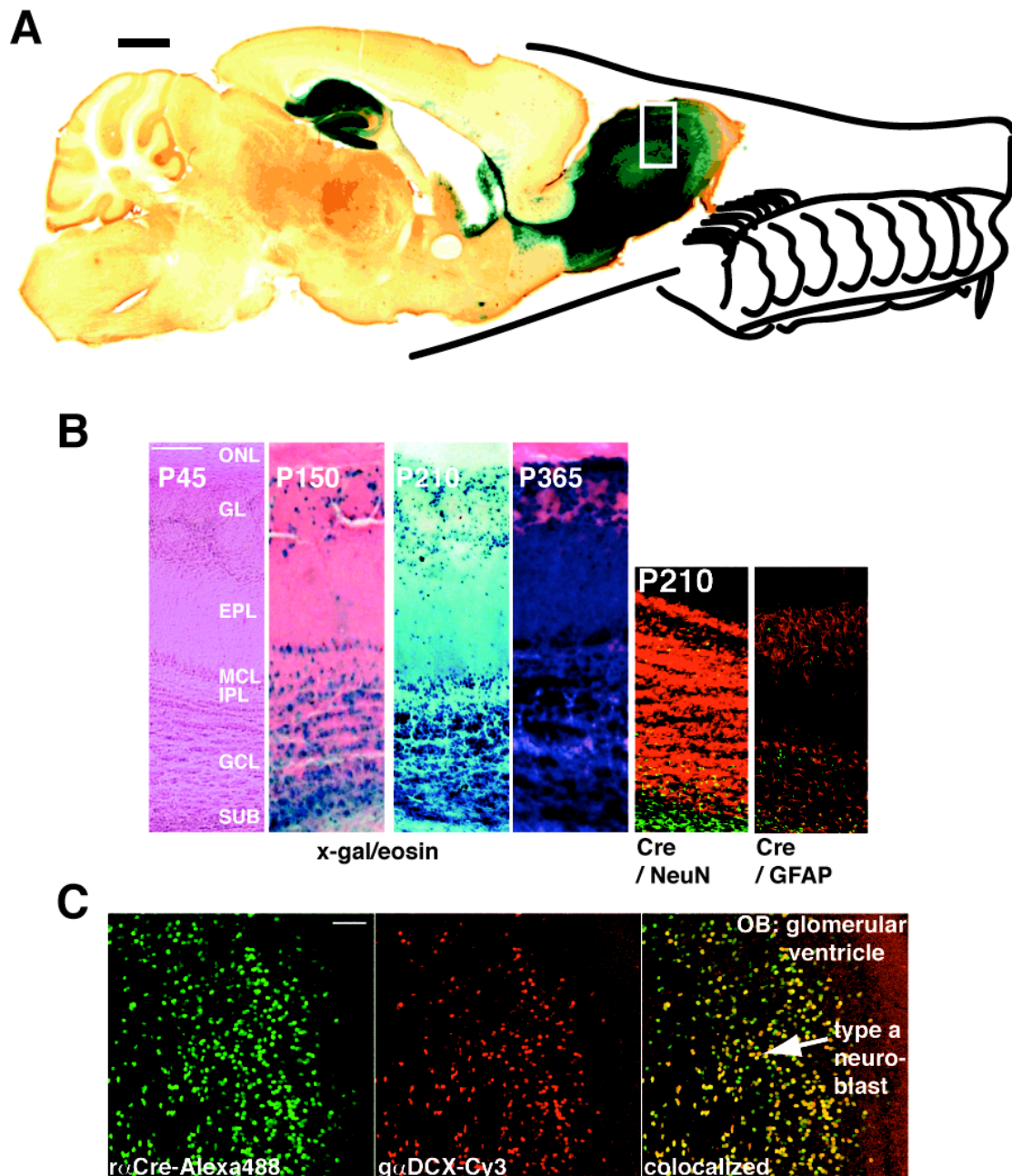
Fig. 2.1.6. Recombination in olfactory neurogenesis

All structures that contribute to the replacement of inhibitory MOB neurons were targeted in *Rosa26R^{ΔHipOlf}* mice and increased with age. A. X-gal staining of sagittal section of *Rosa26R^{ΔHipOlf}* mice (P180) showed labeling of the rostral migratory stream (RMS) and MOB, next to hippocampal sublayers. B. Temporal increase of recombination events in all cellular MOB layers (first four panel). Cre expression was found mainly in non-neuronal cells (rαCre, Alexa488, green, mαNeuN, Cy3, red, fifth panel). A small subset of Cre expressing cells in the inner supendymal layer (SUB) colocalized with a glial cell marker (mαGFAP, Cy3, red, sixth panel). C. Immunostaining against *Tg^{CN12-itTA}* / *Tg^{LC1}*-driven Cre expression (Alexa488, green) colocalized mainly in the SUB where newborn cells migrate and differentiate into the MOB layers involved in olfactory processing. In SEL, all visible migratory neural stem cells (nES) expressing doublecortin (DCX, Cy3, lower panel) contained the

transgenic Cre protein. EPL, external plexiform layer; GCL, granular cell layer; GL, glomerular layer; IPL, internal plexiform layer; MCL, mitral cell layer; ONL, outer nerve layer. Scale bar, overviews, 1 mm; higher magnifications in B, 100 µm; magnification in C, 20 µm.

2.2. Depletion of excitatory receptor pools in adult neuronal networks

Restricted recombination in adult $Rosa26R^{\Delta HipOlf}$ mice was achieved by transgenes of mouse lines $Tg^{CN12-itTA}$ and Tg^{LC1} that utilize the tet system to arrest Cre expression in the mouse embryo. Cre-mediated recombination remained highly concentrated in restricted sublayers of the hippocampal formation and the olfactory system until the very end of behavioral analysis. In the following, this mouse model was employed to manipulate prominent, excitatory glutamate receptors in these restricted areas ($iGluR^{\Delta HipOlf}$) by generating double transgenic mice of lines $Tg^{CN12-itTA}$ and Tg^{LC1} in homozygous background of loxP-flanked receptor gene alleles. Embryonic Cre recombinase was suppressed with 50 mg/l dox in the drinking water of the mothers until birth of the offspring. Negative and single transgene-positive individuals served as litter controls.
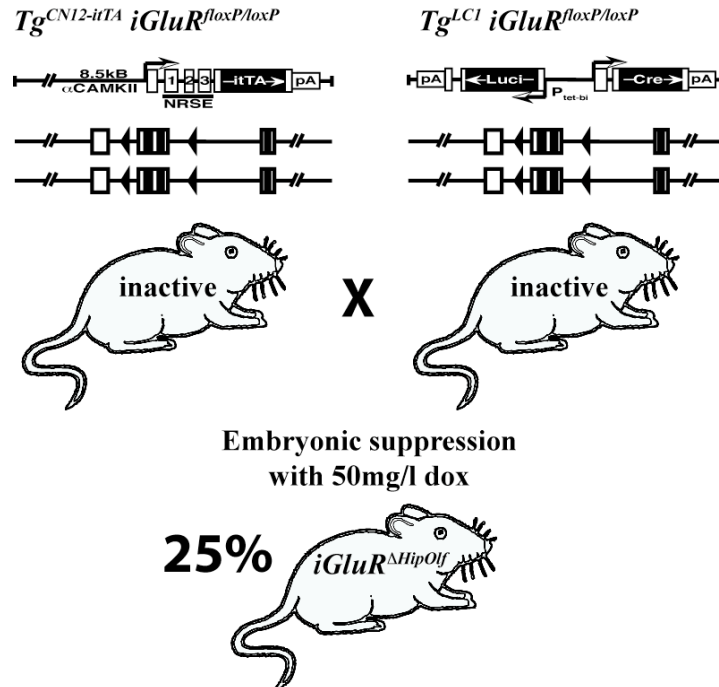

Fig. 2.2. Breeding scheme of $iGluR^{\Delta HipOlf}$ mice
Mice homozygous for the floxed receptor gene ($iGluR^{loxP/loxP}$) and heterozygous for one transgene of the $Tg^{CN12-itTA}$/ Tg^{LC1} model (inactive) were bred with their counterparts to generate $Tg^{CN12-itTA}$ / Tg^{LC1} /

iGluR^{*loxP/loxP*} mice. Embryonic Cre recombinase was suppressed by 50 mg/l dox. On average, ~25% *iGluR*^{*ΔHipOlf*} mice were born.

2.2.1. GluR-A depletion in *Gria1*^{*ΔHipOlf*} mice

The AMPAR subunit GluR-A is encoded by the *Gria1* locus on mouse chromosome 11 (57.02-57.14Mb). In gene-targeted *Gria1*^{*loxP*} mice, exon 11 encoding the membrane domains 2 and 3 (M2, M3) of GluR-A were flanked with loxP sites to enable conditional gene KO upon Cre activity. To direct GluR-A depletion to hippocampal and olfactory sublayers in the adult mouse brain, *Gria1*^{*ΔHipOlf*} mice were generated by breeding double transgenic mice of lines *Tg*^{*CN12-itTA*} and *Tg*^{*LC1*} in the homozygous background of *Gria1*^{*loxP/loxP*} mice and Cre suppression in the embryo with 50mg/l dox.

Slow and gradual depletion of the GluR-A protein was observed in restricted hippocampal sublayers of *Gria1*^{*ΔHipOlf*} mice. Whereas GluR-A signals remained stable in the CA3 and CA4 regions, elaborate GluR-A depletion occured in dCA1, dCA2, DG but was not completed before P150. However, loss of the GluR-A protein in the cell bodies (gcl, pcl) was detected even at the first time point of analysis (P60), although GluR-A signals persisted in the neuronal processes of DG granule cells (ml) as well as of dCA1 and dCA2 principal neurons (so, srad). Surprisingly, the GluR-A signals declined very slowly in these neuronal processes. Additional loss of the GluR-A protein was observed in the neuronal cell layers (gcl, pcl) at P100, whereas no remarkable difference was seen in the layers of corresponding processes. At P150, however, GluR-A staining decreased enormously in these layers (ml, so, srad). Now, even the entire cell shape of sparse GluR-A expressing neurons was visible along all layers of hippocampal subfields (so, pcl, srad, gcl, ml). The location and shape of these residual neurons indicated an interneuronal character. In co-localization studies against inhibitory neuronal marker proteins (GAD67, parvalbumin), further evidence was collected. Most of the remaining GluR-A neurons were co-localized with GAD67 or parvalbumin (data not shown).

The GluR-A depletion in the hippocampal sublayers leveled off at P150 since the pattern of DAB immunostainings remained stable at older ages (P240 – P320 tested, not all data shown). The loss of GluR-A in additional *Tg*^{*CN12-itTA*} / *Tg*^{*LC1*}-

affected brain regions (vCA1, MOB, PC etc.) with lower recombination efficiency was barely visible.
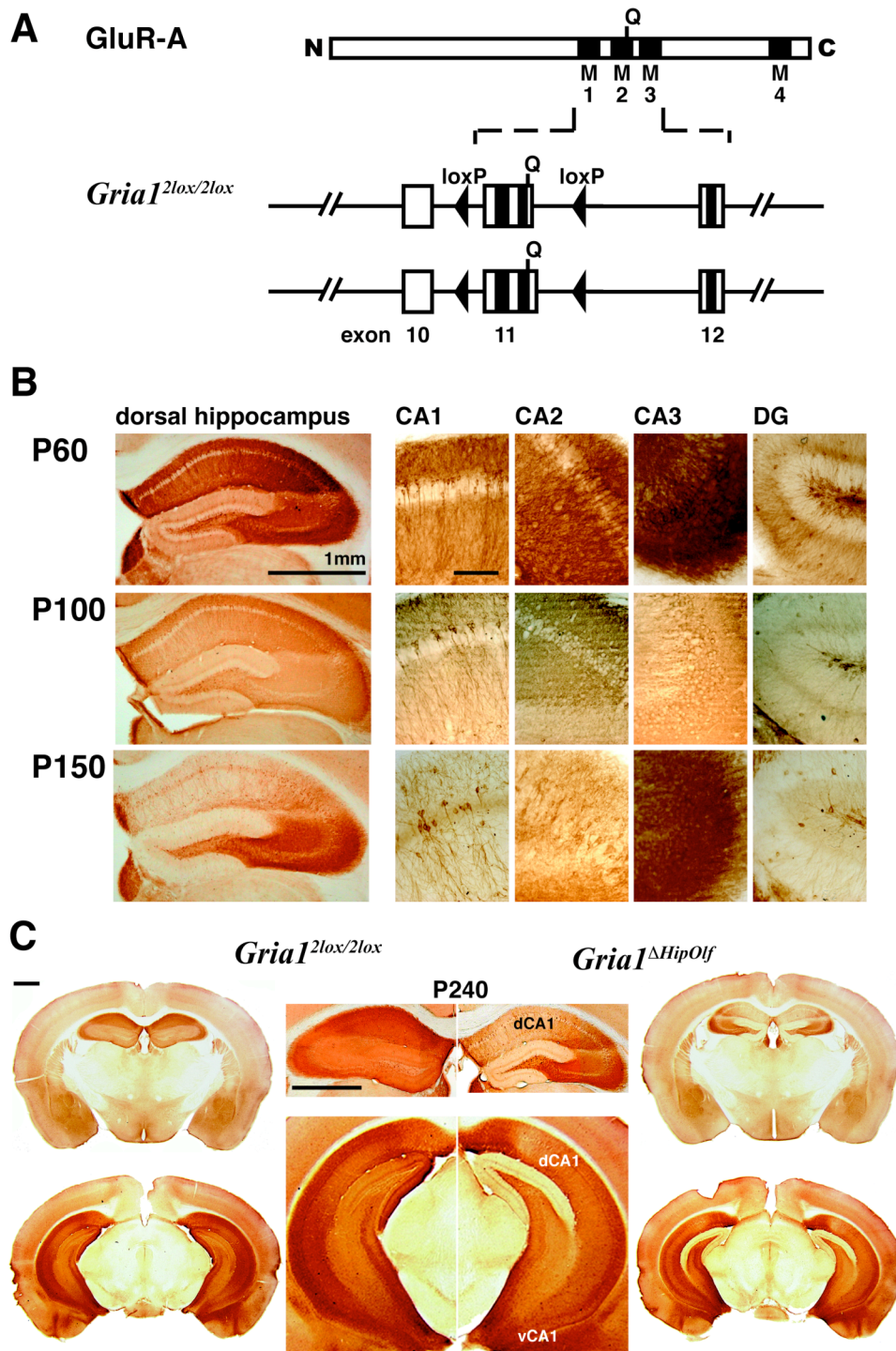
Fig. 2.1.1. GluR-A depletion in hippocampal sublayers of adult *Gria1^{ΔHipOlf}* and litter control (*Gria1^{loxP/loxP}*) mice

(A) Diagram of the GluR-A protein with its four transmembrane domains (M1-M4) and the gene-targeted *Gria1* alleles in *Gria1^{loxP/loxP}* mice. N, amino-terminus; C, carboxyl-terminus; M1-M4, membrane domains 1-4; Q, glutamine in channel pore **(B)** Temporal depletion of the GluR-A protein in

hippocampal sublayers visualized by DAB immunostaining at different ages (P60, P100, P150). **(C)** DAB immunostaining against the GluR-A protein in P240 mice. The magnification in the inner panel indicated elaborate loss of GluR-A in DG, dCA1 and dCA2 in conditional GluR-A KO but not in controls. No obvious depletion was observed in extrahippocampal brain regions in these stainings. Scale bar, hippocampal and coronal slice overviews, 1 mm; magnifications of individual sublayers, 100 µm.

Quantification of GluR-A depletion in the hippocampal formation was performed by immunoblotting of whole-cell lysates from $Gria1^{\Delta HipOlf}$ and litter control mice (>P150). As expected from the immunostainings against the GluR-A protein, strong depletion was detected in the dorsal hippocampus (13.9 ± 4.4% residual GluR-A signal) and more modest depletion in the ventral hippocampus (39.4 ± 21.8%).
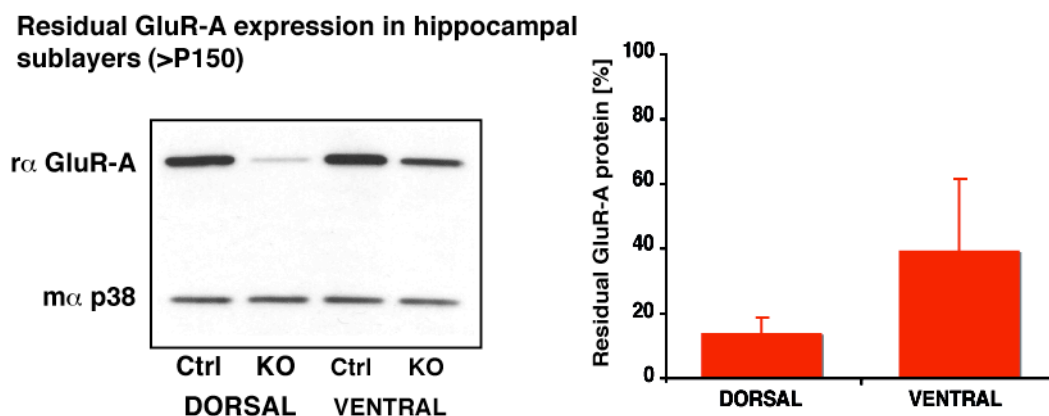
Fig. 2.1.2. Quantification of GluR-A in the hippocampal formation of adult $Gria1^{\Delta HipOlf}$ mice (>P150)
Whole cell lysates were prepared from dorsal (upper third) and ventral hippocampus (lower third). Residual GluR-A protein was determined by calculation of rα-GluR-A/mα–p38 ratios and comparison to litter control mice.

Although anatomical changes in the hippocampal formation have not been reported for the complete *Gria1* KO mice (Zamanillo *et al.* 1999, Mack *et. al.* 2001), immunostaining against different markers of interneurons (GAD67, Parvalbumin, Calbindin) and of glial cells (GFAP) were performed to evaluate potential consequences in $Gria1^{\Delta HipOlf}$ mice. Compared to litter control mice, the elaborate GluR-A depletion in excitatory neurons of the dCA1, dCA2 and DG sublayers did not result in obvious changes of the inhibitory networks or the glial system (data not shown)

2.2.2. GluR-B depletion in *Gria2$^{\Delta HipOlf}$* mice

The main AMPA receptor subunit GluR-B regulating Ca^{2+}-impermeability of functional AMPA receptors is encoded by the *Gria2* locus on mouse chromosome 3 (80.77-80.89Mb). In *Gria2^{loxP}* mice, exon 11 encoding the membrane domains 2 and 3 (M2, M3) of the GluR-B protein was flanked with loxP sites to allow for gene manipulation upon Cre activity (Shimshek *et al.* 2005). To deplete the GluR-B protein leading to Ca^{2+}-permeable AMPA receptor in olfactory and hippocampal networks of adult mice, double transgenic mice of lines *Tg$^{CN12-itTA}$* and *Tg^{LC1}* were bred in homozygous background of gene-targeted *Gria2$^{loxP/loxP}$* and suppressed embryonic itTA activity by administration of 50mg/l dox-containing drinking water (termed *Gria2$^{\Delta HipOlf}$*).

The spatial and temporal pattern of GluR-B depletion, observed in DAB immunostainings of vibratome sections in *Gria2$^{\Delta HipOlf}$* mice, was similar to the depletion of the GluR-A protein in *Gria1$^{\Delta HipOlf}$* mice. At higher age ($\geq$P150), extensive loss of the GluR-B protein remained restricted to dCA1, dCA2 and DG of the hippocampal formation. Notably, residual GluR-B expression was only detected in the cell bodies and initial dendritic or axonal segment of sparse neurons. GluR-B signals in vCA1, vCA2 or additional *Tg$^{CN12-itTA/LC1}$*-affected brain regions (RMS neuroblasts, Tu, PC etc.) were indistinguishable from those of DAB stainings in the litter control mice. Depletion of the GluR-B protein in dorsal CA1/2 and DG was not visualized explicitly at younger age (P60-P120, data not shown), mainly due to the low signal-to-noise ratio of the anti-GluR-B antibody.

Quantification of GluR-B depletion in the hippocampal formation was performed by immunoblotting of hippocampal protein lysates of adult *Gria2$^{\Delta HipOlf}$* and litter control mice (n=2, each genotype, >P150). Ratios of GluR-B vs. β-Actin levels were examined and compared between genotypes. The GluR-B protein level in the hippocampal formation of adult *Gria2$^{\Delta HipOlf}$* mice was decreased to 32.3 ± 21.2% of control mice.

A

GluR-B

N — M1 M2 M3 M4 — C (R)

Gria2^{2lox/2lox}

exon 10 / loxP / 11 (Q/R) / loxP / 12

B

Gria2^{2lox/2lox}   *Gria2^{ΔHipOlf}*

dorsal hippocampus CA1   CA2   CA3   DG

Gria2^{2lox/2lox}

Gria2^{ΔHipOlf}

C

Residual GluR-B expression in the hippocampal formation (>P150)

rα GluR-B

mα Actin

KO   Ctrl

Residual GluR-B protein [%]
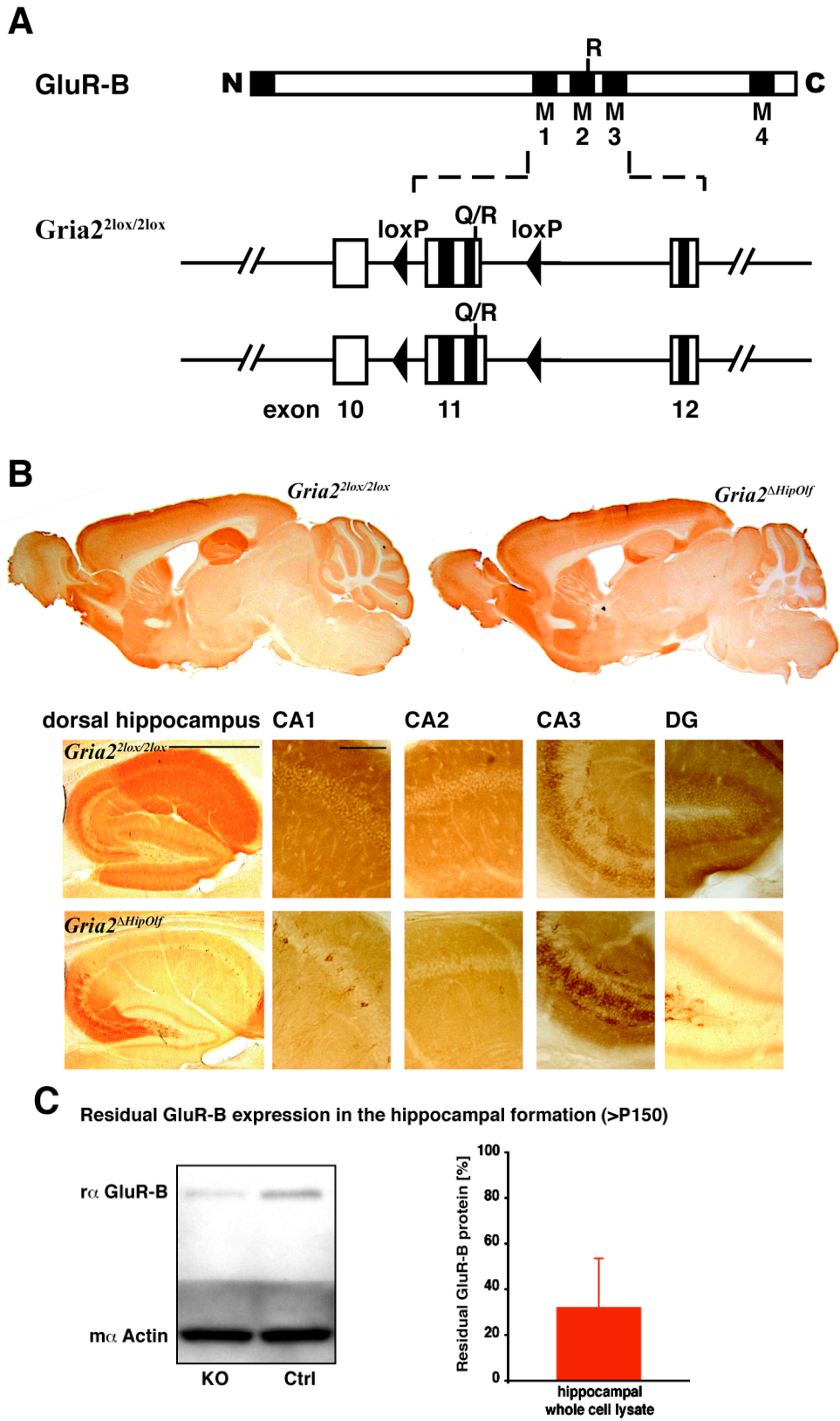
hippocampal whole cell lysate

Fig. 2.2.1. GluR-B depletion in adult *Gria2^{ΔHipOlf}* mice

(A) Diagram of the GluR-B protein with its four membrane domains (M1-M4) and the gene-targeted *Gria2* alleles in *Gria2^{loxP/loxP}* mice. N, amino-terminus; C, carboxyl-terminus; M1-M4, membrane domains 1-4; Q/R, critical amino acid (RNA-editing from glutamine/Q to arginine/R **(B)**

Immunostaining against the GluR-B protein in sagittal vibratome sections of *Gria2^ΔHipOlf* and litter control mice (>P150). Higher magnifications demonstrated elaborate loss of GluR-B in CA1, CA2 and DG in conditional GluR-B KO but not in controls. Scale bar, 1mm, sagittal and hippocampal overviews, 100 μm, sublayer magnifications. **(C)** Quantification of GluR-B depletion in the hippocampus of *Gria2^ΔHipOlf* and litter control mice (>P150). GluR-B expression was examined relative to β-actin by immunoblotting. Residual GluR-B expression in *Gria2^ΔHipOlf* and litter control mice is depicted in the diagram.

Previous observations in *Gria2^ΔFb* mice (Shimshek *et al.* 2006) revealed long-lasting consequences upon GluR-B depletion in the hippocampal formation. Next to a loss of parvalbumin-positive DG interneurons, moderate DG mossy fiber sprouting was observed. To check these parameters in the hippocampal formation of adult *Gria2^ΔHipOlf* and litter control mice (9-11 months old), the number of parvalbumin-positive interneurons in CA1/2 (*so* and *pcl*) and DG in DAB stainings (fig. 2.2.2.B) and Timm-stained granules in the inner molecular layer (*iml*, fig.2.2.2.A) were quantified. Neither the number of parvalbumin-positive interneurons nor the extent of DG mossy fiber sprouting and number of Timm-stained granules in the DG inner molecular layer (iml) were significantly different between adult *Gria2^ΔHipOlf* (n = 2-4, 9-11 months old) and litter control mice (n = 2).

In addition, immunostainings against marker proteins of the glial system (glial fibrillar acidic protein, GFAP) and the inhibitory networks (67 kDa glutamic acid decarboxylase, GAD67, calbindin, parvalbumin) were performed in vibratome sections of adult *Gria2^ΔHipOlf* and control mice. No obvious changes in GFAP-, GAD67- and calbindin-expressing components of the hippocampal formation were observed upon GluR-B depletion (data not shown).

In summary, inactivation of the *Gria2* locus in *Gria2^ΔHipOlf* mice resulted in GluR-B depletion in restricted sublayers of hippocampal and olfactory sublayers at adult age (≥P150). The AMPA receptor-mediated Ca^{2+}-influx upon GluR-B depletion did not mediate any structural or cellular changes in the dorsal hippocampal formation, as described upon forebrain, principal neuron-specific *Gria2* inactivation at early postnatal ages (*Gria2^ΔFb*; Shimshek *et al.* 2006).
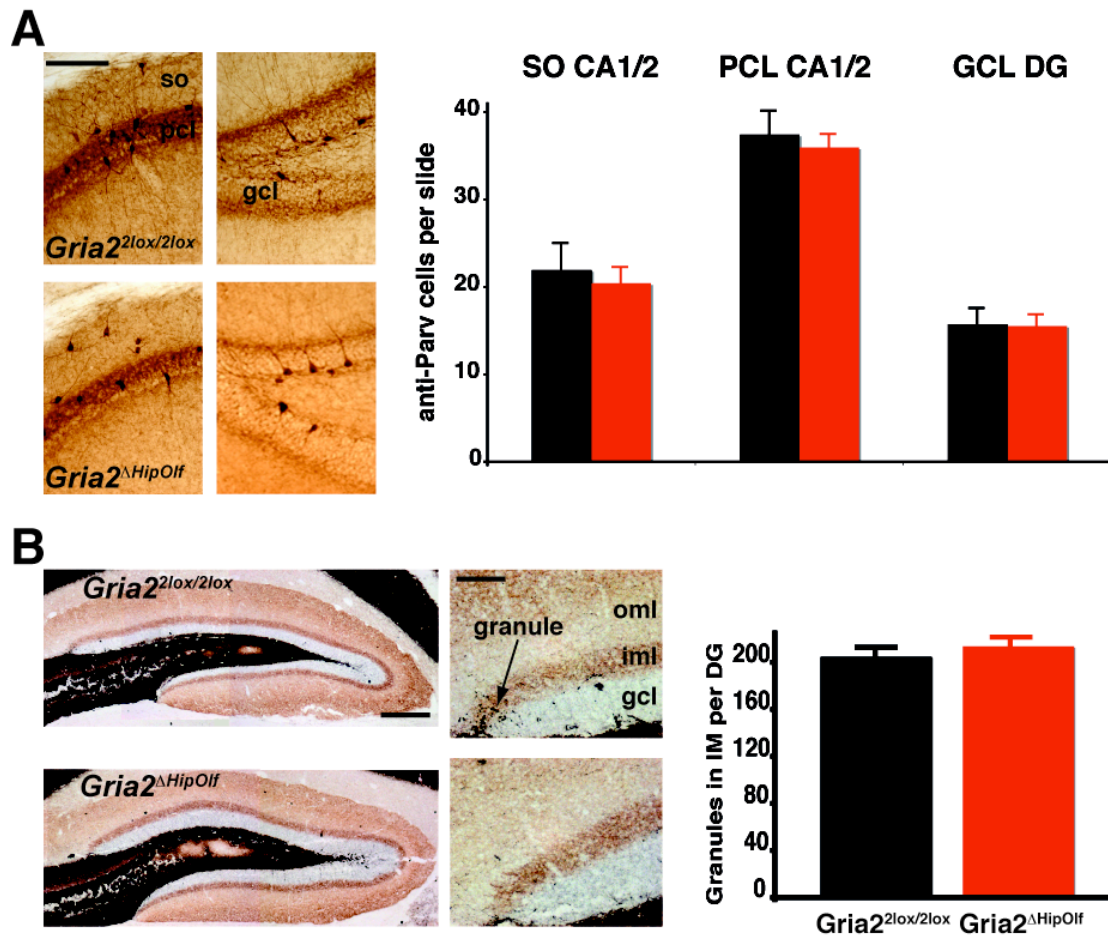
Fig. 2.2.2. Anatomical consequences in the hippocampal formation of adult *Gria2^ΔHipOlf* and litter control mice (8-11 months old)

(A) No difference in number of parvalbumin-positive interneurons. DAB immunostaining of 8-15 slices of different coronal or sagittal hippocampal levels were performed and cell numbers of parvalbumin-stained interneurons were counted in so and pcl of CA1/2 and in gcl of DG. **(B)** Normal mossy fiber sprouting. Timm staining revealed no aberrant sprouting of DG mossy fibers in the granule cell layer (gcl) and no difference in Timm-stained granules in the inner molecular layer (iml) representing axon terminals of DG mossy fibers. Scale bar, 1 mm, DG overview of Timm stainings, 100 µm, higher magnifications.

2.2.3. NR1 depletion in *Grin1*[ΔHipOlf] mice

The principal subunit NR1 is essential for the formation of functional tetrameric NMDA receptors. The *Grin1* gene on mouse chromosome 2 (25.11-25.14Mb) encodes the NR1 protein. Exons 11 to 18 containing M1 to M3 sequences were flanked by loxP sites in *Grin1*[loxP/loxP] mice (F.N. Single, dissertation 1999; Shimshek *et al.* 2006) to allow for Cre-mediated recombination of the *Grin1* loci. As in the other two mouse models of this study, *Tg*[CN12-itTA] / *Tg*[LC1] mice were bred in the homozygous background of *Grin1*[loxP/loxP] to achieve the restricted NR1 depletion upon Cre suppression in the mouse embryo with 50mg/l dox.

Several antibodies against the NR1 protein were tested in various protocols[8] (Fukaya *et al.* 2003, McHugh *et al.* 2007, Niewoehner *et al.* 2007) to visualize NR1 depletion in *Grin1*[ΔHipOlf] mice. Perfused and 1h post-fixed vibratome sections stained with the rabbit anti-NR1 antibody (1:50, Chemicon, USA) and enhanced DAB development was the only protocol that showed the expected staining in control mice and the depletion of the NR1 protein in the dorsal hippocampal formation (dCA1, dCA2, DG) of *Grin1*[ΔHipOlf] mice (fig. 2.3.1). Nevertheless, the low signal-to-noise ratio of this approach hindered cellular resolution of the NR1 signals and hence, verification of the NR1 depletion by immunostainings.

Whereas most commercial antibodies against the NR1 protein had low signal-to-noise ratios in immunohistochemical approaches, the specificity in detection of denatured NR1 protein in immunoblotting was excellent (fig. 2.3.2). Hence, protein lysates from the dorsal hippocampus (upper third) were immunoblotted and residual NR1 protein (relative to p38 MAP kinase) in *Grin1*[ΔHipOlf] analyzed compared to litter control mice at different ages (P100-P365). As expected from the previous *iGluR*[ΔHipOlf] mouse models, the NR1 protein level decreased slowly over time and depletion was not final before P120. The main loss occurred between P100 (56.5 ±12.1%) and P120 (28.6 ± 21.7%), indicating the strong depletion in the processes of principal CA1/2 and DG neurons (in so, srad, ml). NR1 depletion was finished between P120 and P150, since the residual protein level did not change significantly up to P365 (P150, P240, P365 tested, n=1-2 at each age, data not shown). The protein

---

[8]We tested paraffin sections with pepsin pretreatment and DAB development (Fukaya *et al.* 2003) or fluorescent visualization (McHugh *et al.* 2007), vibratome sections with PFA post fixation overnight or for only 1h at 4°C with four different antibodies.

level, summarized for P150 until P365 (n=5), decreased to 27 ± 8.9% in $Grin1^{\Delta HipOlf}$ compared to litter control. The NR1 depletion in the ventral hippocampus (lower third of freely prepared structure) in adult mice (P > 150) was also quantified. The residual NR1 protein in $Grin1^{\Delta HipOlf}$ mice decreased significantly (69.6 ± 14%) but not as strongly as in the dorsal part.
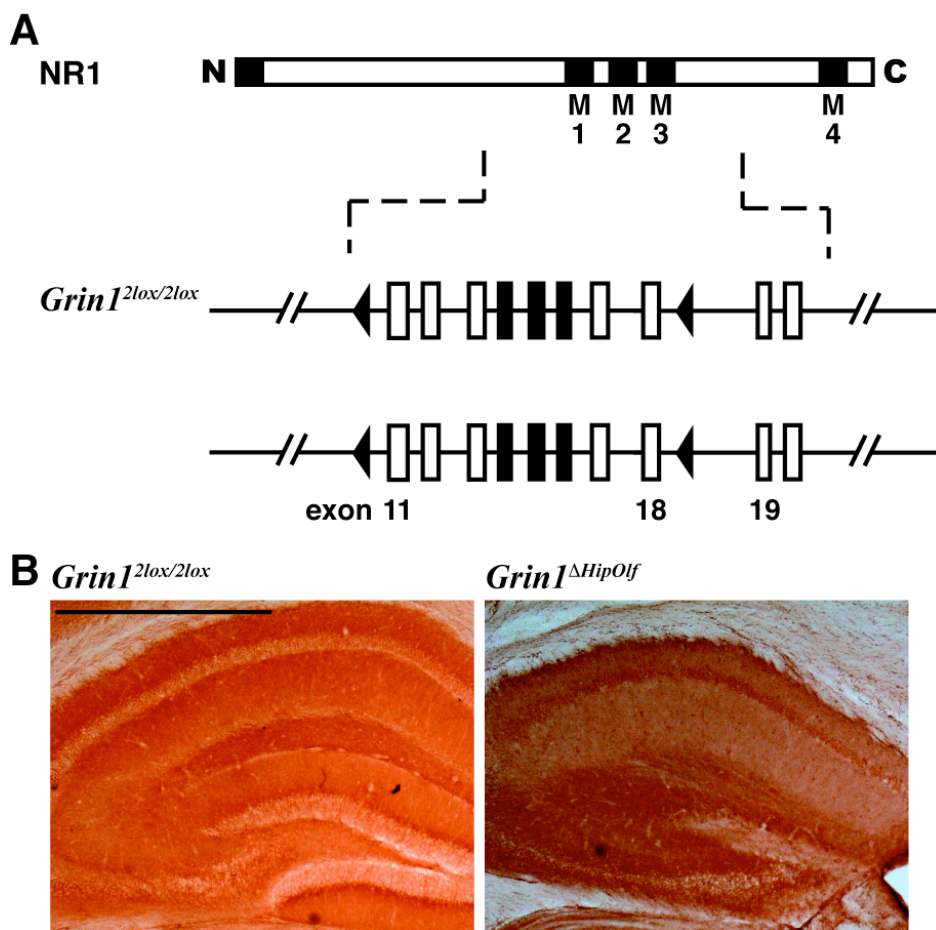
Fig. 2.3.1. NR1 depletion in adult $Grin1^{\Delta HipOlf}$ mice

(A) The NR1 protein (first row) depicted schematically with its four membrane domains (M1-M4) is encoded by the *Grin1* gene. In $Grin1^{2lox/2lox}$ mice, exons 11 to 18 containing M1 to M3 sequences were flanked with Cre recognition sites (loxP) to enable conditional gene manipulation. N, amino-terminus; C, carboxyl-terminus. **(B)** DAB immunostaining against the NR1 protein in coronal vibratome sections of litter control (left panel) and $Grin1^{\Delta HipOlf}$ mice (> 1 year, right panel). Overview of dorsal hippocampus indicated NR1 depletion in CA1, CA2 and DG. The higher magnification of hippocampal demonstrated extensive loss of NR1 in CA1, 2 and DG in dorsal hippocampus. Signals in the CA3 region seemed unaffected. Scale bar, 1 mm.
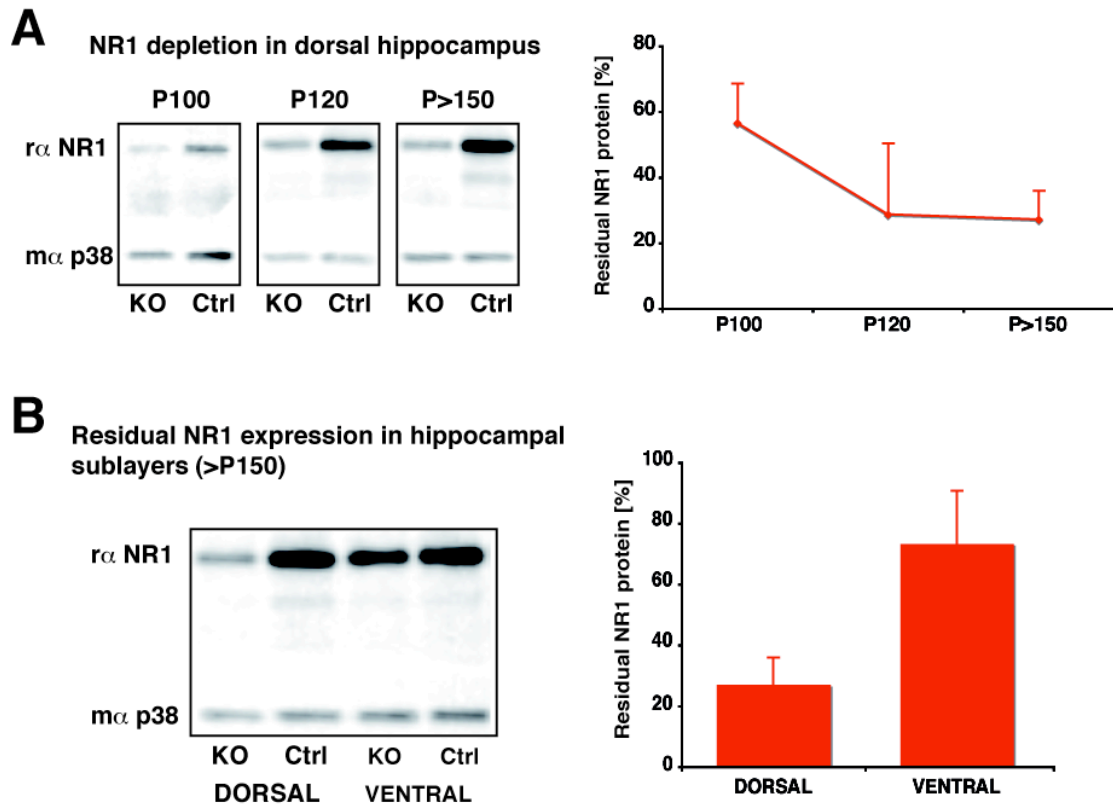
Fig. 2.3.2. Quantification of NR1 depletion in *Grin1^ΔHipOlf* and litter control mice by immunoblotting against the NR1 protein and the p38 MAP kinase as reference protein

(A) NR1 depletion in the dorsal hippocampus. Protein lysates of the dorsal hippocampus (upper third) were prepared at different ages (P100-P365). Relative NR1 protein levels (to MAP kinase p38) were examined and compared between conditional KOs and litter control mice. Protein levels of P150, P240, P365 are summarized as P>150. Residual NR1 protein levels of *Grin1^ΔHipOlf* mice were plotted against the animals´ age in the diagram. **(B)** Residual NR1 expression in dorsal and ventral hippocampus. Relative NR1 protein levels (to MAP kinase p38) were examined also in the ventral hippocampus (lower third) and compared between conditional KOs and litter control mice (P150, P240, P365 are summarized as P>150). Data reflect mean ± SD.

Previous studies on conditional *Grin1* KO mouse models (Tsien *et al.* 1996, McHugh *et al.* 2007, Niewoehner *et al.*, 2007) investigated extensively the entire anatomy of the hippocampal formation upon NR1 depletion and did not find any loss of neurons, degeneration or axonal rearrangements. Parallel to the previous two *iGluR^ΔHipOlf* mouse models, immunostainings against marker proteins of the glial system (GFAP) and the inhibitory networks (GAD67, calbindin, parvalbumin) were performed as well as Nissl stainings of vibratome sections of adult *Grin1^ΔHipOlf* and control mice (data not shown). No obvious changes were observed in the glial system, inhibitory networks or principal cell layers of the dorsal, hippocampal formation

between both genotypes. The pronounced ablation of NMDA receptors in DG did not trigger any obvious rearrangement of axonal processes. In calbindin stainings, the DG mossy fibers were labeled similar in *Grin1$^{\Delta HipOlf}$* and control mice.

Field recordings of synaptic plasticity by Vidar Jensen and ∅ivind Hvalby (University of Oslo, Norway) obtained evidence for functional depletion of NMDA receptors in restricted sublayers of the dorsal hippocampus. First, NMDAR-dependent fLTP measurements at Schaffer collateral – CA1 synapses (Collingridge *et al.*, 1983) were performed to assess functional NR1 depletion in the dorsal CA1 subfield. Repeated tetanic stimulation (100 Hz, 1 s, repeated four times at 5 min intervals) of Schaffer collateral-commissural fibers in stratum radiatum elicited a robust, homosynaptic fLTP in control mice (n=4, >P150), whereas synaptic responses upon stimulation of the untetanized, control pathway remained at baseline activity (nEPSP = 0.97 ± 0.04). 40-45 min after tetanization the normalized fEPSP slope showed an increase of 60% compared to the pretetanic activity upon stimulation of Schaffer collaterals in stratum radiatum (1.60 ± 0.07, n=18). In contrast, normalized field potentials in the tetanized pathway (0.99 ± 0.03, n=14) were indistinguishable compared to the untetanized, control pathway (1.03 ± 0.04) in the dorsal hippocampus of adult *Grin1$^{\Delta HipOlf}$* mice (n=4, >P150, p=0.35, paired t-test). The absence of fLTP at Schaffer collateral – CA1 synapses clearly demonstrates the functional loss of NMDA receptors upon NR1 depletion.

In the next experiment, NMDAR-dependent synaptic plasticity at CA1 and CA3 synapses at the same time was assessed to test the restricted ablation of functional networks in the dorsal hippocampus of *Grin1$^{\Delta HipOlf}$* mice. Therefore, the CA1/CA3 border in stratum radiatum was stimulated and recorded simultaneously at CA1 and at CA3 in stratum radiatum. Repeated tetanic stimulation (100 Hz, 1 s, repeated four times at 5 min intervals) in stratum radiatum produced robust fLTP of CA1 (nEPSP = 1.37 ± 0.11) and CA3 synapses (1.33 ± 0.12, n=11) in control mice (n=3, > P150). In *Grin1$^{\Delta HipOlf}$* mice (n=3, >P150), as seen earlier, fLTP is absent in CA1 (0.94 ± 0.09) but was still well evoked in CA3 (1.20 ± 0.07, n=8). Our initial experiments to assess electrophysiological functions in *Grin1$^{\Delta HipOlf}$* mice revealed a functional dissection of the CA1 and CA3 sublayers in the dorsal hippocampal formation. Whereas the elaborate NR1 depletion in the dorsal hippocampus ablated NMDAR-dependent synaptic plasticity in the CA1 subfield, the field property in CA3 was not affected.

Field LTP in Schaffer collateral - CA1 synapses
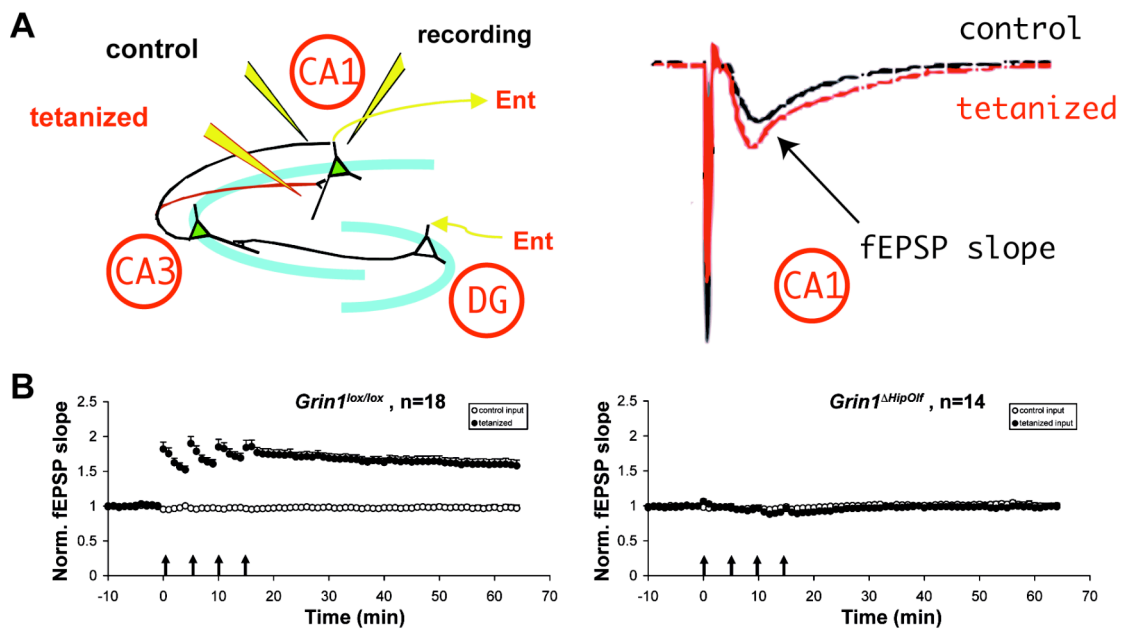
Simultaneous fLTP at CA1 and CA3 synapses
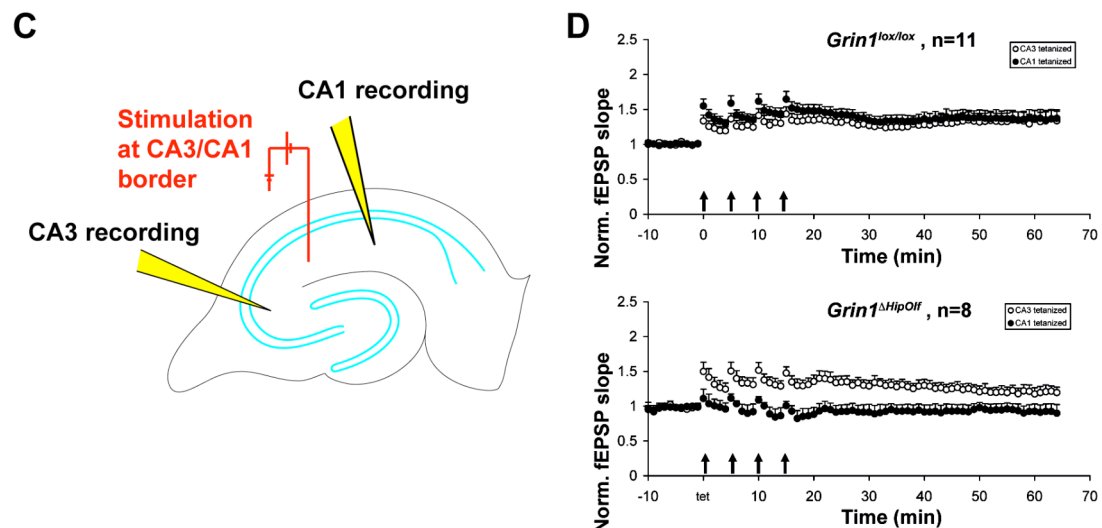
Fig. 2.3.1. Sublayer-restricted ablation of NMDAR-dependent fLTP in adult *Grin1^{ΔHipOlf}* mice (V. Jensen and ∅. Hvalby, University of Oslo, Norway)

(A) *Left panel*, schematic depiction of the trisynaptic hippocampal pathway and the electrode placement in field LTP recordings at Schaffer collaterals (red axon) – CA1 synapses. *Right panel*, example of an evoked excitatory postsynaptic potential (fEPSP) of extracellular field recordings after stimulation of the control (black) and the tetanized input (red). **(B)** Repeated tetanization (100 Hz, 1 s, 4x 5 min intervals) elicited robust fLTP in control slices (n=18) but failed to potentiate CA1 synapses upon NR1 depletion in dorsal slices (n=14) of *Grin1^{ΔHipOlf}* mice. C. Electrode placement in simultaneous fLTP recordings at CA1 and CA3 synapses. D. Repeated tetanization (100Hz, 1s, 4x, 5min interval) elicited robust fLTP in CA1 and CA3 of control slices (n=11). In dorsal slices (n=8) of

Grin1^{ΔHipOlf} mice tetanization failed again to induce fLTP at CA1 synapses but elicited potentiation of synapses in the CA3 subfield.

2.3. Behavioral analysis

The depletion of NMDA receptors or one of the two AMPA receptor subtypes GluR-A and GluR-B was achieved in restricted hippocampal sublayers (dCA1, dCA2, DG) of adult mice by transgenes of mouse models *Tg^{CN12-itTA}* and *Tg^{LC1}* and Cre suppression in the mouse embryo. Depletion of GluR-A in *Gria1^{ΔHipOlf}*, GluR-B in *Gria2^{ΔHipOlf}* and NMDA receptor in *Grin1^{ΔHipOlf}* mice with a similar spatial and temporal specificity allowed the functional dissection of excitatory glutamate receptors in three main properties within hippocampal sublayers (CA1/2, DG vs. CA3/4, Sub, Ent) and towards cortical and subcortical brain regions of adult mice.

As presented in the introduction, excitatory, AMPA and NMDA receptor-mediated neurotransmission in the hippocampal formation plays a crucial role in distinct forms of cognitive spatial learning and memory mechanisms (O´Keefe and Nadel, 1978; Tsien *et al.* 1996; Zamanillo *et al.* 1999; Shimshek *et al.* 2006). In particular, the dorsal subregion of the hippocampal formation is thought to be crucial for normal spatial memory performance (Moser et al. 1995; Bannerman et al. 1999). With improvement of transgenic manipulation of AMPA and NMDA receptors (e.g. Tsien *et al.* 1996; Zamanillo *et al.* 1999; Mack *et al.* 2001; Niewoehner *et al.* 2005), molecular mechanisms were dissected and supported the idea of distinct spatial working and reference memory systems in the hippocampal formation (first mentioned by Honig 1978; Olton *et al.* 1979).

Spatial working memory was tested in the delayed non-matching-to-place task on the elevated T-maze (discrete trial, rewarded alternation; Rawlins and Olton 1982, Deacon *et al.* 2002, Reisel *et al.* 2002). Further, acquisition of spatial reference memory was assessed in the matching-to-place task on the elevated Y-maze (Deacon *et al.* 2002, Reisel *et al.* 2002). We concentrated on *Grin1^{ΔHipOlf}* mice because acquisition of the delayed match-to-place task in the Morris watermaze was severely impaired in mice (< P90; Tsien *et al.* 1996, Fukaya *et al.* 2003) upon ablation of NMDA receptors in hippocampal CA1 neurons during pubertal and early adult ages. The initial T- and Y-maze tasks were performed in our laboratory and will be shown in the following.

D. Bannerman and co-workers in the department of N. Rawlins (Department of Experimental Psychology, University of Oxford, England) performed more extensive analysis of spatial behavior in $Gria1^{\Delta HipOlf}$ and $Grin1^{\Delta HipOlf}$ mice. In addition to critical repetitions of our T-maze data, certain components (spontaneous vs. rewarded; acquisition vs. reversal learning) of spatial working and reference memory systems were tested in various tasks with different complexity (T-maze vs. radial maze) and environment (Y-maze vs. watermaze). Results of selected tasks are summarized in the chapter 2.3.3.

2.3.1. Delay-dependent spatial working memory on the elevated T-maze

Spatial working memory performance in rodents can be studied using the delayed non-matching-to-place (DNMTP) paradigm on a simple three-arm maze with a defined start arm and two identical target arms, such as the elevated T-maze or Y-maze (Rawlins and Olton 1982, Bannerman *et al.* 1999). The relationship between spatial cues and the goal location changes from trial to trial in a pseudo-variant manner. Each trial on the elevated T-maze consists of two runs. In the first, the sample run, the mouse is directed to a certain target arm by blocking the other one. The conditional information of space has to be stored and maintained across a certain delay (inter-session interval, ISI, usually 15 sec in a cage). In the subsequent choice run, both target arms are accessible, and the animal uses the conditional information to choose the previously unvisited arm (goal location). The appropriate response is based on exploratory activity and curiosity, namely the alternation behavior in rodents. The rewarded alternation task (Rawlins and Olton, 1982) takes further advantage of a reward (droplet of sweet milk) to motivate the mouse for searching the goal location in multiple trials (usually 40 trials in total, with a daily performance of 8 trials).

Rewarded alternation on the elevated T-maze is especially sensitive to hippocampal dysfunction. It was shown that dorsal but not ventral lesions impaired T-maze performance completely (Hock *et al.* 1998, Bannerman *et al.* 1999, 2002). Extensive literature (e.g. Steele and Morris 1994, McHugh *et al.* 2007) and our own previous work suggested an essential role of certain iGluR-subtypes in the dorsal hippocampal formation in performing the DNMTP paradigm in different spatial tasks (Morris watermaze, T-maze or radial maze). Global $Gria1^{-/-}$ mice performed rewarded

alternation at chance level (50% total trials), as observed in dorsally lesioned mice (Reisel *et al.* 2002) and partial restoration of GFP-tagged GluR-A in the postnatal forebrain improved performance (Schmitt *et al.* 2005). Furthermore, forebrain-restricted depletion of GluR-B in *Gria2^ΔForebrain* mice mediated impairment of the spatial working memory (Shimshek *et al.* 2006). Impaired T-maze performance upon NMDA receptor manipulation was observed upon AP-5 infusion in the dorsal hippocampus (McHugh *et al.* 2007), and even dentate gyrus-restricted depletion of NMDA receptors in *Grin1^ADG* mice resulted in reduced spatial working memory performance when tested in the six-arm radial maze (Niewoehner *et al.* 2007). Based on previous experience and a widely accepted hypothesis, strong impairment in the rewarded alternation T-maze task was expected in our *iGluR^ΔHipOlf* mice with restricted depletion of GluR-A, GluR-B or NMDA receptors in the CA1/2 and DG sublayers of dorsal hippocampus.

The rewarded alternation task was performed in an elevated T-maze (Deacon *et al.* 2002) and extra-maze cues[9] were minimized to direct the animal's attention to the black-painted maze with identical target arms. Spatial working memory was assessed with the standard delay between the sample and choice run (IRI = 15 sec in cage) in *Gria1^ΔHipOlf*, *Gria2^ΔHipOlf* and litter control mice. Based on observations of the mouse's behavior at the entrance into the target arms[10], further training of the *Gria1^ΔHipOlf* and *Grin1^ΔHipOlf* genotype was performed with modified delays to evaluate the persistence of spatial working memory. *Gria1^ΔHipOlf* and control mice were tested additionally for a long delay (IRI = 1 min in cage for 32 trials totally). Rewarded alternation in *Grin1^ΔHipOlf* and control mice was assessed for a very short delay (IRI = 3 sec on the experimenter hand), and in presence of an extra-maze cue[11], for a long delay (IRI = 1 min in a cage for 40 trials totally). Previous reports suggested that hippocampal NMDA receptors are not essential for spatial short-term memory but play a role in a

---

[9] The elevated T-maze was placed in an aluminum cage (usually used for electrophysiological set-up) that was enclosed by a black curtain. Only the start arm-facing side was open and it was luminated by two 100 Watt lamps (app. 50 cm above, , 8-12 lux in T-maze).

[10] Upon short IRI, even by resting in a cage, the mouse was so active that it ran directly in the appropriate target arm in the choice run.

[11] We added an extra-maze cue (checkerboard pattern) in the left corner of the surrounding curtain to improve the spatial representation of the individual target arm and simplify spatial differentiation of target arms for the mouse.

delay-dependent working memory task (Steele and Morris, 1999; Rawlins and Olton, 1982).

Unexpected from our previous work (Reisel *et al.* 2002, Schmitt *et al.* 2005), *Gria1$^{\Delta HipOlf}$* mice exhibited an intact spatial working memory. Rewarded alternation performance was indistinguishable compared to litter controls at any single day, and *Gria1$^{\Delta HipOlf}$* mice (n = 8) alternated significantly and similarly compared to litter controls (n = 7) after 40 trials with the standard delay (IRI = 15 sec) between the sample and the choice run (68.1 ± 1.8 % vs. 69.2 ± 1.6 %, p = 0.660). Surprisingly, intact alternation behavior was even observed in the additional task with a 1 min delay. *Gria1$^{\Delta HipOlf}$* and control mice performed this difficult task similarly well, and both showed significant alternation after 40 trials (62.5 ± 3.2 % vs. 64.7 ± 4.3 %, p = 0.676).

In contrast, some impairment was observed upon GluR-B depletion in dorsal CA1/2 and DG sublayers. Whereas *Gria2$^{\Delta HipOlf}$* mice alternated significantly better than chance level, success rates (correct trials in %) on the last two days of the standard T-maze task (ISI = 15 sec) were significantly lower compared to control mice (day 4, 75 ± 5.1 % vs. 93.8 ± 3.6 %, p = 0.035; day 5, 78.1 ± 3.1 % vs. 90.6 ± 3.1 %, p = 0.043). In fact, rewarded alternation after the total 40 trials showed only a weak tendency for impaired working memory (71.9 ± 5.1 % vs. 83.1 ± 4.1 %, p = 0.141) but presumably, this was due to the small animal cohort tested (n = 4 of each genotype).

Upon depletion of NMDA receptors in CA1/2 and DG neurons, *Grin1$^{\Delta HipOlf}$* mice alternated successfully in the simple short-term alternation task (ISI = 1 sec) but failed to alternate in the difficult intermediate-term task. In fact, *Grin1$^{\Delta HipOlf}$* mice (n = 6) exhibited a low success rate on the first (54.2 ± 5.3 % vs. 65.6 ± 6 %, p = 0.194) and second day (56.3 ± 2.8 % vs. 75 ± 7.2 %, p = 0.074) compared to controls (n = 4) in the simple task. But *Grin1$^{\Delta HipOlf}$* mice improved rewarded alternation on the following days (day 5, 70.8 ± 7 % vs. 75 ± 10.2 %, p = 0.748). Performance after 40 trials did not differ significantly between both genotypes (61.1 ± 3.6 % vs. 74 ± 6.5 %, p = 0.144). Spatial working memory performance in the difficult task was severely impaired in *Grin1$^{\Delta HipOlf}$* mice. Whereas *Grin1$^{\Delta HipOlf}$* and control mice showed both rewarded alternation with low success rates on the first day (54.2 ± 7 % vs. 65.6 ± 7.9 %, p = 0.312), only litter controls increased performance significantly during the

training (day 5 vs. day 1, p = 0.033). Significant differences in success rates between genotypes were observed at day 2 (50 ± 3.2 % vs. 68.8. ± 3.6 %, p = 0.006), day 4 (54.2 ± 4.2 % vs. 81.3 ± 8.1 %, p = 0.034) and day 5 (60.4 ± 6 % vs. 93.8 ± 6.2 %, p = 0.006). After 40 trials, $Grin1^{\Delta HipOlf}$ mice did not alternate and were significantly different to control mice (55.8 ± 4.1 % vs. 76.2 ± 1.6 %, p = 0.003).
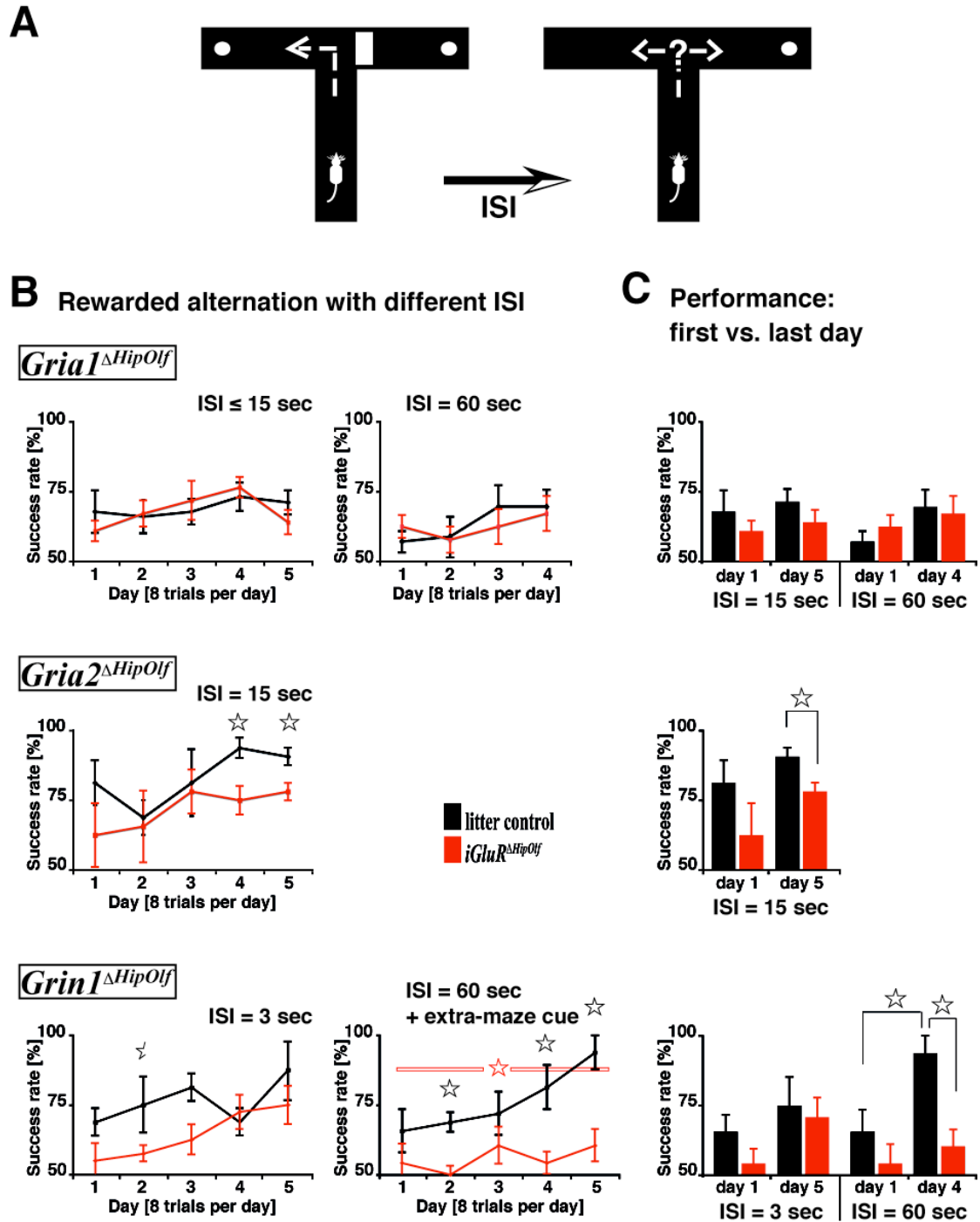

Fig. 2.3.1 Rewarded alternation with short (≤ 15 sec) and long (1 min) ISI of $iGluR^{\Delta HipOlf}$ and litter control mice on the elevated T-maze

(A) Each trial of the delayed match-to-sample task on the T-maze consisted of two runs. In the first (sample) run (left panel), the mouse was forced to choose and find the reward (sweet milk droplet) at the end of one target arm by blocking the other. The blocked target arm in the sample run was changed in a pseudorandom order (four trials of left arm, four trials of right arm, ≤ 2 times repetition per target arm). After resting for a certain delay (≤ 15 sec or 1 min in a new cage; ≤ 5 sec on the hand of the experimentator), the mouse was placed again in the T-maze with access to both target arm. Reward in the previously blocked arm was only achieved by successful performance when the mouse entered directly the rewarded arms. **(B + C)** Rewarded alternation with different IRI of the *Gria1*$^{\Delta HipOlf}$ (IRI of 15 sec and 1 min, n = 8 cKOs, n = 7 control, *first row*), *Gria2*$^{\Delta HipOlf}$ (ISI of 15 sec, n = 4 cKOs, n = 4 control, *second row*) and *Grin1*$^{\Delta HipOlf}$ (IRI of 3 sec and 1 min, n = 6 cKOs, n = 4 control, *third row*). **(B)** Learning curves of daily performance. **(C)** Diagram of performance on the first and last days for certain IRIs. Surprisingly, *Gria1*$^{\Delta HipOlf}$ showed no impairment. Even, alternation in the difficult task (IRI = 1 min) was similar to control. *Gria2*$^{\Delta HipOlf}$ mice were impaired at the last two days of the simple task (IRI = 15 sec), but neither learning (ratio of last vs. first day performance) nor total alternation (performance in all trials) was significantly different. Notably, only a small animal group was tested. *Grin1*$^{\Delta HipOlf}$ mice increased performance in a very simple task (IRI = 3 sec) but even with adding an extra-maze cue, alternation with 1 min ISI was strongly impaired. Alternation on day 4 and 5 (*black star*) and the total performance (*red bar and star*) were significantly different to control mice that even show significant learning during this task. Values represent mean ± SE.

2.3.2. Acquisition of spatial reference memory in *Grin1*$^{\Delta HipOlf}$ mice

Spatial reference memory can be assessed in rodents using the matching-to-place (MTP) paradigm, usually performed on a simple Y-maze, a more complex radial maze or in the Morris watermaze. In contrast to rewarded alternation in the T-maze, the relationship between the spatial cues and the goal location is fixed during all training trials. During the acquisition phase, the mouse learns to find a spatially defined target (sweet milk reward in a certain target arm or hidden platform to escape from water) from different start positions. Subsequently, memory can be tested by minimizing spatial cues in the Y-maze or by removing the hidden platform of the Morris watermaze.

Previous studies indicated controversial observations on the role of hippocampal NMDA receptors on acquisition of spatial reference memory. Whereas AP-5 infusion in the dorsal hippocampus failed to abolish the acquisition of spatial reference memory (Bannerman *et al.* 1999), young animals (< P 75) were severely impaired upon deletion of the NR1 gene exclusively in CA1 neurons (Tsien *et al.* 1996). To investigate the role of NMDA receptors in dorsal CA1/2 and DG neurons of adult

mice, we performed acquisition of the DMTP paradigm on a standard Y-maze for seven days (10 trials daily) in *Grin1^{ΔHipOlf}* and litter control mice (n = 6 each).

Grin1^{ΔHipOlf} mice showed a tendency for impaired performance on day 3 (46.7 ± 7.1 % vs. 68.3 ± 7.5 %, p = 0.063), but performances on all other days were similar to litter controls. Both genotypes exhibited significant acquisition of spatial reference memory (1.84 ± 0.29, p = 0.0399 vs. 2.27 ± 0.56, p = 0.011) in the elevated Y-maze with a similar increase in the success rate (performance ratio of day 7 vs. day 1) compared to litter controls (p = 0.524) and achieved high success rates on day 7 (78.3 ± 10.8 % vs. 80 ± 10 %, p = 0.912).
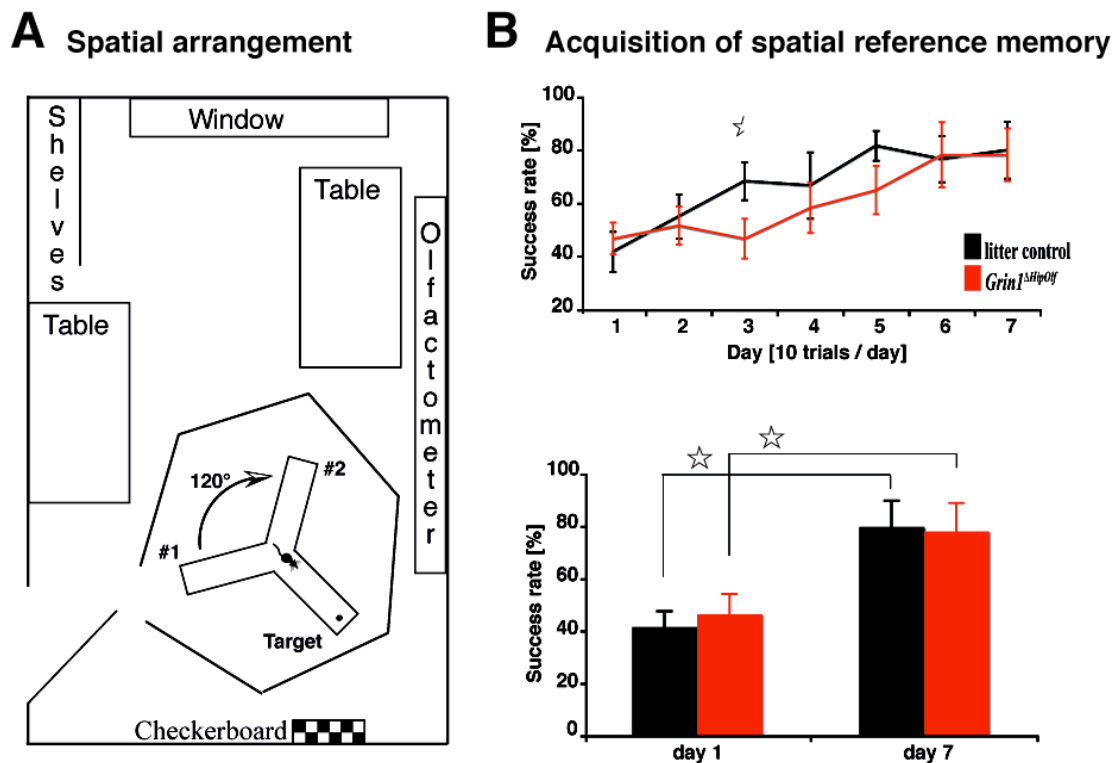
Fig. 2.3.2. Acquisition of spatial reference memory in the elevated Y-maze of *Grin1^{ΔHipOlf}* (n = 6) and litter control mice (n = 6)

(A) Arrangement of spatial cues during rewarded spatial reference learning. Elevated Y-maze was placed in our olfactometer room (white noise, 80 dB, olfactometer turned off) and surrounded by a bast curtain (open six-edged box). Positions of Y-maze arms were marked with three different symbols (green star, blue circle, black-white checkerboard) on the curtain and turned by 120° upon each trial to avoid olfactory intra-maze cues. Direction of turns was also changed daily. **(B)** Learning curves of spatial reference memory in the elevated Y-maze were similar between *Grin1^{ΔHipOlf}* and litter control mice (except tendency of difference on day 3, half of black, open star) and indicated significant improvement in finding the rewarded target arm. Success rates increased significantly from the beginning (day 1) to the end (day 7) of spatial learning in *Grin1^{ΔHipOlf}* and litter control (black, open star) but were similar between genotypes. Values represent mean ± SE.

2.3.3. Additional results in spatial cognitive tasks of Gria1$^{\Delta HipOlf}$ and Grin1$^{\Delta HipOlf}$ mice (D.M. Bannerman, Exp. Psychology, Oxford)

D. Bannerman and co-workers in the department of N. Rawlins (Department of Experimental Psychology, University of Oxford, England) performed more extensive analysis of spatial behavior in *Gria1$^{\Delta HipOlf}$* and *Grin1$^{\Delta HipOlf}$* mice. Results of selected tasks and preliminary figures are summarized here and will be used for discussion of the role of glutamatergic neurotransmission in hippocampal CA1/2 and DG neurons of adult mice. Behavioral values or detailed statistics are not included.

Of particular interest in *Gria1$^{\Delta HipOlf}$* mice, spatial working memory was tested in spontaneous alternation and rewarded alternation on the elevated T-maze as well as in the working memory task on the six-arm radial maze (Reisel *et al.* 2002). *Gria1$^{\Delta HipOlf}$* mice showed significant difference in the spontaneous alternation task on the elevated T-maze but alternated successfully in the rewarded alternation task and displayed similar decrease in working memory errors on the six-arm radial maze (3 arms rewarded, 3 arms not rewarded, re-entry possible) compared to litter controls.

Spatial reference learning and memory was investigated in the Morris watermaze. As expected from global *Gria1* KO mice, depletion of GluR-A in hippocampal CA1/2 and DG neurons of adult mice was not essential for the acquisition of spatial reference memory in the Morris watermaze. *Gria1$^{\Delta HipOlf}$* mice learned and remembered the position of the hidden platform, indicated by a similar decrease in distance traveled in the acquisition trials and similar time spent in the training quadrant during the probe test upon acquisition (after 36 trials), compared to litter controls. Even upon re-positioning of the hidden platform in the opposite quadrant of the initial training quadrant (reversal learning), *Gria1$^{\Delta HipOlf}$* mice showed similar learning (decrease in path length) and memory (time spent in probe test) of spatial reference as do litter controls. In fact, *Gria1$^{\Delta HipOlf}$* mice showed some differences in the Morris watermaze task (less time spent in the first probe test after 24 trials and more distance traveled during the four trials in the second block of reversal learning). But as expected from global *Gria1$^{-/-}$* mice, GluR-A depletion in dorsal CA1/2 neurons and the entire DG sublayer did not affect spatial reference memory in the Morris watermaze in *Gria1$^{\Delta HipOlf}$* mice.

Spatial behavior of Gria1$^{\Delta HipOlf}$ mice

A. Spontaneous alternation
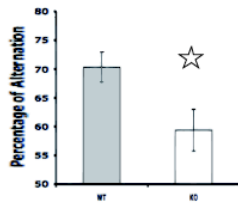
B. Rewarded alternation
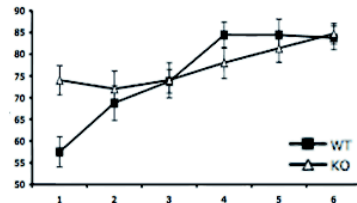
C. Radial six arm maze working memory task
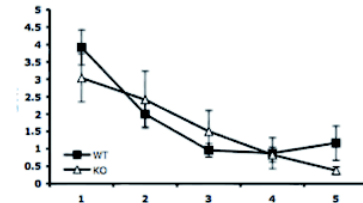
D. Morris watermaze

1. Acquisition and reversal learning of spatial reference memory
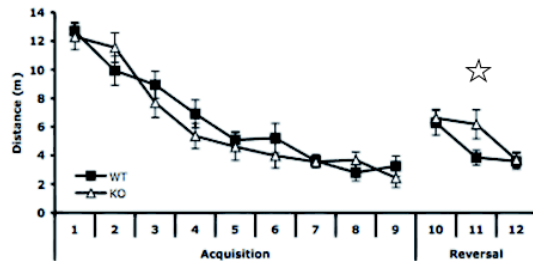
2. Probe tests after 6, 9 and 12 blocks

Fig. 2.3.3. Hippocampus-dependent spatial behavior in *Gria1$^{\Delta HipOlf}$* and litter control mice (n>10, each genotype)

Spatial working memory was assessed in **(A)** the spontaneous alternation (10 trials without reward), **(B)** rewarded alternation (48 trials in 6 days) on the elevated T-maze and **(C)** the working memory task on the six arm radial maze (20 trials in 5 days). *Gria1$^{\Delta HipOlf}$* showed significantly less spontaneous alternation but rewarded learning tasks on T- and radial maze were performed successfully. **(D)** Spatial reference learning and memory was tested in the Morris watermaze. *Gria1$^{\Delta HipOlf}$* and litter control mice exhibited a similar decrease in distance traveled in the acquisition trials and similar time spent in the training quadrant during the probe test upon acquisition (after 36 trials). Re-positioning the hidden platform in the opposite quadrant assessed reversal learning and memory. *Gria1$^{\Delta HipOlf}$* and litter control mice exhibited a similar decrease in distance traveled in the 12 reversal trials and similar time spent in the training quadrant during the probe test upon reversal learning. Significant differences were observed in time spent in the first probe test (after 24 trials) and distance traveled during the second block (of 4 trials) of reversal learning. Values represent mean ± SE.

Spatial working memory in $Grin1^{\Delta HipOlf}$ and control mice was assessed in the spontaneous and the rewarded alternation tasks on the elevated T-maze as well as in the working memory task on the six arm radial maze. $Grin1^{\Delta HipOlf}$ mice showed less spontaneous alternation on the T-maze but rewarded alternation with the standard delay of 15 sec between sample and choice run was similar to litter controls. However, $Grin1^{\Delta HipOlf}$ mice made more errors in the spatial working memory task on the radial maze and did not reduce the error rate during training as observed in litter controls.

Of particular interest in $Grin1^{\Delta HipOlf}$ mice, acquisition of spatial reference was assessed on the elevated Y-Maze, the six arm radial maze and in the Morris watermaze. In general, $Grin1^{\Delta HipOlf}$ mice were able to acquire spatial reference memories on Y-maze and in watermaze. Choosing the right of two target arms to find a milk reward (correct choice in %) and finding a hidden platform to escape from water (path length in m) was learned significantly and similarly as by litter controls. $Grin1^{\Delta HipOlf}$ mice were also able to recall the acquired spatial reference. When tested in probe tests after 24 and 36 trials (removal of hidden platform), $Grin1^{\Delta HipOlf}$ mice and litter controls spent more than 50% of the total time in the training quadrant for searching the platform. In contrast, $Grin1^{\Delta HipOlf}$ mice were impaired in the acquisition of spatial reference on the radial maze. Choosing three of six arms to find milk rewards (in errors, re-entry blocked) was learned in $Grin1^{\Delta HipOlf}$ mice as indicated by a significant decrease in error rate, but not as efficiently as in litter controls. $Grin1^{\Delta HipOlf}$ mice showed also impairment in reversal learning of spatial reference in the Morris watermaze. After initial acquisition and probe tests, the hidden platform was placed in the quadrant opposite of the initial training quadrant. $Grin1^{\Delta HipOlf}$ mice traveled more distance (path length in m) to find the new-placed platform. In the probe test after 12 trials of reversal learning, $Grin1^{\Delta HipOlf}$ mice did not prefer significantly the new training quadrants as litter controls.
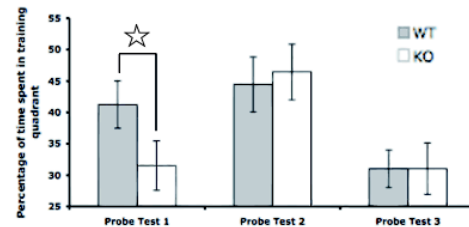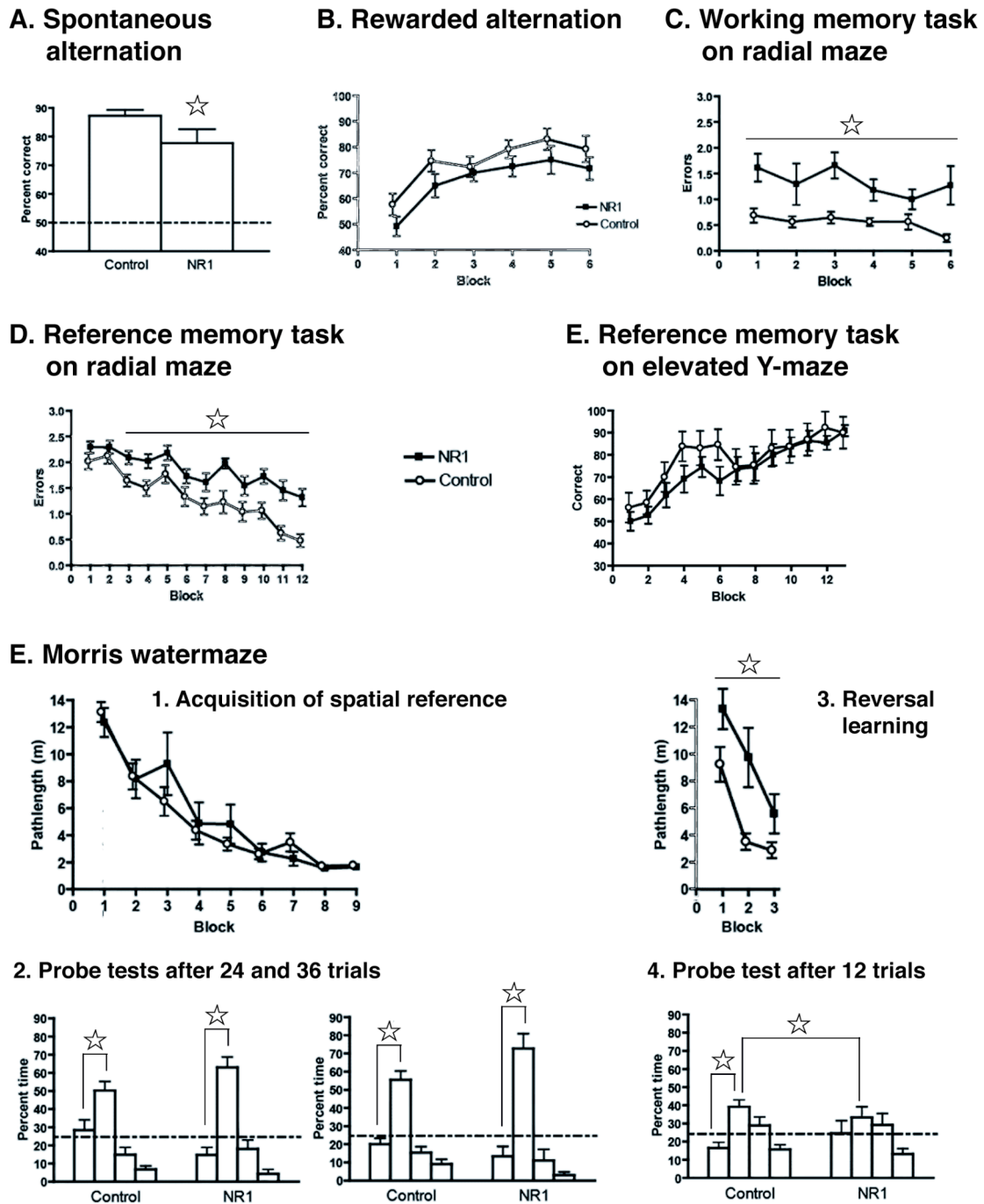
Fig. 2.3.4. Hippocampus-dependent, spatial behavior in *Grin1*^{ΔHipOlf} **and litter control mice (n>10, each genotype).**

Spatial working memory was assessed in **(A)** the spontaneous alternation and **(B)** the rewarded alternation task on the elevated T-maze as well as **(C)** the *delayed non-matching to sample* task on the six arm radial maze. *Grin1*^{ΔHipOlf} mice showed less spontaneous alternation on the T-maze but rewarded alternation with the standard delay of 15 sec between sample and choice run was similar to litter controls. However, spatial working memory on the six arm radial maze (three arms baited vs. three not baited, re-entry possible) was impaired in *Grin1*^{ΔHipOlf} mice. Acquisition of spatial reference was assessed on **(D)** the elevated Y-Maze, **(E)** the six arm radial maze and **(F)** in the Morris watermaze. Whereas, *Grin1*^{ΔHipOlf} mice were impaired to acquire spatial reference on the radial maze, acquisition

spatial reference memories on Y-maze and in watermaze were intact. *Grin1*$^{\Delta HipOlf}$ mice were also able to recall the acquired spatial reference. *Grin1*$^{\Delta HipOlf}$ mice and litter controls spent more than 50% of the total time in the training quadrant for searching the platform in the probe tests. But *Grin1*$^{\Delta HipOlf}$ mice showed impaired in reversal learning of spatial reference in the Morris watermaze. *Grin1*$^{\Delta HipOlf}$ mice traveled more distance to find the new-placed platform. *Grin1*$^{\Delta HipOlf}$ mice did not prefer significantly the training quadrants as litter controls the probe test, subsequent to the reversal training. Values represent mean ± SE.

3. Discussion

In the present study, functional segregation of ionotropic glutamate receptor function (AMPA receptors that contain the GluR-A or GluR-B subunit or all NMDA receptors) in restricted principal cell layers of the well-developed hippocampal formation (deficient in DG, CA1, CA2, Sub vs. intact in CA3, PreS, ParS, Ent) in adult mice was achieved. Cre suppression in the mouse embryo of double transgenic $Tg^{CN12\text{-}itTA}$ / Tg^{LC1} mice and selective recombination of floxed $Gria1$, $Gria2$ or $Grin1$ loci allowed the generation of three mutant mouse models with similar spatial and temporal specificity. Behavioral analysis of $Gria2^{\Delta HipOlf}$ or $Grin1^{\Delta HipOlf}$ mice indicated impairment in spatial working memory. However, the expected impairment of GluR-A-depleted $Gria1^{\Delta HipOlf}$ mice was not observed. In contrast to previous reports (Morris et al., 1982; Tsien et al., 1996), NR1 depletion in adult $Grin1^{\Delta HipOlf}$ mice did not impair the acquisition of spatial reference in the Morris watermaze or in the Y-maze. Impairment in spatial reference was observed in the six-arm radial maze and in the efficiency of reversal learning in the Morris watermaze.

3.1. Temporal control of $Tg^{CN12\text{-}itTA}$ / Tg^{LC1}-driven recombination in the mouse brain

Embryonic suppression of itTA activity in the mouse embryo permitted a sublayer-restricted recombination in the hippocampal formation (DG, CA1, CA2) and olfactory system (PC) of transgenic $Tg^{CN12\text{-}itTA}$ / Tg^{LC1} / $Rosa26R$ mice (termed as $Rosa26R^{\Delta HipOlf}$ mice) at a young post-pubertal age (P45). This transgenic activity resembled the expression profile of $Tg^{CN12\text{-}itTA}$-induced β-gal and GFP-tagged GluR-B fusion protein from the Tg^{OCN1} locus in dox-naive, so-called $GluR\text{-}B^{Rescue}$ mice, generated in a previous study (Shimshek et al., 2005).

However, the Cre expression and recombination profile in dox-naive $Tg^{CN12\text{-}itTA}$ / Tg^{LC1} / $Rosa26R$ mice and $Rosa26R^{\Delta HipOlf}$ mice at adult ages revealed additional transgenic itTA-induced activity. Most obviously, dox-naive animals showed a widespread β-gal activity (monitored by sensitive X-gal staining; 24 h at 37°C) in the whole forebrain but a restricted Cre protein pattern (visualized by anti-Cre DAB immunostaining) at P45. Notably, while the Cre protein expression was dependent on permanent itTA-dependent induction of the P_{tetBi} promoter in the Tg^{LC1} locus, the

Rosa26 promoter expressed β-galactosidase constitutively upon Cre-mediated recombination. Hence, the widespread X-gal pattern in dox-naive $Tg^{CN12\text{-}itTA}$ / Tg^{LC1} / *Rosa26R* mice was presumably evoked by embryonic itTA expression in $Tg^{CN12\text{-}itTA}$ mice. Administration of 50 mg/l dox-containing drinking water during breeding and pregnancy of mothers generating triple positive $Tg^{CN12\text{-}itTA}$ / Tg^{LC1} / *Rosa26R* mice (dox until birth, now termed $Rosa26R^{\Delta HipOlf}$) confirmed this hypothesis. $Rosa26R^{\Delta HipOlf}$ mice exhibited now both, the expected Cre protein and X-gal profile at P45. The slow induction of postnatal Cre expression in $Rosa26R^{\Delta HipOlf}$ mice upon dox treatment until birth was already observed previously (Krestel et al., 2004).

In addition to the unexpected embryonic activity in the $Tg^{CN12\text{-}itTA}$ / Tg^{LC1} model, the recombination profile in $Rosa26R^{\Delta HipOlf}$ mice showed an age-dependent accumulation of transgenic activity, often observed in transgenic mice (e.g. Fukaya et al., 2003). From P45 until the age of the first behavioral analysis (P150), $Tg^{CN12\text{-}itTA}$ / Tg^{LC1}-mediated recombination were observed in additional sublayers of the hippocampal formation (IG, S) and in particular, of the olfactory system (e.g. OB, DTT, VTT, Tu). Sparse cellular X-gal signals were also detected in the CA3 subfield and in defined layers (II and V/VI) of cortical (e.g. FrA, M1, M2, AuD) and subcortical (e.g. BLA) structures. With a few, astonishing exceptions, recombination was still restricted to principal cell layers and is highly concentrated in specific sublayers in the hippocampal formation and the olfactory system.

Strong recombination in the hippocampal formation was restricted mainly to CA1, CA2, DG and the anterior part of the subiculum, suggesting functional segregation from the other hippocampal sublayers (CA3, PrS, PaS and Ent) and cortical brain areas when the $Tg^{CN12\text{-}itTA}$ / Tg^{LC1} genotype will be used to manipulate certain ionotropic glutamate receptors. Importantly for the generation and behavioral analysis of conditional gene KOs, this pattern remained stable in one-year-old $Rosa26^{\Delta HipOlf}$ mice.

However, strong recombination in the olfactory system was not only observed in the piriform cortex (PC) or other parts of the primary olfactory cortex (POC) but spread also to other functional sublayers of the olfactory system Transgenic activity was also observed in certain parts of the medial olfactory cortex (MOC; including tenia tecta, TT, dorsal peduncle, DPC) and *pars medialis* of the anterior olfactory nucleus (AON), but only sparsely in the anterior olfactory cortex (AOC; reviewed in

Brujnes et al., 2005). These brain areas were not investigated systematically with lesion and tracing studies, and their exact role in the olfactory system is still not resolved. However, based on the wiring model proposed by Haberly (2001), the AOC is innervated directly by mitral and tufted cells, the projection neurons of the MOB, and is implicated in the direct processing of olfactory information before transmitting the "olfactory code" to the primary olfactory cortex (POC). In contrast, MOC and *pars medialis* do not receive direct input from the MOB, but innervate the AOC after receiving information of higher brain areas such as via back propagation of information from the POC or via the indusium griseum (IG) from the hippocampal formation. Presumably, these structures have an indirect modulatory activity to the processing of the olfactory code by the AOC.
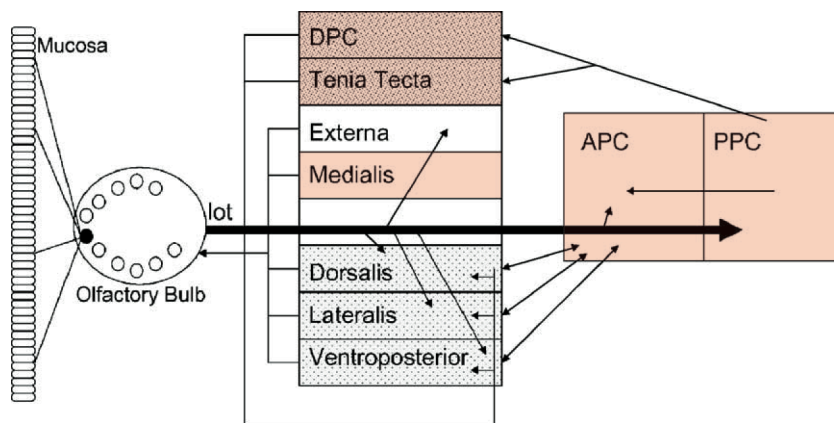
Fig. 3.1. Wiring model of the olfactory cortex proposed by L.B. Haberly (2001)

Pars externa, medialis, dorsalis, lateralis and *ventroposterior* are commonly summarized as anterior olfactory nucleus (AON). Based on its wiring, Haberly and others examined *pars medialis* separately and summarized the residual layers as anterior olfactory cortex (AOC) APC, anterior piriform cortex; DPC, dorsal peduncle; lot, lateral olfactory tract; PPC, posterior piriform cortex. Red boxes indicate strong recombination in the $iGluR^{\Delta HipOlf}$ mouse models.

But surprisingly, $Tg^{CN12\text{-}itTA}$ / Tg^{LC1}-mediated recombination was also observed in inhibitory neurons of the main olfactory bulb (MOB), the subventricular zone (SVZ), the rostral migratory stream (RNS), the caudate putamen (CPu) and within the corpus callosum (CC). These structures are characteristic for neurogenesis (e.g. Reyes et al., 1992). Radial glia cells divide asymmetrically within the SVZ in intermediate progenitor cells and give rise to all classes of brain cells (Merkle et al., 2004). Most prominent are olfactory neuroblasts that replace inhibitory granule and perigranule cell in the main olfactory bulb (reviewed e.g. in Lledo et al., 2007). The nature of

olfactory neuroblasts was definitely proven by a temporal X-gal accumulation along the RMS and subsequently in MOB sublayers. Transgenic Cre expression was predominately found in RMS brain areas and not in cellular MOB layers. In addition, transgenic Cre expression was highly co-localized with doublecortin (DCX), characteristic for olfactory neuroblasts. However, further evidence is needed to verify the transgenic activity in additional progenitor cell types throughout the brain, generated by dividing radial glia cells (RC2, radial glial process; CD24, ependymal cell; Olig2, oligodendrocyte; GFAP, glial fibrillary acidic protein; Merkle et al., 2004).

In summary, the analysis of the recombination efficiency in dox-naive and embryonic dox-suppressed, triple positive $Tg^{CN12\text{-}itTA}$ / Tg^{LC1} / $Rosa26R$ mice at various ages of the behavioral training period revealed many additional brain areas (esp. neural stem cells and MOC) with $Tg^{CN12\text{-}itTA}$-induced transgenic activity that had never been observed in $GluR\text{-}B^{Rescue}$ mice ($Tg^{CN12\text{-}itTA}$ / Tg^{OCN1} in forebrain-specific GluR-B deleted background; Shimshek et al., 2005). As observed in different mouse models with itTA or tTA expression (e.g. KT1, Mayford et al., 1996; Gnit, Th. Bus, diploma thesis, Uni Heidelberg, 2005) to induce transgenic activity from different tet-responder mouse lines (e.g. G3, Krestel et al., 2003; SA, Mack et al., 1999), the Cre-expressing tet-responder line Tg^{LC1} was the most accessible transgenic tet-responder in the mouse brain, whereas the Tg^{OCN1} responder line was not inducible in all neurons (Th. Bus, diploma thesis, Uni Heidelberg, 2005).

The high recombination efficiency in additional sublayers of the hippocampal formation and the olfactory system, observed in adult $Rosa26R^{\Delta HipOlf}$ mice, will exacerbate the interpretation of behavioral phenotypes in $Tg^{CN12\text{-}itTA}$ / Tg^{LC1}-mediated gene KOs of excitatory glutamate receptors. Nevertheless, $Tg^{CN12\text{-}itTA}$ / Tg^{LC1}-driven recombination affected restricted sublayers, and might prove invaluable for separating explicit functions in these brain systems.

3.2. Depletion of excitatory receptor pools in adult neuronal networks

The depletion of NMDA receptors or any of the two AMPA receptor subtypes GluR-A and GluR-B was achieved in restricted hippocampal sublayers (DG, CA1, CA2) of adult $Gria1^{\Delta HipOlf}$, $Gria2^{\Delta HipOlf}$ and $Grin1^{\Delta HipOlf}$ mice. Depletion of receptor subtypes with a similar spatial and temporal specificity allowed the dissection of

ionotropic glutamate receptor (iGluR) function in three main properties (GluR-A dependent LTP; GluR-B restricted Ca^{2+} permeability of AMPA receptors; NMDA receptor dependent LTP) within individual hippocampal sublayers (DG, CA1, CA2, vs. CA3, Ent) and towards cortical and subcortical brain regions of adult mice.

Surprisingly, the temporal decrease in the protein levels of manipulated iGluR subtypes was not finished before P120-P150 in DG and CA1 of $Gria1^{\Delta HipOlf}$, $Gria2^{\Delta HipOlf}$ or $Grin1^{\Delta HipOlf}$ mice. Depletion of iGluR subtypes in the soma of affected principal neurons was relatively rapidly, however, a detectable protein level in the layers of apical and basal processes remained for three to four months. The slow depletion in neuronal processes was not observed in previous mouse models using the αCaMKII promoter (e.g. in $GluR-B^{\Delta Fb}$ using $Tg^{CaMKII-Cre}$ generated by Mantamadiotis et al., 2002). But these mutant mice expressed the Cre recombinase in early postnatal days before the increase in iGluR expression between P7 and P14 (Jensen et al., 2003). In contrast to these models, Cre expression in $iGluR^{\Delta HipOlf}$ mice was not induced before P28 when the expression of iGluR subtypes was already high in the hippocampus.

Additional support for the importance of temporally restricted gene manipulation in well-established neuronal networks of the hippocampal formation was observed in $Gria2^{\Delta HipOlf}$ mice. Previous studies suggested that GluR-B-lacking AMPA receptors are expressed predominantly in response to excessive glutamatergic neurotransmission, e.g. in kainate-induced or electroconvulsive ("kindled mice") epileptic seizures. It was further hypothesized that the excessive influx of Ca^{2+} through NMDA receptors and AMPA receptors lacking GluR-B upon the endogenous glutamate release is sufficient to induce a cascade of reactions leading to cell death (Ca^{2+}-induced neuro-toxicity; Lipton and Rosenberg, 1994, Tanaka et al. 2000). However, our previous observations in forebrain-specific $GluR-B^{\Delta FB}$ and RNA editing-deficient $GluR-B^{QFb}$ mice (Shimshek et al., 2006) did not confirm but qualified this 'GluR-B hypothesis' (Pollard et al., 1993; Friedman et al., 1994; 1997). Gene manipulation of the $Gria2$ loci in the early postnatal forebrain, resulting either in GluR-B-lacking or GluR-B(Q)-containing AMPA receptors, had long-lasting functional and structural consequences in the hippocampus. However, loss of principal neurons was only observed in CA3 neurons of $GluR-B^{\Delta FB}$ mice but not in any other hippocampal sublayer and not even in CA3 neurons of $GluR-B^{QFb}$ mice that

exhibited a much stronger Ca^{2+} influx through functional AMPA receptors and were prone to epileptic seizures (Krestel et al., 2004). Nevertheless, both mouse models showed rearrangements of DG mossy fiber terminals (termed as 'sprouting'), although the extent of mossy fiber sprouting was much lower than characteristically observed in brains of "kindled mice" (e.g. Vaidya et al., 1999). Most impairment in *GluR-B^{ΔFB}* or *GluR-B^{QFb}* mice were not directly mediated by changes in AMPA receptor signaling, but were more likely secondary to the AMPA receptor-mediated Ca^{2+} influx. Parvalbumin-positive interneurons in the DG subfield (and somatostatin-positive interneurons in CA1 and DG of *GluR-B^{QFb}* mice) were significantly reduced, neurogenesis at the DG subgranular zone (SGZ) was nearly absent in *GluR-B^{ΔFB}* mice and was increased in *GluR-B^{QFb}* mice compared to litter control mice. Postnatal GluR-B depletion in the hippocampus of *GluR-B^{ΔFB}* mice did not impair fLTP at Schaffer collateral - CA1 synapses, but these synapses exhibited reduced excitatory neurotransmission with increased synaptic excitability, indicating lower expression of AMPA receptors at synapses of GluR-B depleted neurons (Shimshek et al., 2006). Hence, manipulations of the GluR-B gene in forebrain-specific *GluR-B^{ΔFB}* and *GluR-B^{QFb}* mice had long-lasting consequences for hippocampal anatomy and function.

However, upon GluR-B depletion in DG, CA1 and CA2 of *Gria2^{ΔHipOlf}* mice, no long-lasting anatomical changes were detected in the well-established network of the adult hippocampus. We quantified axonal terminals of sprouting DG mossy fibers in the inner molecular layer (Timm staining) and parvalbumin-positive interneurons in DG and CA1. Initial results indicated also no remarkable difference in the number of BrdU-labeled newborn cells at the SGZ, although additional experiments are needed. Of particular interest, Vidar Jensen and ∅ivind Hvalby (University of Oslo, Norway) investigate the electrophysiological properties in the anatomically well-established hippocampus at the moment. Nevertheless, adult GluR-B depletion in DG, CA1 and CA2 had no remarkable and long-lasting consequences for hippocampal anatomy. Therefore, electrophysiological investigation of the hippocampal circuitry and more extensive behavioral analysis of *Gria2^{ΔHipOlf}* mice might yield further insight into synaptic plasticity-underlying memory and behavior.

Our initial experiments to assess electrophysiological functions in *Grin1^{ΔHipOlf}* mice revealed a functional dissection of the CA1 and CA3 sublayers in the dorsal hippocampal formation. Whereas the elaborate NR1 depletion in the dorsal

hippocampus ablated NMDAR-dependent synaptic plasticity (field LTP) in the CA1 subfield, the field property in CA3 was not affected. However, field recordings stimulate and measure a large number of neurons. Known from the extensive recombination analysis of $Rosa26R^{AHipOlf}$ mice (please refer to 2.1.3.), sparse CA3 neurons exhibited $Tg^{CN12\text{-}itTA}$ / Tg^{LC1}-mediated recombination and will deplete the NR1 protein. Nevertheless, NR1 depletion in the CA3 subfield was minor and not sufficient to impair fLTP in comparison to litter control mice.

The functional segregation of ionotropic glutamate receptor function in the CA1 subfield relative to the CA3 region, entorhinal cortex and other cortical brain areas (e.g. perirhinal cortex, temporal association cortex) in well-established networks of the adult mouse brain might offer further insight into the hippocampal role in cognitive behavior, independently from developmental aspects. Computational models based on the wiring scheme between principal cell layers of the corresponding brain areas and lesion experiments of individual layers indicated a strong convergence of projection neurons onto the CA3 pyramidal neurons and a great divergence again back to cortical brain areas from the CA1 pyramidal neurons via the subiculum. The CA3 subfield with its extensive auto-associative network (recurrent collaterals) was thought to support rapid spatial one-trial learning, spatial short-term memory, sequence learning and spatial pattern completion, whereas the CA1 subfield was thought to be responsible for processing temporal information required for temporal pattern separation and associations across time. The DG was implicated in spatial pattern separation (Rolls, Kesner, 2006).
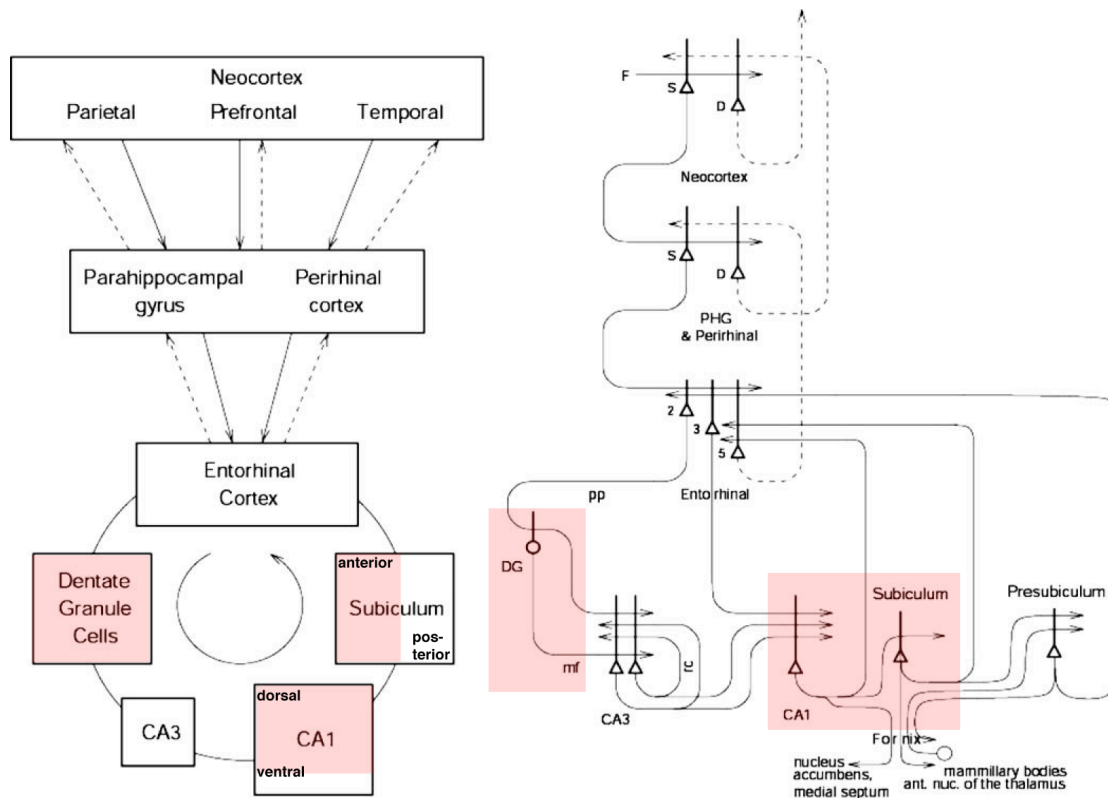
Fig. 3.2. Simplified wiring model of the hippocampal formation and cortical brain areas thought to be involved critically in cognitive, declarative memory

Forward connections (solid lines) from areas of cerebral association neocortex via the parahippocampal gyrus and perirhinal cortex, and entorhinal cortex, to the hippocampus; back-projections (dashed lines) via the hippocampal CA1 pyramidal cells, subiculum, and parahippocampal gyrus to the neocortex. There is great convergence in the forward connections down to the single network implemented in the CA3 pyramidal cells. Great divergence is observed again in the back-projections up, again from the CA1 pyramidal cells via the subiculum. Left: block diagram. Right: more detailed representation of some of the principal excitatory neurons in the pathway. D, deep pyramidal cells; DG, dentate granule cells; F, forward inputs to areas of the association cortex from preceding cortical areas in the hierarchy; mf, mossy fibers; PHG, parahippocampal gyrus and perirhinal cortex; pp, perforant path; rc, recurrent collateral of the CA3 pyramidal cells; S, superficial pyramidal cells; 2, pyramidal cells in layer II of the entorhinal cortex; 3, pyramidal cells in layer III. The thick lines above the cell bodies represent the dendrites. Red boxes indicate strong recombination in the *iGluR*$^{\Delta HipOlf}$ mouse models (adapted from E.T. Rolls, R.P.Kesner, 2006).

3.3. Behavioral analysis

The rodent's hippocampal formation is the most extensively investigated model system for cognitive memory. It is easily accessible by stereo-tactical injections and can be manipulated with various techniques. In addition, multiple behavioral tasks have been developed that monitor the role of the hippocampus in spontaneous, associative and cognitive behavior. Hippocampal function in rodents is mainly tested for spatial forms of cognitive memory, in particular for spatial working memory in the *delayed non-matching-to-place* (DNMTP) paradigm and for spatial reference memory in the *matching-to-place* (MTP) paradigm.

The behavioral analysis of *Gria1*$^{\Delta HipOlf}$ and *Grin1*$^{\Delta HipOlf}$ mice was performed in Heidelberg and more extensively in Oxford (N. Rawlins, D. Bannerman, Exp. Psychology, England). Although, the behavioral analysis in Heidelberg included only the rewarded alternation task on the elevated T-maze for spatial working memory, and the acquisition phase on the Y-maze in *Grin1*$^{\Delta HipOlf}$ mice for spatial reference learning, the behavioral performances in both laboratories revealed reliable phenotypes. Indeed the ratios of performances between genotypes were highly reproducible, although the absolute values of genotypes differed. Variability in behavioral performances was often observed depending on the handling of the mice and other environmental conditions (personal experience & communication with D. Bannerman).

3.3.1 Spatial working memory

The most striking results, unexpected from our previous work, were that adult *Gria1*$^{\Delta HipOlf}$ mice with GluR-A depletion in DG, CA1 and CA2 principal neurons were not impaired in the rewarded learning tasks for spatial working memory. *Gria1*$^{\Delta HipOlf}$ mice performed similar to litter controls, even when a delay of 1 min occurred between the sample run and the choice run on the elevated T-maze and in the more difficult six arm radial maze. Only a small impairment was detected in the eight trials of the spontaneous alternation on the T-maze. However, global depletion of the GluR-A protein in *Gria1*$^{-/-}$ mice abolished spatial working memory, tested on the T-maze with the standard delay of 15 sec. *Gria1*$^{-/-}$ mice performed at chance level (50% alternation; Reisel et al., 2002). In addition, restoration of GFP-tagged GluR-A

in principal neurons of the forebrain rescued the T-maze performance partially (Schmitt et al., 2005; reviewed in Sanderson et al., 2008). Transgenic GluR-A restoration, induced by transgenic αCaMKII promoter-driven tTA (Tg^{KT1}; Mayford et al. 1996), was especially pronounced in the CA1 subfield of the dorsal hippocampus (69 ± 4 %; Schmitt et al., 2005). Combined with findings in lesion studies and of GluR-A dependent LTP at Schaffer collateral - CA1 synapses, the GluR-A subunit in CA1 principal neurons was thought to play an essential role in the spatial working memory, at least to a substantial part. GluR-A containing AMPA receptors in inhibitory neurons (e.g. parvalbumin-positive neurons) might underlie the residual fraction of the spatial working memory, as indicated by parvalbumin-specific *Gria1* deletion in transgenic *GluR-A$^{PVCre -/-}$* mice (Fuchs et al., 2007).
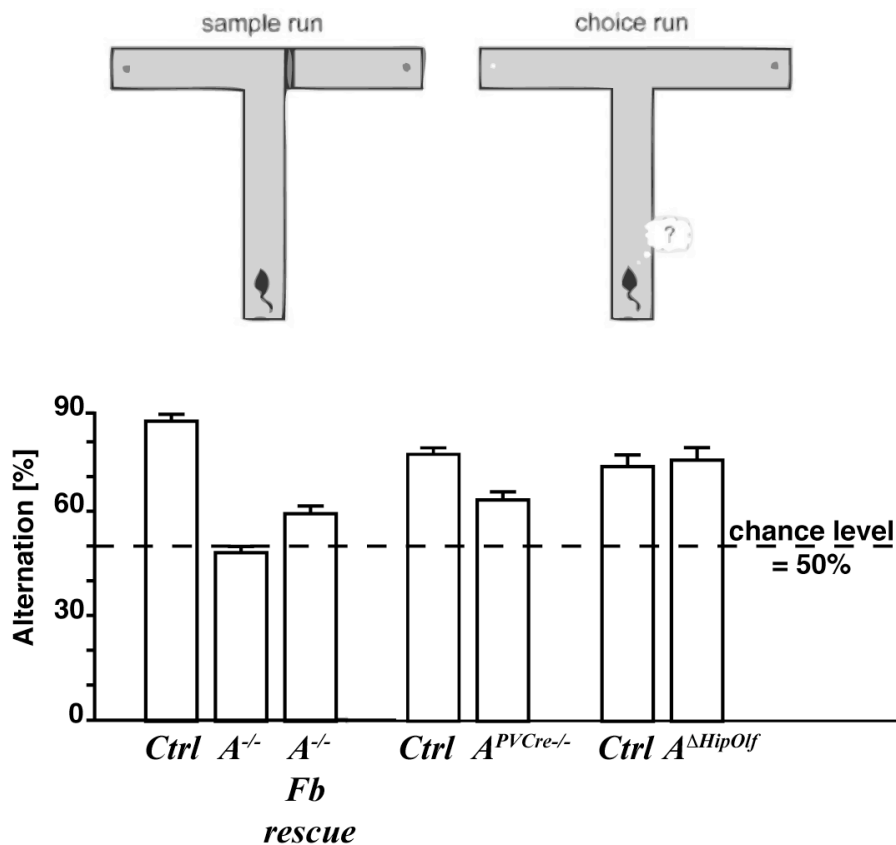
Fig. 3.3. GluR-A deletion, either globally or in parvalbumin-positive interneurons, impaired spatial working memory performance during the DNMTP task on the elevated T-maze. But surprisingly, GluR-A deletion in principal DG, CA1 and CA2 neurons in the adult mouse brain did not impair spatial working memory performance in this rewarded alternation task.

Top: The mouse is forced into either the left or right goal arm, according to a pseudorandom sequence, and receives a milk reward. During the choice run (right) the mouse has to go directly to the opposite (previously unvisited) goal arm to find a second milk reward. Both runs are delayed by the standard

inter run interval (IRI) of 15 seconds. 40 trials in total on 5 successive days were performed. **Bottom:** Mean percentage of trials on which the mouse alternated successfully (± SEM). *Left:*: performance of control (Ctrl) and GluR-A$^{-/-}$ mice (data taken from Reisel et al., 2002). *Center:* Performance of control (Ctrl) and parvalbumin-restricted *GluR-A$^{PVCre-/-}$* mutant (data taken from Fuchs et al. 2007). *Right:* Performance of control (Ctrl) and *Gria1$^{\Delta HipOlf}$* mice. Broken line equates to chance performance of 50%.

The most obvious difference in the hippocampus between these T-maze impaired mouse models and the T-maze intact *Gria1$^{\Delta HipOlf}$* mice was the developmental stage when gene recombination occurred. While the T-maze impaired models affected glutamatergic neurotransmission either globally or at early postnatal age, *Gria1$^{\Delta HipOlf}$* mice grew up normally until at least P28 (initiation of Cre recombinase). Along this line of evidence, the GluR-A protein might play a role in the maturation of a balanced network between hippocampal principal and inhibitory neurons. Additional support for a developmental role of GluR-A in the hippocampus came from viral deletion of the *Gria1* gene. Stereo-tactical injections of neuron-restrictive Cre expressing rAAV (driven by a synapsin promoter) in the hippocampus of adult mice with floxed *Gria1* alleles did not impair spatial working memory performance in rewarded alternation tasks. In addition, conditional restoration by GluR-A expressing rAAV in adult *Gria1$^{-/-}$* mice does not rescue their behavioral performance (F. Freudenberg, Dissertation, Uni Heidelberg, 2009; in preparation).

Gria1$^{\Delta HipOlf}$ mice showed high GluR-A depletion in the DG, CA1 and CA2 subfields, but other parts of the hippocampal formation and cortical brain areas remained manly unaffected. All T-maze impaired models affect the GluR-A protein either globally or in the whole forebrain. A possible role of the frontal association cortex, which is thought to be involved in working memory tasks in primates (Goldman-Rakic, 1987), was excluded by lesion experiments that did not change the rewarded alternation performance in mice (D. Bannerman, unpublished data). This confirmed the pivotal role of the hippocampal formation in the working memory task tested in rodents. Hence, structures of the hippocampal formation that were not affected in *Gria1$^{\Delta HipOlf}$* mice might contribute to the spatial working memory. Most likely, the medial entorhinal cortex (MEnt) might be critically implicated in the hippocampal memory system. The discovery of spatially related firing cells like place cells, grid cells and head direction cells drew more attention to this structure of the

hippocampal formation, but lesion experiments combined with rewarded alternation tasks are still missing.

Different from *Gria1^{ΔHipOlf}* mice, GluR-B in *Gria2^{ΔHipOlf}* mice or all NMDA receptors in *Grin1^{ΔHipOlf}* mice in DG, CA1 and CA2 affected the behavioral performance in rewarded alternation tasks. *Gria2^{ΔHipOlf}* mice alternated significantly on the elevated T-maze but did not increase their alternation in contrast to litter control mice during the five-day training protocol (eight trials per day). Unfortunately, the tested cohort was very small (n=4, each genotype) and thus, further confirmation is needed. *Grin1^{ΔHipOlf}* mice learned the T-maze task with a very short delay (~ 3 sec), but performed nearly at chance level when a long delay (1 min) separated both runs (sample and choice run) of the rewarded alternation trial. This delay-dependent impairment in the spatial working memory was proposed by previous studies that observed the delay-dependent impairment on the T-maze (Rawlins and Olton, 1982; McHugh et al., 2007) and in the water maze (Morris et al., 1982) upon infusion of the NMDA receptor antagonist AP-5 in the dorsal hippocampus. Consistently, *Grin1^{ΔHipOlf}* mice were also impaired in the six-arm radial maze that is more difficult than the short delayed T-maze task, since the animals need to remember three previously visited target arms.

The comparison of behavioral performances in the spatial working memory tasks of *Gria1^{ΔHipOlf}*, *Gria2^{ΔHipOlf}* and *Grin1^{ΔHipOlf}* mice demonstrated clearly that the transgenically affected principal neurons, i.e. DG, CA1 and CA2 pyramidal cells of the hippocampal formation at adult ages, are critically involved in the spatial working memory. While the depletion of GluR-B or NR1 in these neurons confirmed previous observations of an impaired or delay-dependent working memory (Rawlins and Olton; Shimshek et al., 2006), GluR-A containing AMPA receptors in these projection neurons were surprisingly not essential at adult ages for the spatial working memory.

Notably, *Gria1^{ΔHipOlf}* mice showed still a hyperactive phenotype, like the global *Gria1^{-/-}* mice, in novel environments, when observed in an open field and by Pavlovian fear conditioning (data not included in this thesis). Together with the impairment in the spontaneous alternation task, the hyperactivity might be based on impairment in a short-term habituation process. Further analysis of *Gria1^{ΔHipOlf}* mice in one-trial spatial working memory (Sanderson et al., 2007) and non-spatial,

hippocampus-dependent, differential reinforcement of low rates of responding (DLR)-paradigm (impaired in *Gria1*$^{-/-}$; Reisel et al., 2005) is needed.

3.3.2 Spatial reference memory

GluR-A containing AMPA receptors in DG, CA1 and CA2 of adult mice were not essential for the learning or memory of spatial references in the Morris watermaze. This observation was expected since even global *Gria1*$^{-/-}$ mice exhibited normal spatial reference memory (Reisel et al., 2002). In fact, *Gria1*$^{\Delta HipOlf}$ mice spent less time than litter control mice in the training quadrant upon removal of the hidden platform in the first probe test. Nevertheless, *Gria1*$^{\Delta HipOlf}$ mice remembered the training quadrant. They spent more than 25 % (chance level) of the total time in the appropriate quadrant of the watermaze. The observed deficit might be based on the hyperactive phenotype in these mice. Hyperactivity in global *Gria1*$^{-/-}$ mice was often observed (Bannerman et al., 2004) and even *Gria1*$^{\Delta HipOlf}$ mice showed hyperactivity in response to novelty in spontaneous and associative tasks (spatial open field, cued and contextual fear conditioning, not included in the thesis). However, the hyperactive phenotype did not account for impairment in spatial reference memory. Performance of *Gria1*$^{\Delta HipOlf}$ mice was indistinguishable to controls in all acquisition trials and also in the second probe test after 36 acquisition trials.

Unfortunately, GluR-B depleted *Gria2*$^{\Delta HipOlf}$ mice were not yet tested in any spatial reference memory paradigm. Based on previous observations in forebrain-specific GluR-B mutant mice (*GluR-B*$^{\Delta Fb}$, Shimshek et al., 2006), the spatial reference memory might require GluR-B containing AMPA receptors. However, the depletion of GluR-B in these *GluR-B*$^{\Delta Fb}$ mice mediated also long-lasting effects in the hippocampal architecture that hindered the interpretation of the observed behavioral impairment. In contrast, GluR-B depletion in restricted hippocampal sublayers of adult *Gria2*$^{\Delta HipOlf}$ mice did not reveal any obvious change in the hippocampal network. Neither loss of neurons nor mossy fiber sprouting was observed upon Ca^{2+} influx via GluR-B lacking AMPA receptors in eight- to eleven-month-old animals. Hence, *Gria2*$^{\Delta HipOlf}$ mice will serve as an important model for the behavioral analysis of the GluR-B subunit in the adult hippocampus. The hypothesized role of GluR-B in spatial reference memory will be evaluated soon.

Presumably, the most discussed role of ionotropic glutamate receptors in spatial forms of cognitive behavior is the acquisition of spatial reference in the Morris watermaze in dependence to NMDA receptors in the CA1 subfield of the hippocampus (Tsien et al., 1996; Bannerman et al., 1995). Discrepancies between CA1-restricted NR1 mutant mice (Tsien et al., 1996), which were shown to fail in the acquisition phase of the hidden platform task but exhibited an age-dependent NR1 gene recombination in cortex (Fukaya et al., 2003) and confusing results of AP5-infused mice (Morris et al., 1982; Bannerman et al., 1995) hindered a consistent hypothesis of the role of NMDA receptors in the spatial reference memory.

The ablation of all NMDA receptors in hippocampal DG, CA1 and CA2 of adult $Grin1^{\Delta HipOlf}$ mice did not impair spatial reference memory. In total, three cohorts of adult $Grin1^{\Delta HipOlf}$ mice (five- to eleven-month-old) were analyzed in different tasks (Y-maze, radial maze, Morris watermaze) for learning and memory of spatial references. Adult $Grin1^{\Delta HipOlf}$ mice were able to acquire and recall spatial reference memory in all these tests. Performances on the Y-maze and in the Morris watermaze were indistinguishable from litter controls. In fact, $Grin1^{\Delta HipOlf}$ mice learned less efficient than litter control mice in the six-arm radial maze but still, they decreased the error rate for the finding of previously unvisited arms.

Specific impairment was observed in reversal learning in the Morris watermaze. $Grin1^{\Delta HipOlf}$ mice traveled more distance to find the new position of the hidden platform in the quadrant opposite to the initial training quadrant. Consistently, these mice spent less time compared to litter controls in the appropriate quadrant in the subsequent probe test. This deficit was already reported for mice given AP5 infusion into the hippocampus. Reversal learning in the water maze was more sensitive to AP5 infusion than learning an entirely new spatial task in a second, different environment (Morris et al., 1990; Bannerman et al., 1995). It appeared somewhat surprising that learning an entirely new spatial representation of a novel environment appeared easier than simply re-encoding the goal location of a familiar environment in reversal learning. Based on observation of reversal learning deficit in global $GluR\text{-}A^{-/-}$ mice in an elevated plus maze task, a deficit in short-term, flexible, spatial working memory may underlie this kind of re-encoding memory (Bannerman et al., 2003). Two hippocampal mechanisms were found in global $GluR\text{-}A^{-/-}$ mice; GluR-A dependent spatial working memory and GluR-A independent spatial reference memory. Both

mechanisms might be essential in reversal learning. Spatial reference memory may underlie the gradual improvement in choice accuracy during reversal, whereas working memory may contribute to the efficacy of flexible re-encoding of spatial reference memory. $Grin1^{\Delta HipOlf}$ mice exhibited a delay-dependent impairment in the flexible, spatial working memory, but learned spatial reference memory as efficiently as litter control mice.

3.4. Genetic investigations into the role of ionotropic glutamate receptors in hippocampal learning

Genetic manipulation of the main ionotropic glutamate receptors in the three mutant mouse models $Gria1^{\Delta HipOlf}$, $Gria2^{\Delta HipOlf}$ and $Grin1^{\Delta HipOlf}$ offered an invaluable system to investigate the role of AMPA and NMDA receptors in principal DG, CA1 and CA2 neurons of adult mice in hippocampal learning and memory. Using the same recombination system, i.e. $Tg^{CN12-itTA}$ / Tg^{LC1} suppressed with doxycycline in the mouse embryo, to manipulate either the GluR-A, GluR-B or NR1 subunit in these restricted neurons allowed to dissect the role of certain ionotropic glutamate receptors in hippocampal learning in spatial working and reference memory tasks.

While AMPA receptors containing the GluR-B subunit and NMDA receptors are essentially involved in the spatial working memory, AMPA receptors containing the GluR-A subunit are not required in principal DG, CA1 and CA2 neurons of adult mice to remember the relationships between spatial cues and a milk reward for a certain delay.

Consistent with previous reports of global $Gria1^{-/-}$ mice (Reisel et al., 2002), AMPA receptors containing GluR-A are not required for spatial reference memory performance in various tasks. Similar results were observed upon NMDA receptor ablation in $Grin1^{\Delta HipOlf}$ mice. The acquisition and recall of spatial reference memory in the Morris watermaze and on the Y-maze were not affected. However, $Grin1^{\Delta HipOlf}$ mice exhibited some associative mismatches in the acquisition phase on the six-arm radial maze and in the reversal-learning task in the Morris watermaze. Impairment in spatial working memory in $Grin1^{\Delta HipOlf}$ mice might account for the effects in these spatial reference memory tasks.

Unfortunately, behavioral analysis of spatial reference memory in $Gria2^{\Delta HipOlf}$ mice is still missing. Based on previous work with $Gria2$ mutant mice (Shimshek et al., 2006) the GluR-B protein is the most important subunit of functional AMPA receptors. Combined with additional observations of $Gria1^{\Delta HipOlf}$, $Gria2^{\Delta HipOlf}$ and $Grin1^{\Delta HipOlf}$ mice in spontaneous and emotional behavior (not included in the Ph.D. thesis), depletion of the GluR-B subunit might cause stronger effects in spatial behavior than ablation of all NMDA receptors in principal DG, CA1 and CA2 neurons of adult mice. Hence, spatial reference memory in $Gria2^{\Delta HipOlf}$ mice has to be addressed soon.

4. Methods

4.1. Mice and housing

Experiments were approved under protocol 35-9185.81/MPI/T-9/06 at the Regierungspräsidium Karlsruhe, Germany. Animal breeding was performed in SPF-controlled rooms at the Interdisciplinary Breeding Facility (IBF; Unit 5) of the University of Heidelberg. Mice were housed in temperature (22°C) and light (on 08.00-20.00 h)-controlled rooms with *ad libitum* access to food and water. For experiments, mice were transported to the Department of Molecular Neurobiology in the MPI for Medical Research at Heidelberg, Germany or by air (World Courier) to the Department of Experimental Psychology, University of Oxford in England. In Heidelberg, individuals were isolated from litter and housed them in a single cage (Makrolon 2). A ventilated rack was used to ensure stable air conditions. Animals were kept for at least two weeks in a single cage to compensate for potential dominance disadvantages, witnessed by short whiskers and missing patches of fur in very rare cases. We also added a small house made of reused cardboard to offer additional climbing opportunity and a minimum of "privacy".

4.1.1. Mouse lines, genotyping and doxycycline treatment

Tg^{CN12-itTA} mice (J. Kim, Dissertation Uni Heidelberg, 2001) express the improved version of the tetracycline-dependent trans-activator (itTA) under the control of the 8.5 kb CaMKIIα promoter fragment and the 1.0 kb NR2C silencing element. ***Tg^{LC1}*** mice (K. Schoenig et al., 2003) contain the bidirectional tTA responder element with Luciferase and Cre Recombinase expression. ***Rosa26R.lacZ*** mice (Soriano et. al., 1999) with Rosa26 locus targeted β-Galactosidase gene fragment under expression control of a floxed transcription stop cassette were employed as functional Cre recombinase indicator. ***Gria1^{loxP/loxP}*** mice carry gene-targeted AMPA receptor subunit GluR-A alleles in which exon 11 are flanked by loxP elements. In ***Gria2^{loxP/loxP}*** mice, loxP sites flank exons 11. ***Grin1^{loxP/loxP}*** mice exhibit gene-targeted NMDA receptor subunit 1 genes with floxed exons 11 to 18.

For determination of transgenic specificity during lifetime Tg^{CN12} / Tg^{LC1} / $R26R$ mice were bred with all loci in heterozygous state. Adult and sublayer specific depletion of AMPA or NMDA receptor subunits was achieved by generating transgenic mice heterozygous for Tg^{CN12} / Tg^{LC1} and in $Gria1^{\Delta HipOlf}$ homozygous for $Gria1^{loxP/loxP}$, in $Gria2^{\Delta HipOlf}$ homozygous for $Gria2^{loxP/loxP}$ or in $Grin1^{\Delta HipOlf}$ homozygous for $Grin1^{loxP/loxP}$ mice. Doxycycline hydrochloride (Sigma) at a concentration of 50 mg/l, supplemented with 1 % sucrose, was dissolved in drinking water and provide to the parental mice in light-protected bottles. Animal breeding was kept under doxycycline to prevent embryonic itTA activity. At birth of offspring doxycycline was removed from the drinking water.

Mice were genotyped by PCR of tail DNA with specific primers. Indicated below are the used primer and the approximate lengths of the amplified DNA fragments. Primer sequences are listed in materials.

$Tg^{CN12\text{-}itTA}$: rsphtTA1 and rsphtTA2 produce a 600 bp band.

Tg^{LC1}: rspCre1 and rspCre2 with a 200 bp positive PCR band.

$Gria1^{loxP}$: MH60 and 3´intro3 with 200 bp for wild type and 250 bp for mutant alleles.

$Gria2^{loxP}$: VM10 and VM12 with 250 bp for wild type and 350 bp for mutant alleles.

$Grin1^{loxP}$: NR1 Ex18 do1 and NR1 Ex18up1 with 450 bp for wild type and 500 bp for mutant alleles.

4.1.2. General appearance of mice

Upon acclimatization in our department, all $iGluR^{\Delta HipOlf}$ mice generated by embryonic arrest of Cre activity in the Tg^{CN12} / Tg^{LC1} model ($Gria1^{\Delta HipOlf}$, $Gria2^{\Delta HipOlf}$, $Grin1^{\Delta HipOlf}$) showed normal general appearance (fur, whisker, exploratory behavior during handling) compared to litter control mice. To exclude interference of gross abnormalities with behavioral testing, we checked the eye-blink, ear-twitch and whisker-orientating reflex (Paylor 1998) as well as motor learning on the accelerated rota-rod. All neurological reflexes were well established in all tested mice.

4.2. Molecular analysis

For the applied standard molecular biological techniques refer to:

Current Protocols in Molecular Biology; Ausubel, Brent, Kingston, Moore, Seidman, Smith, Struhl, Wiley Interscience, 1989

Molecular Cloning, A Laboratory Manual; Sambrook, Fritsch, Maniatis, 2nd Edition, Cold Spring Harbor Laboratory Press, 1989

4.2.1 Immunochemistry

Mice were anesthetized with isoflurane (Hoechst, Germany) and intracardially perfused with phosphate-buffered saline (PBS, pH 7.4, 37°C) followed by 4 % paraformaldehyde (PFA) in PBS. Brains were removed and post-fixed in 4 % PFA (2-24 h at 4°C). Afterwards the brains were rinsed with PBS and embedded in 2 % agarose in PBS. Coronal, horizontal or sagittal sections of 70μm thickness were performed on a vibratome (VT 1000S, Leica, Germany).

In DAB immunostaining, selected sections were pretreated for 10 min in 0.5 % H_2O_2/PBS to erase the activity of endogenous peroxidases. After repeated washing for 10 min with PBS, sections were permeabilized for 2 h in Day 1 buffer (0.3% Triton X-100, 1 % bovine serum albumin (BSA) in PBS), supplemented with 4 % normal goat serum (NGS) for blocking of perturbing antigens. For binding of the primary antibody against certain proteins, the sections were incubated overnight in Day 1 buffer containing 1 % NGS and the corresponding antibody dilution (refer to materials) The following day, sections were washed three times for 10 min in Day 2 buffer (0.1 % Triton X-100 and 0.3 % BSA in PBS) and incubated for 1 h in Day 2 buffer supplemented with peroxidase-conjugated secondary antibody (1:600; Vector Laboratories, USA). After repeated washing for 10 min in Day 2 buffer, sections were cleared twice for 10 min in PBS. The staining reaction of the antibody coupled peroxidase was performed in 0,4 mg/ml diaminobenzidine (DAB, Sigma, Germany) in 20 mM Tris/HCl at pH 7.6 (Sigma, Germany) and stopped by repeated washing in PBS. After a brief wash in 10 mM Tris/HCl (pH 7.6), sections were mounted on glass slides and dehydrated in 70, 90, 99.5 % (v/v) EtOH. After brief wash in xylol, slices were embedded in Eukitt (Kindler GmbH, Germany).

In immunhistofluorescence staining, sections were permeabilized and blocked in 4 % NGS-containing buffer 1, incubation of primary antibody overnight and detection by fluorescent secondary antibody (1:200; Jackson Immunolabs or Sigma) that was incubated for 1 h in Day 2 buffer. After clearing of sections with day 2 buffer and PBS, sections were dried briefly, embedded in Aqua mount and coverslipped.

4.2.2 X-gal staining for vibratome sections

Brains were removed and fixed for 1 h in 4 % paraformaldehyde in PBS (137 mM NaCl, 2.7 mM KCl, 4.3 mM $Na_2HPO_4/2H_2O$, 1.4 mM KH_2PO_4). Afterwards, the brains were rinsed wit PBS, embedded in 2 % agarose (Seakem LE) in PBS and cut in 70-100 μm sagittal or coronal sections on a vibratome (Leica VT 1000S, Leica). The sections were incubated for 24 h at 37°C in X-Gal staining solution (5 mM $K_4Fe(CN)_6$, 5 mM $F_3Fe(CN)_6$, 2 mM MgCL2, 2 mg/ml X-gal in dimethyl-fornamid/PBS). Sections were washed twice in PBS and once 10 mM Tris/HCl, pH7.6. Sections were immediately counterstained with eosin (Sigma) for 1 min and rapidly and successively dehydrated in ethanol 70, 90, 99.5 % (v/v). The dry sections were dehydrated in xylene and embedded in EuKitt (Kindler GmbH, Germany).

4.2.3. Mossy fiber visualization by Timm stain

Timm staining was performed as described (Danscher et al., 1982, 1985) with some modifications. Briefly, one hour after sodium selenite (Na2SeO3, 15mg/kg) injection intraperitoneally mice were anaesthetized with halothane (Hoechst, Frankfurt, Germany) and perfused intracardically with 1% phosphate buffered sodium (PBS) at room temperature. Brains were isolated and frozen on solid CO2 and stored at -70 °C until use. Cryostat sections (15 μm) were cut through the entire extent of the hippocampus and mounted on poly-lysine coated slides, fixed in 4% PFA for 5 min, dehydrated in 100% alcohol and stored at 4°C. Prior to development, mounted sections were dipped in 0.5% gelatin, developed in the dark for 10-30 min in developer solution (100 ml 50% Gum Arabic solution, 20 ml Citrate buffer of 25.5% citric acid and 23.5% tri-sodium citrate, 30 ml 3.3% hydroquinone, ddH2O 70 ml, with additional 30 ml 0.7% Ag lactate added immediately before use). After washing, the slices were dehydrated in alcohol, cleared in xylene and cover-slipped. Timm staining was analyzed by manual counting of Timm-stained granules in the inner

molecular layer of the DG. Both DG on four slices per animals were quantified. Data are presented as mean of two mice per genotype ± SD. Statistical significance was evaluated by two-tailed, unpaired Student's t test.

4.2.4. Immunoblotting

Mouse brains were removed and the hippocampus was isolated. Whole protein cell lysates in 25 mM HEPES (pH7.6; including protein inhibitor cocktail) was prepared and immunoblots were performed as described (Mack et al., 2001). Antibodies against GluR-B (1:800, Chemicon, monoclonal), GluR-A (1:2000, Chemicon, polyclonal), NR1 (1:600, Chemion, polyclonal) and actin (1:80000, Sigma, monoclonal) or p38 (1:2000, rabbit polyclonal) as an internal standard were used. HRP-coupled secondary goat anti-rabbit and goat anti-mouse antibodies (Vector, 1:15000) were used to label primary antibodies. Immunoreactivity was detected with ECLplus (Amersham Pharmacia Biotech, UK). Immunoblots were scanned and quantitatively analyzed with ImageJ. Data are presented as mean ± SEM. Statistical significance was evaluated by two-tailed, unpaired Student's t test.

4.3. Long-term potentiation in field recordings

Orthodromic synaptic stimulation in CA1 was delivered alternately through two tungsten electrodes (0.2 Hz) to activate synapses in apical (stratum radiatum) and basal dendrites (stratum oriens), respectively. Extracellular potentials were monitored by glass electrodes filled with ACSF, which were placed in the corresponding synaptic layers. After stable synaptic responses in both pathways for at least 15 min, one pathway was tetanized (with either a single 100 Hz tetanization for 1 sec or four such tetanization given at 5 min intervals), the other pathway served as a control. To standardize tetanization strength in different experiments, the tetanic stimulation strength was set in response to a single shock at intensity just above the threshold for generating a population spike. Synaptic efficacy was assessed measuring the slope of the fEPSP in the middle third of its rising phase. Six consecutive responses (1 min) were averaged and normalized to the mean value recorded 4-7 min prior to tetanic stimulation. In some experiments, DL-2-amino-5-phosphonopentanoicacid (DL-AP5, 50 μM, Sigma) was present during the recordings. Data are mean ± SEM; the statistical significance of LTP levels between tetanized and non-tetanized inputs were

calculated by Student's paired two-tailed t test. LTP levels between genotypes or resulting from different tetanization paradigms were evaluated by linear mixed model statistical analysis.

4.4. Behavioral analysis

4.4.1. Spatial working memory (non-matching-to-place alternating T-maze)

The alternating T-maze consists of a start arm (47 X 10 cm) and two identical goal arms (35 X 10 cm) with 10 cm high walls out of black-painted wood (Reisel et al., 2002). The mice were held on a diet as described above and were habituated to the T-maze several days before the testing. Each trial consisted of a sample run and a choice run with a 3 - 60 sec interval. On the sample run the mouse was forced to either left or right by the presence of a wooden block. A reward of 30 µl sweetened, condensed milk was available at the end of the arm in a food well. The block was then removed and the choice run was performed, allowing a free choice of either arm. The animal was rewarded for choosing the previously blocked arm and unrewarded for the previously visited. The intertrial interval was approx. 10-20 min. Each daily session (5 sessions in total) consisted of 4 trials in the morning and 4 trials in the afternoon.

4.4.2. Spatial reference memory (elevated Y-maze)

We used the elevated Y-maze, consisting of three arms (angle: 120°, arm length: 50 cm) made of black painted wood, as described (Reisel et al., 2002). Before the experiment, mice were put on a diet and held at 85% of the starting weight. Mice were accustomed to the Y-maze, and sweetened, condensed milk served as reward. After pre-training, mice were trained in the Y-maze. One session per day consisted of 10 trials with an inter-trail interval of about 10-15 min. The target arm (baited with sweetened milk) was fixed in one direction and the mice were put randomly during one session five times on the left and five times on the right starting arm. In the first two days (sessions 1 and 2) mice were allowed to find the sweetened milk even when entering the wrong arm. At day 3-7 (sessions 3-7) mice were removed to their cages after entering the un-baited arm. The maze was rotated by 120° randomly between

each trial, to prevent usage of olfactory, visual or tactile cues unique to a particular arm.

4.4.3. Assessment of Spatial Memory on the Radial Maze.

Spatial memory was assessed using a 6 arm radial maze, which was made of wood and painted gray (Schmitt et al., 2003). Each arm (60 x 7 cm) was surrounded by a 1 cm raised edge and extended from a circular central platform (18 cm diameter). At the end of each arm was a stainless steel food well. Mice were rewarded with 0.1 ml sweetened, condensed milk (diluted 50/50 with water). The maze was elevated 80 cm above the floor in a well-lit laboratory (6.3 x 2.7 m) which contained various extra-maze cues (e.g. laboratory equipment, stools, bench, posters). The central platform was surrounded by a transparent Perspex cylinder (18 cm diameter, 30 cm high). At the entrance to each arm of the maze was a Perspex door (6 cm wide, 7 cm high) which could be controlled by the experimenter using a series of strings. Mice were maintained on a restricted feeding schedule at 85% of their free feeding weights. The mice were first habituated to drinking sweetened, condensed milk on two arms of an elevated Y-maze (Reisel et al., 2002)in their colony holding room (i.e. not the testing room). Once all the mice were running freely on the Y-maze and readily consuming the milk rewards, testing on the radial arm maze began.

4.4.3.1. Spatial reference memory acquisition.

Mice were first trained to discriminate between baited and non-baited arms on a radial maze task in which the same 3 out of 6 arms were always baited. The three baited arms were allocated such that two of these arms were adjacent and the third was between two non-rewarded arms (e.g. arms 1, 2 and 4). Different combinations of arms were used as far as possible, although the arm allocations were counterbalanced across groups. At the start of a trial, a mouse was placed individually on the central platform. Mice were allowed to explore freely and consume all the milk rewards available. During this acquisition phase, Perspex doors prevented mice from re-entering an arm that they had already visited on that trial (Schmitt et al., 2003). All the doors were closed each time the mouse returned to the central platform, and confined the mouse there for 5 s until the next choice. Once an arm had been visited, its door remained closed for subsequent choices. Thus, all 6 doors were open for the

first choice, 5 for the second choice, 4 for the third choice, and so on. Using this testing procedure it was not possible for the mice to make working memory errors. This provides a pure test of SRM acquisition, and is dependent upon the hippocampus (Schmitt et al., 2003). SRM errors were defined as entries into arms that were never baited (maximum of 3 errors per trial). The maze was rotated periodically to prevent the mice from using intra-maze cues to solve the task. Mice received 32 trials in total. Data were arranged in 8 blocks of 4 trials for analysis. By this stage all of the animals had acquired the SRM component of the task and were making very few, if any, errors.

4.4.3.2. Simultaneous assessment of spatial working and reference memory

The SWM component of the task was then introduced. The mice received a further 24 trials (with an inter-choice interval of 5 s) in which the same 3 out of 6 arms were baited, but now they were no longer prevented from re-entering a previously chosen arm. The doors were solely used to retain the animals on the central platform between choices. SWM errors were scored when a mouse entered an arm that had already been visited on that trial. SRM errors were scored as before. The effect of increasing the retention interval between successive choices was then assessed (Tonkiss & Rawlins, 1991; Steele & Morris, 1999; Lee & Kesner, 2002). The minimum amount of time that the animal spent on the central platform between choices with all doors closed was increased from 5 to 15 s and a further 24 trials were conducted.

4.4.4. Morris watermaze

Spatial reference memory was also assessed in an open-field water maze (Morris et al., 1981; 1984), consisting of a large circular tank (diameter 2.0 m, depth 0.6 m) containing water at $25 \pm 1°C$ to a depth of 0.3 m. To escape from the water, the mice had to find a hidden platform (diameter 21 cm) submerged approximately 1 cm below the waters surface. The water was made opaque by the addition of 2 l of milk, which not only prevented the animals from seeing the platform but also allowed efficient tracking of swim paths. The pool was located on an elevated platform 60 cm above the floor in another new, well lit laboratory containing prominent extra-maze cues. Swim paths were monitored by a video camera mounted in the ceiling. The video signal was relayed to a video recorder allowing both on- and off-line analysis, and

from there to an image analyzer (HVS VP112, HVAS Image, Hampton, UK). The x and y coordinates of the animals´ position were sampled in real-time at 10 Hz by an Acorn computer, using specialized software that provided measures of latency, swim speed and path length during acquisition, and the percentage of time spent in each quadrant of the pool during the probe trial.

Each type of memory error (SRM and SWM) was analyzed separately. The data were analyzed in blocks of 4 trials. Where the assumptions of normality and equal variance were met, data were analyzed by ANOVA with subsequent analysis of simple main effects where appropriate. If the data failed to satisfy these assumptions, transformations (square root transform) were applied and ANOVA performed on the transformed data set. To make the figures more legible, however, all the data are presented as un-transformed means (± SEM.).

The platform was located at the center of one of the four quadrants of the pool (arbitrarily designated NE, NW, SE, SW). The number of mice trained to each platform position was counterbalanced with respect to group. Animals had no swim pre-training before the start of spatial testing in the water maze. All mice were trained to find a hidden escape platform, which remained in a fixed location throughout testing. They received 4 trials per day for 9 days with an ITI of approximately 15 s. The mice were placed into the pool facing the side wall at one of 8 start locations (nominally N, S, E, W, NE, NW, SE and SW; chosen randomly across trials), and allowed to swim until they reached the platform, or for a maximum of 90 s. Any mouse that failed to find the platform within the allotted time was lifted out of the water by experimenter and placed onto the platform. The animal then remained on the platform for 30 s before commencing the next trial.

On the tenth day of testing (24 h after spatial training trial 36), a probe trial was conducted to determine the extent to which the mice had learned about the spatial location of the platform. The platform was removed from the pool, and the mice were allowed to swim freely fro 90 s. The percentage of time that animals spent in each quadrant of the maze was recorded.

5. Material

5.1. Mouse lines

C57Bl/6:   Charles River (Basel)

NMRI: Charles River (Basel)

Rosa26R: Soriano et al., 1999

$Tg^{CN12\text{-}itTA}$:   R. Sprengel, P.H. Seeburg

Tg^{LC1}:   Schonig et al., 2002

$Gria1^{loxP}$:   R. Sprengel, P.H. Seeburg

$Gria2^{loxP}$:   R. Sprengel, P.H. Seeburg

$Grin1^{loxP}$:   R. Sprengel, P.H. Seeburg

5.2. Sequences of PCR primer

htTA1   AGA GCA AAG TCA TCA ACT CTG CC

htTA2   GTG AGA GCC AGA CTC ACA TTT CA

rspCre1   ACC AGG TTC GTT CAC TCA TGG

rspCre2   AGG CTA AGT GCC TTC TCT ACA C

Lac3'   TTA CCC GTA GGT AGT CAC GCA

Lac5'   TTA CGA TGC GCC CAT CTA CAC

MH60   CAC TCA CAG CAA TGA AGC AGG

3´intro3   CTG CCT GGG TAA AGT GAC TTG G

VM12   GCG TAA GCC TGT GAA ATA CCT G

VM10   GTT GTC TAA CAA GTT GTT GAC C

NR1 Ex18 do1   CTG GGA CTC AGC TGT GCT GG

NR1 Ex18 up1   AGG GGA GGC AAC ACT GTG GAC

5.3. Antibodies

Rabbit polyclonal anti-glutamate receptor 1, AB1504, Chemicon; IHC, 1:200, IB: 1:2000

Rabbit polyclonal anti-glutamate Receptor 2, AB1768, Chemicon; IHC: 1:60, IB: 1:600

Rabbit polyclonal anti-NMDA Receptor 1, AB AB1516 Chemicon; IB: 1:100

Rabbit polyclonal anti-GFAP, Z0334, DAKO; IHC: 1:400

Rabbit polyclonal anti-Cre (Cre Recombinase), G. Schuetz, DKFZ Heidelberg; IHC: 1:3000

Rabbit polyclonal anti-Cre (Cre Recombinase), PRB-106C, BabCo; IHC: 1:8000

Rabbit polyclonal anti-p38, Abcam, IB: 1:2000

Mouse monoclonal anti-NeuN (Neuronal Nuclei), MAB377, Chemicon; IHC: 1:1000

Mouse monoclonal anti-β-Actin, Clone AC-15, A5441, Sigma; IB: 1:80000

Mouse monoclonal anti-Parvalbumin, P 3088, Sigma; IHC: 1:1000

Rat monoclonal anti-BrdU, OBT 0030, Acurate; IHC: 1:400

Peroxidase-conjugated goat anti-rabbit IgG (H+L), PI-1000, Vector

Peroxidase-conjugated horse anti-mouse IgG (H+L), PI-2000, Vector

Biotinylated goat anti-mouse IgG (H+L), BA-9200, Vector

Biotinylated goat anti-rabbit IgG (H+L), BA-1000, Vector

Biotinylated rabbit anti-rat (H+L), BA-4001, Vector

TexasRed dye-conjugated goat anti-mouse IgG (H+L), 115-075-146, Dianova

TexasRed dye-conjugated goat anti-rabbit IgG (H+L), 111-075-144, Dianova

Fitc dye-conjugated goat anti-mouse IgG (H+L), 115-095-146, Dianova

Fitc dye-conjugated goat anti-rabbit IgG (H+L), 111-095-144, Dianova

TexasRed dye-conjugated avidin, A-1100, Vector

Fitc dye-conjugated avidin, A-1100, Vector

6. Abbreviations

6.1. General

α alpha

β beta

Δ delta

μ micro

AMPA   L-α-amino-3-hydroxy-5-methyl-4-isoxalepropionic acid

AP   action potential

AP5   2-Amino-5-phosphonopentanoic acid

ATP   adenosin-tri-phophat

BrdU   Bromodeoxyuridine

C   Celsius

Ca^{2+} calcium ion

CAMKII Ca^{2+}/calmodulin-depdendent protein kinase II

cKO   conditional gene knock-out

Cl^{-} chlorid ion

CNS   central nervous system

DCX   doublecortin

et al.   et alii

Fig.   Figure

gal   galactosidase

GFAP   glial fibrillary acidic protein

GFP   green fluorescent protein

GluR   glutamate receptor

HEPES   N-(2-hydroxyethyl)piperazine-N´-ethansulfonic acid

Hz   Hertz

I   current intensity

i.e.   id est

k   kilo

K^{+} kalium ion

kb   kilo bases

l	liter
loxP	locus of crossover in P1 phage, Cre recombinase recognition sites
LTD	long-term depression
LTP	long-term potentiation
n	nano, number (of experiments or mice)
Na$^+$	sodium ion
m	meter, milli or miniature
ms	millisecond
mV	millivolt
NGS	normal goat serum
NMDA	N-methyl-D-aspartate
P	postnatal day
PBS	phosphate buffered saline
PCR	polymerase chain reaction
PFA	paraformaldehyde
Ph.D.	philosophiae doctor, Doctor of Philosophy
PSD	postsynaptic density
P$_{tet-Bi}$	bidirectional Tet promoter
rAAV	recombinant Adeno-Associated Virus
s	second
SEM	standard error of the mean
t	time
Tet	tetracycline
Tg	transgenic line
Tris	Tris-(hydroxymethyl)-aminomethan
tTA	tetracycline dependent transactivator
V	volt
vs.	versus
Xgal	5-bromo-4-chloro-3-indolyl-β-D-galactoside

6.2. Brain structures

ACo	anterior cortical amygdaloid nucleus
Amy	amygdala

AOB	accessory olfactory bulb
AOC	anterior olfactory cortex
AOD	anterior olfactory nucleus, dorsal part
AOE	anterior olfactory nucleus, external part
AON	anterior olfactory nucleus
AOM	anterior olfactory nucleus, medial part
APir	amygdalopiriform transition zone
AuD	secondary auditory cortex
BLA	basolateral amygdala
CA	Cornu Ammonis or Ammon´s horn
CPu	caudate putamen
CxA	cortex-amygdala transition zone
DG	dentate gyrus
DP	dorsal peduncular cortex
DTT	dorsal tenia tecta
ff	fimbria-fornix
FrA	frontal association cortex
ICj	islands of Calleja
IG	indusium griseum, also termed as "hippocampal attenuation"
LEnt	lateral entorhinal cortex
M1, M2	primary, secondary motor cortex
MEnt	medial entorhinal cortex
MOC	medial olfactory cortex
mf	DG mossy fibers
ml	DG molecular layer
OB	olfactory bulb
PC	piriform cortex
pcl	pyramidal cell layer
POC	primary olfactory cortex
PaS	parasubiculum
PrS	presubiculum
S	subiculum
S1, S2	primary, secondary somatosensory cortex
SEL	subendymal layer of the main olfactory bulb

SNL	substantia nigra
so	stratum oriens
sr	stratum radiatum
SVZ	subventricular zone
Tu	olfactory tubercle
VP	ventral pallidum
VTT	ventral tenia tecta

7. References

Amaral, D. G. (1978). "A Golgi study of cell types in the hilar region of the hippocampus in the rat." J Comp Neurol **182**(4 Pt 2): 851-914.

Amaral, D. G. and M. P. Witter (1989). "The three-dimensional organization of the hippocampal formation: a review of anatomical data." Neuroscience **31**(3): 571-91.

Andersen, P. (1975). "[Isolated brain slices. A new preparation for theoretical and clinical research]." Tidsskr Nor Laegeforen **95**(6): 349-51.

Andersen, P., T. V. Bliss, et al. (1971). "Unit analysis of hippocampal polulation spikes." Exp Brain Res **13**(2): 208-21.

Andersen, P., B. Holmqvist, et al. (1966). "Entorhinal activation of dentate granule cells." Acta Physiol Scand **66**(4): 448-60.

Ascher, P. and L. Nowak (1986). "A patch-clamp study of excitatory amino acid activated channels." Adv Exp Med Biol **203**: 507-11.

Bagal, A. A., J. P. Kao, et al. (2005). "Long-term potentiation of exogenous glutamate responses at single dendritic spines." Proc Natl Acad Sci U S A **102**(40): 14434-9.

Bannerman, D. M., R. M. Deacon, et al. (2004). "A comparison of GluR-A-deficient and wild-type mice on a test battery assessing sensorimotor, affective, and cognitive behaviors." Behav Neurosci **118**(3): 643-7.

Bannerman, D. M., R. M. Deacon, et al. (2002). "Double dissociation of function within the hippocampus: spatial memory and hyponeophagia." Behav Neurosci **116**(5): 884-901.

Bannerman, D. M., M. A. Good, et al. (1995). "Distinct components of spatial learning revealed by prior training and NMDA receptor blockade." Nature **378**(6553): 182-6.

Bannerman, D. M., J. N. Rawlins, et al. (2006). "The drugs don't work-or do they? Pharmacological and transgenic studies of the contribution of NMDA and GluR-A-containing AMPA receptors to hippocampal-dependent memory." Psychopharmacology (Berl) **188**(4): 552-66.

Bannerman, D. M., J. N. Rawlins, et al. (2004). "Regional dissociations within the hippocampus--memory and anxiety." Neurosci Biobehav Rev **28**(3): 273-83.

Bannerman, D. M., B. K. Yee, et al. (1999). "Double dissociation of function within the hippocampus: a comparison of dorsal, ventral, and complete hippocampal cytotoxic lesions." Behav Neurosci **113**(6): 1170-88.

Baron, U., S. Freundlieb, et al. (1995). "Co-regulation of two gene activities by tetracycline via a bidirectional promoter." Nucleic Acids Res **23**(17): 3605-6.

Baron, U., M. Gossen, et al. (1997). "Tetracycline-controlled transcription in eukaryotes: novel transactivators with graded transactivation potential." Nucleic Acids Res **25**(14): 2723-9.

Barria, A., D. Muller, et al. (1997). "Regulatory phosphorylation of AMPA-type glutamate receptors by CaM-KII during long-term potentiation." Science 276(5321): 2042-5.

Benke, T. A., A. Luthi, et al. (1998). "Modulation of AMPA receptor unitary conductance by synaptic activity." Nature 393(6687): 793-7.

Benveniste, M. and M. L. Mayer (1991). "Kinetic analysis of antagonist action at N-methyl-D-aspartic acid receptors. Two binding sites each for glutamate and glycine." Biophys J 59(3): 560-73.

Betz, W. J. (1970). "Depression of transmitter release at the neuromuscular junction of the frog." J Physiol 206(3): 629-44.

Bliss, T. V. and G. L. Collingridge (1993). "A synaptic model of memory: long-term potentiation in the hippocampus." Nature 361(6407): 31-9.

Bliss, T. V. and T. Lomo (1970). "Plasticity in a monosynaptic cortical pathway." J Physiol 207(2): 61P.

Bliss, T. V. and T. Lomo (1973). "Long-lasting potentiation of synaptic transmission in the dentate area of the anaesthetized rabbit following stimulation of the perforant path." J Physiol 232(2): 331-56.

Brunjes, P. C., K. R. Illig, et al. (2005). "A field guide to the anterior olfactory nucleus (cortex)." Brain Res Brain Res Rev 50(2): 305-35.

Burnashev, N., H. Monyer, et al. (1992). "Divalent ion permeability of AMPA receptor channels is dominated by the edited form of a single subunit." Neuron 8(1): 189-98.

Cacucci, F., C. Lever, et al. (2004). "Theta-modulated place-by-direction cells in the hippocampal formation in the rat." J Neurosci 24(38): 8265-77.

Cajal, S. R. (2006). "The impossible interview with the man of the neuron doctrine. Interview by Edward G Jones." J Hist Neurosci 15(4): 326-40.

Carroll, R. C., D. V. Lissin, et al. (1999). "Rapid redistribution of glutamate receptors contributes to long-term depression in hippocampal cultures." Nat Neurosci 2(5): 454-60.

Cenquizca, L. A. and L. W. Swanson (2007). "Spatial organization of direct hippocampal field CA1 axonal projections to the rest of the cerebral cortex." Brain Res Rev 56(1): 1-26.

Chen, H. X., N. Otmakhov, et al. (1999). "Requirements for LTP induction by pairing in hippocampal CA1 pyramidal cells." J Neurophysiol 82(2): 526-32.

Chen, L. W., K. K. Yung, et al. (2000). "Co-localization of NMDA receptors and AMPA receptors in neurons of the vestibular nuclei of rats." Brain Res 884(1--2): 87-97.

Choi, T., M. Huang, et al. (1991). "A generic intron increases gene expression in transgenic mice." Mol Cell Biol 11(6): 3070-4.

Chung, H. J., J. Xia, et al. (2000). "Phosphorylation of the AMPA receptor subunit GluR2 differentially regulates its interaction with PDZ domain-containing proteins." J Neurosci 20(19): 7258-67.

Coan, E. J., W. Saywood, et al. (1987). "MK-801 blocks NMDA receptor-mediated synaptic transmission and long term potentiation in rat hippocampal slices." Neurosci Lett **80**(1): 111-4.

Collingridge, G. L., S. J. Kehl, et al. (1983). "The antagonism of amino acid-induced excitations of rat hippocampal CA1 neurones in vitro." J Physiol **334**: 19-31.

Crair, M. C. and R. C. Malenka (1995). "A critical period for long-term potentiation at thalamocortical synapses." Nature **375**(6529): 325-8.

Cull-Candy, S., S. Brickley, et al. (2001). "NMDA receptor subunits: diversity, development and disease." Curr Opin Neurobiol **11**(3): 327-35.

Danscher, G. (1982). "Exogenous selenium in the brain. A histochemical technique for light and electron microscopical localization of catalytic selenium bonds." Histochemistry **76**(3): 281-93.

Danscher, G. and B. Moller-Madsen (1985). "Silver amplification of mercury sulfide and selenide: a histochemical method for light and electron microscopic localization of mercury in tissue." J Histochem Cytochem **33**(3): 219-28.

de Hoz, L., J. Knox, et al. (2003). "Longitudinal axis of the hippocampus: both septal and temporal poles of the hippocampus support water maze spatial learning depending on the training protocol." Hippocampus **13**(5): 587-603.

Deacon, R. M., D. M. Bannerman, et al. (2002). "Effects of cytotoxic hippocampal lesions in mice on a cognitive test battery." Behav Brain Res **133**(1): 57-68.

Deadwyler, S. A., T. Dunwiddie, et al. (1987). "A critical level of protein synthesis is required for long-term potentiation." Synapse **1**(1): 90-5.

Derkach, V. A., M. C. Oh, et al. (2007). "Regulatory mechanisms of AMPA receptors in synaptic plasticity." Nat Rev Neurosci **8**(2): 101-13.

Devenish, R. J., M. Prescott, et al. (2008). "The structure and function of mitochondrial F1F0-ATP synthases." Int Rev Cell Mol Biol **267**: 1-58.

Dingledine, R., K. Borges, et al. (1999). "The glutamate receptor ion channels." Pharmacol Rev **51**(1): 7-61.

Errington, M. L., M. A. Lynch, et al. (1987). "Long-term potentiation in the dentate gyrus: induction and increased glutamate release are blocked by D(-)aminophosphonovalerate." Neuroscience **20**(1): 279-84.

Esteban, J. A., S. H. Shi, et al. (2003). "PKA phosphorylation of AMPA receptor subunits controls synaptic trafficking underlying plasticity." Nat Neurosci **6**(2): 136-43.

Ferbinteanu, J. and R. J. McDonald (2001). "Dorsal/ventral hippocampus, fornix, and conditioned place preference." Hippocampus **11**(2): 187-200.

Fields, R. D. and B. Stevens-Graham (2002). "New insights into neuron-glia communication." Science **298**(5593): 556-62.

Forrest, D., M. Yuzaki, et al. (1994). "Targeted disruption of NMDA receptor 1 gene abolishes NMDA response and results in neonatal death." Neuron **13**(2): 325-38.

Freudenberg, F. (2009). in preparation. Molecular Neurobiology, MPI for Medical Research, Ruprecht-Karls-Universität, Heidelberg.

Frey, U., M. Krug, et al. (1988). "Anisomycin, an inhibitor of protein synthesis, blocks late phases of LTP phenomena in the hippocampal CA1 region in vitro." Brain Res **452**(1-2): 57-65.

Friedman, L. K. and A. R. Koudinov (1999). "Unilateral GluR2(B) hippocampal knockdown: a novel partial seizure model in the developing rat." J Neurosci **19**(21): 9412-25.

Friedman, L. K., D. E. Pellegrini-Giampietro, et al. (1994). "Kainate-induced status epilepticus alters glutamate and GABAA receptor gene expression in adult rat hippocampus: an in situ hybridization study." J Neurosci **14**(5 Pt 1): 2697-707.

Friedman, L. K., E. F. Sperber, et al. (1997). "Developmental regulation of glutamate and GABA(A) receptor gene expression in rat hippocampus following kainate-induced status epilepticus." Dev Neurosci **19**(6): 529-42.

Fuchs, E. C., A. R. Zivkovic, et al. (2007). "Recruitment of parvalbumin-positive interneurons determines hippocampal function and associated behavior." Neuron **53**(4): 591-604.

Fukaya, M., A. Kato, et al. (2003). "Retention of NMDA receptor NR2 subunits in the lumen of endoplasmic reticulum in targeted NR1 knockout mice." Proc Natl Acad Sci U S A **100**(8): 4855-60.

Fukunaga, K., L. Stoppini, et al. (1993). "Long-term potentiation is associated with an increased activity of Ca2+/calmodulin-dependent protein kinase II." J Biol Chem **268**(11): 7863-7.

Fyhn, M., S. Molden, et al. (2004). "Spatial representation in the entorhinal cortex." Science **305**(5688): 1258-64.

Goldman-Rakic, P. S. (1987). "Development of cortical circuitry and cognitive function." Child Dev **58**(3): 601-22.

Gossen, M. and H. Bujard (1992). "Tight control of gene expression in mammalian cells by tetracycline-responsive promoters." Proc Natl Acad Sci U S A **89**(12): 5547-51.

Gouaux, E. (2004). "Structure and function of AMPA receptors." J Physiol **554**(Pt 2): 249-53.

Haberly, L. B. (2001). "Parallel-distributed processing in olfactory cortex: new insights from morphological and physiological analysis of neuronal circuitry." Chem Senses **26**(5): 551-76.

Hafting, T., M. Fyhn, et al. (2005). "Microstructure of a spatial map in the entorhinal cortex." Nature **436**(7052): 801-6.

Hasselmo, M. E., E. Schnell, et al. (1995). "Dynamics of learning and recall at excitatory recurrent synapses and cholinergic modulation in rat hippocampal region CA3." J Neurosci **15**(7 Pt 2): 5249-62.

Hatten, M. E. (1999). "Central nervous system neuronal migration." Annu Rev Neurosci **22**: 511-39.

Haydon, P. G. and G. Carmignoto (2006). "Astrocyte control of synaptic transmission and neurovascular coupling." Physiol Rev **86**(3): 1009-31.

Higuchi, M., F. N. Single, et al. (1993). "RNA editing of AMPA receptor subunit GluR-B: a base-paired intron-exon structure determines position and efficiency." Cell **75**(7): 1361-70.

Hock, B. J., Jr. and M. D. Bunsey (1998). "Differential effects of dorsal and ventral hippocampal lesions." J Neurosci **18**(17): 7027-32.

Hoffman, D. A., R. Sprengel, et al. (2002). "Molecular dissection of hippocampal theta-burst pairing potentiation." Proc Natl Acad Sci U S A **99**(11): 7740-5.

Hrabetova, S. and T. C. Sacktor (1996). "Bidirectional regulation of protein kinase M zeta in the maintenance of long-term potentiation and long-term depression." J Neurosci **16**(17): 5324-33.

Isaac, J. T., R. A. Nicoll, et al. (1995). "Evidence for silent synapses: implications for the expression of LTP." Neuron **15**(2): 427-34.

Ismailov, I., D. Kalikulov, et al. (2004). "The kinetic profile of intracellular calcium predicts long-term potentiation and long-term depression." J Neurosci **24**(44): 9847-61.

Jarrard, L. E. (1989). "On the use of ibotenic acid to lesion selectively different components of the hippocampal formation." J Neurosci Methods **29**(3): 251-9.

Jensen, V., K. M. Kaiser, et al. (2003). "A juvenile form of postsynaptic hippocampal long-term potentiation in mice deficient for the AMPA receptor subunit GluR-A." J Physiol **553**(Pt 3): 843-56.

Jia, Z., N. Agopyan, et al. (1996). "Enhanced LTP in mice deficient in the AMPA receptor GluR2." Neuron **17**(5): 945-56.

Jonas, P. and N. Burnashev (1995). "Molecular mechanisms controlling calcium entry through AMPA-type glutamate receptor channels." Neuron **15**(5): 987-90.

Katz, B. and R. Miledi (1968). "The role of calcium in neuromuscular facilitation." J Physiol **195**(2): 481-92.

Keinanen, K., W. Wisden, et al. (1990). "A family of AMPA-selective glutamate receptors." Science **249**(4968): 556-60.

Kim, J. (2001). Improvement and establishment of the tTA-dependent inducible system in the mouse brain. Molecular Neurobiology, MPI for Medical Research, Ruprecht-Karls-Universität, Heidelberg.

Koester, H. J. and B. Sakmann (1998). "Calcium dynamics in single spines during coincident pre- and postsynaptic activity depend on relative timing of back-propagating action potentials and subthreshold excitatory postsynaptic potentials." Proc Natl Acad Sci U S A **95**(16): 9596-601.

Kohler, M., H. C. Kornau, et al. (1994). "The organization of the gene for the functionally dominant alpha-amino-3-hydroxy-5-methylisoxazole-4-propionic acid receptor subunit GluR-B." J Biol Chem **269**(26): 17367-70.

Krestel, H. E., M. Mayford, et al. (2001). "A GFP-equipped bidirectional expression module well suited for monitoring tetracycline-regulated gene expression in mouse." Nucleic Acids Res **29**(7): E39.

Krestel, H. E., D. R. Shimshek, et al. (2004). "A genetic switch for epilepsy in adult mice." J Neurosci **24**(46): 10568-78.

Lerma, J., M. Morales, et al. (1994). "Rectification properties and Ca2+ permeability of glutamate receptor channels in hippocampal cells." Eur J Neurosci **6**(7): 1080-8.

Liao, D., X. Zhang, et al. (1999). "Regulation of morphological postsynaptic silent synapses in developing hippocampal neurons." Nat Neurosci **2**(1): 37-43.

Ling, D. S., L. S. Benardo, et al. (2002). "Protein kinase Mzeta is necessary and sufficient for LTP maintenance." Nat Neurosci **5**(4): 295-6.

Lipton, S. A. and P. A. Rosenberg (1994). "Excitatory amino acids as a final common pathway for neurologic disorders." N Engl J Med **330**(9): 613-22.

Lisman, J., H. Schulman, et al. (2002). "The molecular basis of CaMKII function in synaptic and behavioural memory." Nat Rev Neurosci **3**(3): 175-90.

Liu, S. Q. and S. G. Cull-Candy (2000). "Synaptic activity at calcium-permeable AMPA receptors induces a switch in receptor subtype." Nature **405**(6785): 454-8.

Lledo, P. M., G. O. Hjelmstad, et al. (1995). "Calcium/calmodulin-dependent kinase II and long-term potentiation enhance synaptic transmission by the same mechanism." Proc Natl Acad Sci U S A **92**(24): 11175-9.

Lledo, P. M. and F. Lazarini (2007). "Neuronal replacement in microcircuits of the adult olfactory system." C R Biol **330**(6-7): 510-20.

Lomeli, H., J. Mosbacher, et al. (1994). "Control of kinetic properties of AMPA receptor channels by nuclear RNA editing." Science **266**(5191): 1709-13.

Lopes da Silva, F. H., M. P. Witter, et al. (1990). "Anatomic organization and physiology of the limbic cortex." Physiol Rev **70**(2): 453-511.

Lynch, M. A. (2004). "Long-term potentiation and memory." Physiol Rev **84**(1): 87-136.

MacDermott, A. B., M. L. Mayer, et al. (1986). "NMDA-receptor activation increases cytoplasmic calcium concentration in cultured spinal cord neurones." Nature **321**(6069): 519-22.

Mack, V., N. Burnashev, et al. (2001). "Conditional restoration of hippocampal synaptic potentiation in Glur-A-deficient mice." Science **292**(5526): 2501-4.

Magee, J. C. and D. Johnston (1997). "A synaptically controlled, associative signal for Hebbian plasticity in hippocampal neurons." Science **275**(5297): 209-13.

Malenka, R. C. and M. F. Bear (2004). "LTP and LTD: an embarrassment of riches." Neuron **44**(1): 5-21.

Malenka, R. C. and R. A. Nicoll (1999). "Long-term potentiation--a decade of progress?" Science **285**(5435): 1870-4.

Malleret, G., U. Haditsch, et al. (2001). "Inducible and reversible enhancement of learning, memory, and long-term potentiation by genetic inhibition of calcineurin." Cell **104**(5): 675-86.

Mammen, A. L., K. Kameyama, et al. (1997). "Phosphorylation of the alpha-amino-3-hydroxy-5-methylisoxazole4-propionic acid receptor GluR1 subunit by calcium/calmodulin-dependent kinase II." J Biol Chem **272**(51): 32528-33.

Mansuy, I. M., D. G. Winder, et al. (1998). "Inducible and reversible gene expression with the rtTA system for the study of memory." Neuron **21**(2): 257-65.

Mantamadiotis, T., T. Lemberger, et al. (2002). "Disruption of CREB function in brain leads to neurodegeneration." Nat Genet **31**(1): 47-54.

Markram, H. and M. Tsodyks (1996). "Redistribution of synaptic efficacy between neocortical pyramidal neurons." Nature **382**(6594): 807-10.

Matsuda, S., S. Mikawa, et al. (1999). "Phosphorylation of serine-880 in GluR2 by protein kinase C prevents its C terminus from binding with glutamate receptor-interacting protein." J Neurochem **73**(4): 1765-8.

Matsuzaki, M., N. Honkura, et al. (2004). "Structural basis of long-term potentiation in single dendritic spines." Nature **429**(6993): 761-6.

Mayer, M. L. (2005). "Glutamate receptor ion channels." Curr Opin Neurobiol **15**(3): 282-8.

Mayer, M. L. and G. L. Westbrook (1987). "Permeation and block of N-methyl-D-aspartic acid receptor channels by divalent cations in mouse cultured central neurones." J Physiol **394**: 501-27.

Mayford, M., M. E. Bach, et al. (1996). "Control of memory formation through regulated expression of a CaMKII transgene." Science **274**(5293): 1678-83.

McHugh, S. B., B. Niewoehner, et al. (2008). "Dorsal hippocampal N-methyl-D-aspartate receptors underlie spatial working memory performance during non-matching to place testing on the T-maze." Behav Brain Res **186**(1): 41-7.

McHugh, T. J., K. I. Blum, et al. (1996). "Impaired hippocampal representation of space in CA1-specific NMDAR1 knockout mice." Cell **87**(7): 1339-49.

McHugh, T. J., M. W. Jones, et al. (2007). "Dentate gyrus NMDA receptors mediate rapid pattern separation in the hippocampal network." Science **317**(5834): 94-9.

McNaughton, N. and R. G. Morris (1987). "Chlordiazepoxide, an anxiolytic benzodiazepine, impairs place navigation in rats." Behav Brain Res **24**(1): 39-46.

Merkle, F. T., A. D. Tramontin, et al. (2004). "Radial glia give rise to adult neural stem cells in the subventricular zone." Proc Natl Acad Sci U S A **101**(50): 17528-32.

Mihaljevic, A. L. A. (2005). Analysis of recombinant glutamate receptors in the hippocampus of the mouse. Molecular Neurobiology, MPI for Medical Research, Ruprecht-Karls-Universität, Heidelberg.

Minichiello, L., M. Korte, et al. (1999). "Essential role for TrkB receptors in hippocampus-mediated learning." Neuron **24**(2): 401-14.

Molnar, E., A. Baude, et al. (1993). "Biochemical and immunocytochemical characterization of antipeptide antibodies to a cloned GluR1 glutamate receptor subunit: cellular and subcellular distribution in the rat forebrain." Neuroscience **53**(2): 307-26.

Monyer, H., R. Sprengel, et al. (1992). "Heteromeric NMDA receptors: molecular and functional distinction of subtypes." Science **256**(5060): 1217-21.

Morris, R. G., E. Anderson, et al. (1986). "Selective impairment of learning and blockade of long-term potentiation by an N-methyl-D-aspartate receptor antagonist, AP5." Nature **319**(6056): 774-6.

Morris, R. G., P. Garrud, et al. (1982). "Place navigation impaired in rats with hippocampal lesions." Nature **297**(5868): 681-3.

Mosbacher, J., R. Schoepfer, et al. (1994). "A molecular determinant for submillisecond desensitization in glutamate receptors." Science **266**(5187): 1059-62.

Moser, E., M. B. Moser, et al. (1993). "Spatial learning impairment parallels the magnitude of dorsal hippocampal lesions, but is hardly present following ventral lesions." J Neurosci **13**(9): 3916-25.

Moser, M. B. and E. I. Moser (1998). "Distributed encoding and retrieval of spatial memory in the hippocampus." J Neurosci **18**(18): 7535-42.

Moser, M. B., E. I. Moser, et al. (1995). "Spatial learning with a minislab in the dorsal hippocampus." Proc Natl Acad Sci U S A **92**(21): 9697-701.

Nakazawa, K., M. C. Quirk, et al. (2002). "Requirement for hippocampal CA3 NMDA receptors in associative memory recall." Science **297**(5579): 211-8.

Niewoehner, B., F. N. Single, et al. (2007). "Impaired spatial working memory but spared spatial reference memory following functional loss of NMDA receptors in the dentate gyrus." Eur J Neurosci **25**(3): 837-46.

Nutt, S. L. and R. K. Kamboj (1994). "Differential RNA editing efficiency of AMPA receptor subunit GluR-2 in human brain." Neuroreport **5**(13): 1679-83.

O´Keefe, J. a. N., L. (1978). "The hippocampus as a cognitive map." Oxford, Clarendon.

Olton, D. S. a. P., B. C. (1979). "Spatial memory and hippocampal function." Neuropsychologia **17**(6): 660-82.

Otmakhov, N., L. C. Griffith, et al. (1997). "Postsynaptic inhibitors of calcium/calmodulin-dependent protein kinase type II block induction but not maintenance of pairing-induced long-term potentiation." J Neurosci **17**(14): 5357-65.

Palmer, C. L., L. Cotton, et al. (2005). "The molecular pharmacology and cell biology of alpha-amino-3-hydroxy-5-methyl-4-isoxazolepropionic acid receptors." Pharmacol Rev **57**(2): 253-77.

Passafaro, M., V. Piech, et al. (2001). "Subunit-specific temporal and spatial patterns of AMPA receptor exocytosis in hippocampal neurons." Nat Neurosci **4**(9): 917-26.

Paylor, R., M. Nguyen, et al. (1998). "Alpha7 nicotinic receptor subunits are not necessary for hippocampal-dependent learning or sensorimotor gating: a behavioral characterization of Acra7-deficient mice." Learn Mem **5**(4-5): 302-16.

Petralia, R. S., J. A. Esteban, et al. (1999). "Selective acquisition of AMPA receptors over postnatal development suggests a molecular basis for silent synapses." Nat Neurosci **2**(1): 31-6.

Petralia, R. S. and R. J. Wenthold (1992). "Light and electron immunocytochemical localization of AMPA-selective glutamate receptors in the rat brain." J Comp Neurol **318**(3): 329-54.

Petralia, R. S. and R. J. Wenthold (1999). "Immunocytochemistry of NMDA receptors." Methods Mol Biol **128**: 73-92.

Pike, F. G., R. M. Meredith, et al. (1999). "Rapid report: postsynaptic bursting is essential for 'Hebbian' induction of associative long-term potentiation at excitatory synapses in rat hippocampus." J Physiol **518 (Pt 2)**: 571-6.

Pollard, H., A. Heron, et al. (1993). "Alterations of the GluR-B AMPA receptor subunit flip/flop expression in kainate-induced epilepsy and ischemia." Neuroscience **57**(3): 545-54.

Pothuizen, H. H., W. N. Zhang, et al. (2004). "Dissociation of function between the dorsal and the ventral hippocampus in spatial learning abilities of the rat: a within-subject, within-task comparison of reference and working spatial memory." Eur J Neurosci **19**(3): 705-12.

Quirk, G. J., R. U. Muller, et al. (1992). "The positional firing properties of medial entorhinal neurons: description and comparison with hippocampal place cells." J Neurosci **12**(5): 1945-63.

Rawlins, J. N. and D. S. Olton (1982). "The septo-hippocampal system and cognitive mapping." Behav Brain Res **5**(4): 331-58.

Reisel, D., D. M. Bannerman, et al. (2002). "Spatial memory dissociations in mice lacking GluR1." Nat Neurosci **5**(9): 868-73.

Resnik, E. (2007). Impaired representation of space in the hippocampus of GluR-A knockout mice. Molecular Neurobiology, MPI for Medical Research, Ruprecht-Karls-Universität, Heidelberg.

Reyes, A., R. Lujan, et al. (1998). "Target-cell-specific facilitation and depression in neocortical circuits." Nat Neurosci **1**(4): 279-85.

Richmond, M. A., B. K. Yee, et al. (1999). "Dissociating context and space within the hippocampus: effects of complete, dorsal, and ventral excitotoxic hippocampal lesions on conditioned freezing and spatial learning." Behav Neurosci **113**(6): 1189-203.

Roberson, E. D., J. D. English, et al. (1999). "The mitogen-activated protein kinase cascade couples PKA and PKC to cAMP response element binding protein phosphorylation in area CA1 of hippocampus." J Neurosci **19**(11): 4337-48.

Roche, K. W., R. J. O'Brien, et al. (1996). "Characterization of multiple phosphorylation sites on the AMPA receptor GluR1 subunit." Neuron **16**(6): 1179-88.

Rolls, E. T. and R. P. Kesner (2006). "A computational theory of hippocampal function, and empirical tests of the theory." Prog Neurobiol **79**(1): 1-48.

Salter, M. W. and L. V. Kalia (2004). "Src kinases: a hub for NMDA receptor regulation." Nat Rev Neurosci **5**(4): 317-28.

Sanderson, D. J., M. A. Good, et al. (2008). "The role of the GluR-A (GluR1) AMPA receptor subunit in learning and memory." Prog Brain Res **169**: 159-78.

Sargolini, F., M. Fyhn, et al. (2006). "Conjunctive representation of position, direction, and velocity in entorhinal cortex." Science **312**(5774): 758-62.

Saucier, D. and D. P. Cain (1995). "Spatial learning without NMDA receptor-dependent long-term potentiation." Nature **378**(6553): 186-9.

Save, E., B. Poucet, et al. (1992). "Object exploration and reactions to spatial and nonspatial changes in hooded rats following damage to parietal cortex or hippocampal formation." Behav Neurosci **106**(3): 447-56.

Schmitt, W. B., R. Arianpour, et al. (2004). "The role of hippocampal glutamate receptor-A-dependent synaptic plasticity in conditional learning: the importance of spatiotemporal discontiguity." J Neurosci **24**(33): 7277-82.

Schmitt, W. B., R. M. Deacon, et al. (2003). "A within-subjects, within-task demonstration of intact spatial reference memory and impaired spatial working memory in glutamate receptor-A-deficient mice." J Neurosci **23**(9): 3953-9.

Schmitt, W. B., R. Sprengel, et al. (2005). "Restoration of spatial working memory by genetic rescue of GluR-A-deficient mice." Nat Neurosci **8**(3): 270-2.

Schonig, K., F. Schwenk, et al. (2002). "Stringent doxycycline dependent control of CRE recombinase in vivo." Nucleic Acids Res **30**(23): e134.

Scoville, W. B. and B. Milner (1957). "Loss of recent memory after bilateral hippocampal lesions." J Neurol Neurosurg Psychiatry **20**(1): 11-21.

Seeburg, P. H., N. Burnashev, et al. (1995). "The NMDA receptor channel: molecular design of a coincidence detector." Recent Prog Horm Res **50**: 19-34.

Seeburg, P. H., M. Higuchi, et al. (1998). "RNA editing of brain glutamate receptor channels: mechanism and physiology." Brain Res Brain Res Rev **26**(2-3): 217-29.

Seidenman, K. J., J. P. Steinberg, et al. (2003). "Glutamate receptor subunit 2 Serine 880 phosphorylation modulates synaptic transmission and mediates plasticity in CA1 pyramidal cells." J Neurosci **23**(27): 9220-8.

Sharp, P. E. (1996). "Multiple spatial/behavioral correlates for cells in the rat postsubiculum: multiple regression analysis and comparison to other hippocampal areas." Cereb Cortex **6**(2): 238-59.

Sharp, P. E. and C. Green (1994). "Spatial correlates of firing patterns of single cells in the subiculum of the freely moving rat." J Neurosci **14**(4): 2339-56.

Sheay, W., S. Nelson, et al. (1993). "Downstream insertion of the adenovirus tripartite leader sequence enhances expression in universal eukaryotic vectors." Biotechniques **15**(5): 856-62.

Shi, S., Y. Hayashi, et al. (2001). "Subunit-specific rules governing AMPA receptor trafficking to synapses in hippocampal pyramidal neurons." Cell **105**(3): 331-43.

Shimshek, D. R. (2003). GluR-B: die wichtigste AMPA-Rezeptor-Untereinheit in der Maus. Molecular Neurobiology, MPI for Medical Research, Ruprecht-Karls-Universität, Heidelberg.

Shimshek, D. R., T. Bus, et al. (2006). "Impaired reproductive behavior by lack of GluR-B containing AMPA receptors but not of NMDA receptors in hypothalamic and septal neurons." Mol Endocrinol **20**(1): 219-31.

Shimshek, D. R., T. Bus, et al. (2005). "Enhanced odor discrimination and impaired olfactory memory by spatially controlled switch of AMPA receptors." PLoS Biol **3**(11): e354.

Shimshek, D. R., V. Jensen, et al. (2006). "Forebrain-specific glutamate receptor B deletion impairs spatial memory but not hippocampal field long-term potentiation." J Neurosci **26**(33): 8428-40.

Sommer, B., K. Keinanen, et al. (1990). "Flip and flop: a cell-specific functional switch in glutamate-operated channels of the CNS." Science **249**(4976): 1580-5.

Sommer, B., M. Kohler, et al. (1991). "RNA editing in brain controls a determinant of ion flow in glutamate-gated channels." Cell **67**(1): 11-9.

Soriano, P. (1999). "Generalized lacZ expression with the ROSA26 Cre reporter strain." Nat Genet **21**(1): 70-1.

Specht, C. G. and A. Triller (2008). "The dynamics of synaptic scaffolds." Bioessays **30**(11-12): 1062-74.

Sprengel, R. (2006). "Role of AMPA receptors in synaptic plasticity." Cell Tissue Res **326**(2): 447-55.

Squire, L. R. (2009). "The legacy of patient H.M. for neuroscience." Neuron **61**(1): 6-9.

Squire, L. R., C. E. Stark, et al. (2004). "The medial temporal lobe." Annu Rev Neurosci **27**: 279-306.

Stanton, P. K. and J. M. Sarvey (1984). "Blockade of long-term potentiation in rat hippocampal CA1 region by inhibitors of protein synthesis." J Neurosci **4**(12): 3080-8.

Steele, R. J. and R. G. Morris (1999). "Delay-dependent impairment of a matching-to-place task with chronic and intrahippocampal infusion of the NMDA-antagonist D-AP5." Hippocampus **9**(2): 118-36.

Stevens, C. F. (1979). "The neuron." Sci Am **241**(3): 54-65.

Stevens, C. F. and Y. Wang (1995). "Facilitation and depression at single central synapses." Neuron **14**(4): 795-802.

Stuart, G. J. and B. Sakmann (1994). "Active propagation of somatic action potentials into neocortical pyramidal cell dendrites." Nature **367**(6458): 69-72.

Swanson, G. T., S. K. Kamboj, et al. (1997). "Single-channel properties of recombinant AMPA receptors depend on RNA editing, splice variation, and subunit composition." J Neurosci **17**(1): 58-69.

Swanson, L. W., J. M. Wyss, et al. (1978). "An autoradiographic study of the organization of intrahippocampal association pathways in the rat." J Comp Neurol **181**(4): 681-715.

Sweatt, J. D. (2004). "Mitogen-activated protein kinases in synaptic plasticity and memory." Curr Opin Neurobiol **14**(3): 311-7.

Tanaka, H., S. Y. Grooms, et al. (2000). "The AMPAR subunit GluR2: still front and center-stage." Brain Res **886**(1-2): 190-207.

Taylor, A. (2007). The role of excitatory AMPA receptor subtypes in hippocampal-dependent learning and memory. Department of Experimental Psychology, Oxford University.

Taube, J. S. (1995). "Place cells recorded in the parasubiculum of freely moving rats." Hippocampus **5**(6): 569-83.

Thomson, A. M. (2003). "Presynaptic frequency- and pattern-dependent filtering." J Comput Neurosci **15**(2): 159-202.

Tolman, E. C. (1948). "Cognitive maps in rats and men." Psychol Rev **55**(4): 189-208.

Tomita, S., V. Stein, et al. (2005). "Bidirectional synaptic plasticity regulated by phosphorylation of stargazin-like TARPs." Neuron **45**(2): 269-77.

Tonegawa, S., J. Z. Tsien, et al. (1996). "Hippocampal CA1-region-restricted knockout of NMDAR1 gene disrupts synaptic plasticity, place fields, and spatial learning." Cold Spring Harb Symp Quant Biol **61**: 225-38.

Tonkiss, J. and J. N. Rawlins (1991). "The competitive NMDA antagonist AP5, but not the non-competitive antagonist MK801, induces a delay-related impairment in spatial working memory in rats." Exp Brain Res **85**(2): 349-58.

Trussell, L. O. and G. D. Fischbach (1989). "Glutamate receptor desensitization and its role in synaptic transmission." Neuron **3**(2): 209-18.

Tsien, J. Z., D. F. Chen, et al. (1996). "Subregion- and cell type-restricted gene knockout in mouse brain." Cell **87**(7): 1317-26.

Tsien, J. Z., P. T. Huerta, et al. (1996). "The essential role of hippocampal CA1 NMDA receptor-dependent synaptic plasticity in spatial memory." Cell **87**(7): 1327-38.

Vaidya, V. A., J. A. Siuciak, et al. (1999). "Hippocampal mossy fiber sprouting induced by chronic electroconvulsive seizures." Neuroscience **89**(1): 157-66.

Wenthold, R. J., R. S. Petralia, et al. (1996). "Evidence for multiple AMPA receptor complexes in hippocampal CA1/CA2 neurons." J Neurosci **16**(6): 1982-9.

Yasuda, H., A. L. Barth, et al. (2003). "A developmental switch in the signaling cascades for LTP induction." Nat Neurosci **6**(1): 15-6.

Zamanillo, D., R. Sprengel, et al. (1999). "Importance of AMPA receptors for hippocampal synaptic plasticity but not for spatial learning." Science **284**(5421): 1805-11.

Zola-Morgan, S., L. R. Squire, et al. (1986). "Human amnesia and the medial temporal region: enduring memory impairment following a bilateral lesion limited to field CA1 of the hippocampus." J Neurosci **6**(10): 2950-67.

Zucker, R. S. (1989). "Short-term synaptic plasticity." Annu Rev Neurosci **12**: 13-31.

8. Scientific contributions

8.1. Diploma thesis

T. Bus, "Selektive Steuerung der Genexpression in GnRH-Neuronen", 2005, Ruprecht-Karls-Universität, Heidelberg, Deutschland

8.2. Publications

Shimshek, D. R., T. Bus, et al. (2005). "Enhanced odor discrimination and impaired olfactory memory by spatially controlled switch of AMPA receptors." <u>PLoS Biol</u> **3**(11): e354.

Shimshek, D. R., T. Bus, et al. (2006). "Impaired reproductive behavior by lack of GluR-B containing AMPA receptors but not of NMDA receptors in hypothalamic and septal neurons." <u>Mol Endocrinol</u> **20**(1): 219-31.

Shimshek, D. R., V. Jensen, et al. (2006). "Forebrain-specific glutamate receptor B deletion impairs spatial memory but not hippocampal field long-term potentiation." <u>J Neurosci</u> **26**(33): 8428-40.

Oberto, A., E. Acquadro, et al. (2007). "Expression patterns of promoters for NPY Y(1) and Y(5) receptors in Y(5)RitTA and Y(1)RVenus BAC-transgenic mice." <u>Eur J Neurosci</u> **26**(1): 155-70.

8.3. Poster

Shimshek D.R., Bus T., Mack V., Kim J., Mihaljevic A., Sprengel R., Seeburg P.H., Schaefer A.T.: "Enhanced Odor Discrimination and Reduced Olfactory Memory by Spatial Controlled Switch of AMPA Receptor Channels." Presented at the Society of Neuroscience 34th annual meeting in San Diego, October 2004

Bus, T; Shimshek, D.R; Schäfer, A.T; Sprengel, R; Seeburg, P.H.: "Genetic dissection of olfactory learning and memory." Presented at the spring school of life science at the Hebrew University of Jerusalem 2006.

Bus, T; Sprengel, R., "Inactivation of AMPA and NMDA receptor genes in specific regions of the hippocampus and olfactory-related cortical fields", A4 project of the Sonderforschungsbereich 636, presented at the ZI Mannheim 2007

Bus T., Grinevich V., Astori S., Seeburg P.H.: "The role of GABA in GnRH neuronal migration and function and the role of the olfactory GnRH system." D12 project of the Sonderforschungsbereich 488, presented at the ZMBH Heidelberg 2008

9. Acknowledgements